

SCIENTIFIC WRITINGS

Academic Projects (Selected)

- **Ahmad, M.S.**, M. Shafique, and M.S. Anwar (Apr 2019). *Physlock: An Entry-Level Low-Cost Lock-In Amplifier Board* (physlab.org).
- Sohail, E., **Ahmad, M.S.**, and M.S. Anwar (Jul 2019). *Experimental Analysis of Superconductivity and Quantum Interference*. (physlab.org).
- **Ahmad, M.S.** (2018a). *Orbital Angular Momentum Generation and Detection* (researchgate.net).
- **Ahmad, M.S.** (2018b). *Reflection and Transmission of Light from Multilayered Films: An easy approach, using MATLAB* (physlab.org).
- Arshad, M.J., **Ahmad, M.S.**, and R. Abbas (2017). *Measurement of Verdet Constant by Faraday Rotation*. (researchgate.net).

LAB Manuals

- **Ahmad, M.S.** and Anwar, M.S. (May 2019). *Newton's cradle observed by video tracking* (physlab.org).
- **Ahmad, M.S.** and Anwar, M.S. (May 2019). *Experiments with a linear air track* (physlab.org).
- **Ahmad, M.S.**, Hussain, A., Salman, R., and M.S. Anwar (Jul 2019). *Tuning a Laser Diode* (physlab.org).
- Hassan, M.U., **Ahmad, M.S.**, and M.S. Anwar (Apr 2019). *PhysLogger – Quick start Guide (App)* (physlab.org).

Physlock: An Entry-Level Low-Cost Lock-In Amplifier Board

Muhammad Shiraz Ahmad, Muhammad Shafique and Muhammad Sabieh Anwar
Department of Physics, Syed Babar Ali School of Science and Engineering

March 25, 2019, Version 2019-01

The design of a simple, entry level low-cost, stand-alone lock-in amplifier is described. The instrument is useful for detecting and amplifying signals that are frequency synchronized with a reference signal. It is particularly important for detecting and measuring small signals in the presence of large noise. The design is based on a modulator/demodulator integrated circuit and uses a minimum number of components to accomplish input amplification, phase-sensitive detection, low-pass filtering, and dc amplification of the output signal. **Physlock** is based on the chip AD630 and will be helpful in teaching students about low-level signal detection which is commonplace in numerous tasks in the experimental physics laboratory. It can also be used in the research laboratory (see specs below).

Major specifications of PhysLock

Power	220 V, 50 Hz
Reference signal amplitude	> 1 V
Dynamic Range	60 dB to 70 dB
DC gains	$1\times$ or $10\times$
AC input gains	$1\times$, $50\times$, $100\times$, $500\times$, $1000\times$, $2000\times$, $5000\times$
Low pass filter time constants	1 s, 0.1 s, 10 ms, 0.1 ms, $10\ \mu\text{s}$
Form of input signal	Low frequency (< 1 KHz) periodic signal (square to sine converter is also provided).

1 Theory of Operation

Figure 1 which shows the block diagram of the lock-in amplifier. The important components of this circuit will now be described. Each component is shown inside a dashed box for greater clarity.

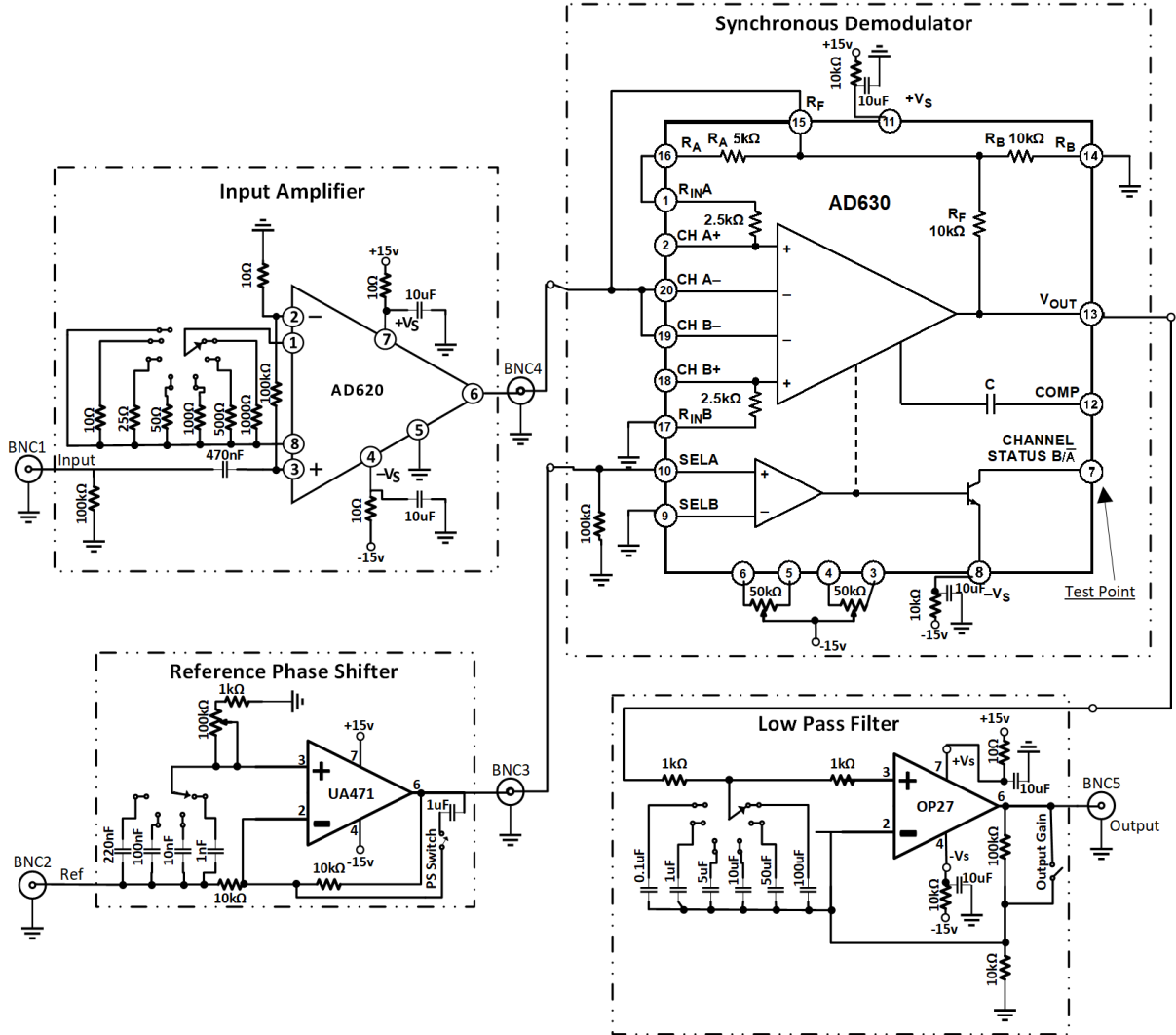


Figure 1: Block diagram of the lock-in amplifier. The input signal is first amplified and then demodulated with a reference signal of known frequency. The output of this stage is then passed through a low pass filter which returns the final DC output. The input and output gains, phase shift of the input signal and the low pass filter threshold can be varied using controls provided on the instrument.

1.1 Input Amplifier

The raw input signal is applied on the BNC1 connector and passes through an amplifier circuit. It's gain can be easily changed to $1\times$, $50\times$, $100\times$, $500\times$, $1000\times$, $2000\times$ or $5000\times$ by changing the feedback resistance of the amplifier chip AD620.

1.2 Reference Phase Shifter

The reference signal applied on the BNC2 connector passes through a buffered phase-shifter. The phase-shifter can also be bypassed by using the PS Switch. This circuit has unity gain.

1.3 Synchronous Demodulator

The functional block diagram of the AD630 chip (see Figure 2) shows the pin connections for the demodulation process. The individual A and B channel preamps, the switch, and the integrator output amplifier are combined in to a single op amp. This amplifier has two differential input channels, only one of which is active at a time.

The basic function of the AD630 may be easier to recognize as two gain amplifiers, which can be inserted into a signal path under the control of a sensitive voltage comparator. When the circuit is switched between inverting and noninverting gain, it provides the basic demodulation function.

Figure 2(a) shows a test configuration to understand the basic functionality of AD630. The comparator selects one of the two input stages to complete an operational feedback connection around AD630. Likewise, when Channel B is selected, the R_A and R_F resistors are connected for inverting feedback as shown in the inverting gain diagram in Figure 2(a). When the sign of comparator input is reversed, Input B is deselected and Input A is selected. The new equivalent circuit is the noninverting gain configuration shown in Figure 2(c). (See AD630's data sheet [1] for further details).

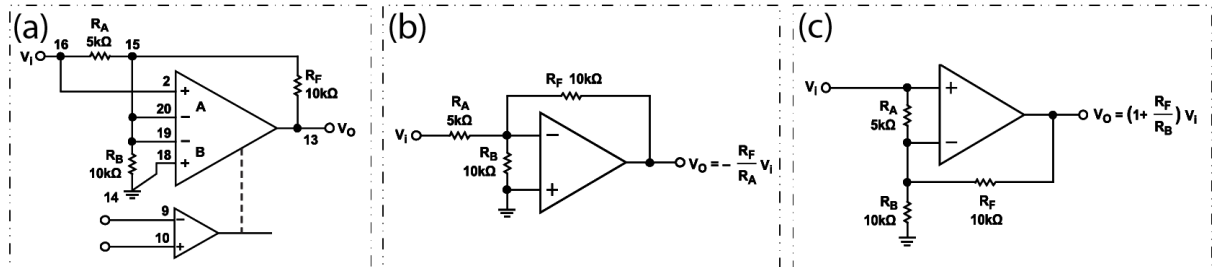


Figure 2: (a) AD630 symmetric gain (2). (b) Inverting gain configuration. (c) Noninverting gain configuration.

In the present configuration, SEL B of voltage comparator is grounded and SEL A is connected to the reference signal followed by the phase shifter. When reference signal goes in its negative half cycle, Channel B is selected. This configuration acts as inverting amplification which yields gain of -2 whereas when reference signal goes in its positive half cycle, Channel A is selected. This is when the configuration achieves non-inverting amplification with a gain factor of $+2$.

1.4 Low Pass Filter

The demodulated signal generated by AD630 passes through a RC Low Pass Filter which has a fixed RC resistance of $1\text{ k}\Omega$. The time constant τ can be changed to 1 s, 0.1 s, 1 ms, 10 ms, 0.1 ms or $1\text{ }\mu\text{s}$ by changing a capacitor. The time constant of the low pass filter determines the bandwidth; larger the time constant, narrower is the bandwidth. This means that signals whose frequencies are within a tighter band around the reference signal will pass through, while others will be blocked.

2 Basic experimental tests of the Lock-In Amplifier

A sinusoidal waveform of amplitude 5 Vp of frequency 60 Hz is generated using a function generator and connected with a voltage divider circuit. This voltage divider circuit produces two frequency synchronized signals of amplitudes 5 Vp and $250\text{ }\mu\text{Vp}$. The $250\text{ }\mu\text{Vp}$ signal is connected to the BNC1 socket and the 5 Vp signal is connected to the BNC2 socket of PhysLock. These signals are used as the input and reference signals for PhysLock. The whole configuration is shown in Figure 3.

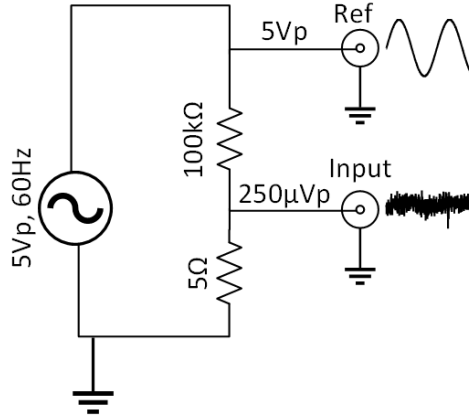


Figure 3: Configuration to produce two synchronized signals, one is used as the reference and other as input signal.

The $250\text{ }\mu\text{Vp}$ signal produced in above configuration also includes noise in the milli volt regime. This signal is shown in Figure 4(a). The gain of input amplifier is set to $5000\times$ which amplifies the reference input to 1.25 Vp (see Figure 4(b)). This amplified signal passes through the chip AD630 followed by a low pass filter. Here switching between inverting and noninverting gain of the chip AD630 is under the direct control of the reference signal. During the positive half cycle of the reference signal, AD630 acts as a noninverting amplifier with a gain of 2, and during the negative half cycle, it acts as an inverting amplifier with a gain of -2 . Figure 4(d) shows switching response of AD630 on its pin 7 which is the output of the comparator controlling the inverting versus noninverting behavior of the input amplifier. Figure 4(e) shows the demodulated signal after passing through AD630, which appears as a positive rectified signal. The time constant of the low pass filter is set to 1 s with gain of 1, which converts this rectified AC signal to pure DC signal. This

DC signal is shown in Figure 4(f). We can switch between positive and negative rectified signals by changing the phase of the reference signal.

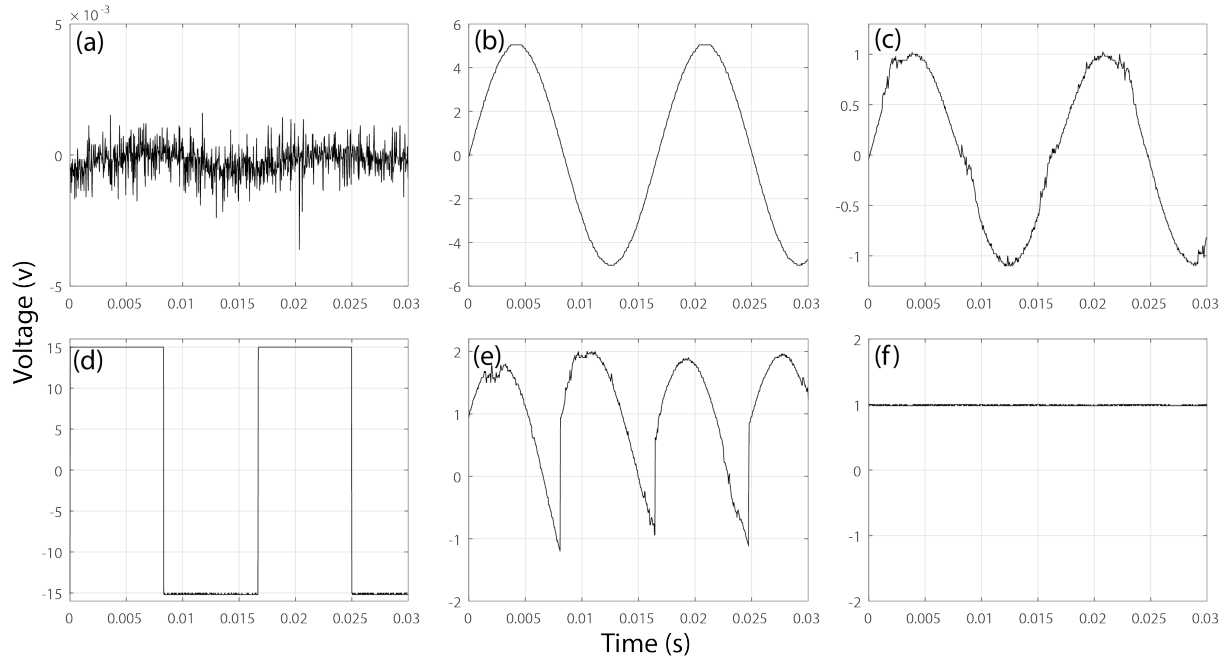


Figure 4: The test waveforms acquired different test points of **PhysLock**; (a) shows the input signal, (b) shows the reference signal, (c) shows the signal after passing through the input amplifier block, (d) shows AD630's pin 07 (Test point) response which is the modulating waveform provided by the switching comparator, (e) shows demodulated signal after passing through AD630, and (f) shows the final output after passing through the low pass filter block.

3 Introduction to PhysLock's Front Panel Controls

Typically, a lock-in amplifier measures the rms value of that component of input signal whose frequency is synchronized with the reference frequency. For example, suppose that the reference waveform is a sine wave of frequency 1 kHz. Furthermore the signal is a wave $A_1 \sin(2\pi \times 10^3 t) + A_2 \sin(2\pi \times 2 \times 10^3 t) + \text{white noise}$. The output of an ideal lock-in should be a DC signal proportional to A_1 , which is the component at the reference frequency. This should also be the case when the noise is much larger than A_1 . Like any other lock-in, **PhysLock** also extracts and amplifies the DC signal but also provides output signals at several intermediate stages. This is how it gives the user more command over the instrument by displaying the performance of every stage of the process. Knobs and switches are provided to adjust different parameters of the process or to switch a part of the internal circuit on or off. BNC sockets are provided for displaying the signal on a voltmeter or an oscilloscope. We now describe the various front panel controls on **PhysLock**

3.1 End User Interface

See Figure 5 which shows different parts of the instrument. The purpose and usage of several important parts will now be described.

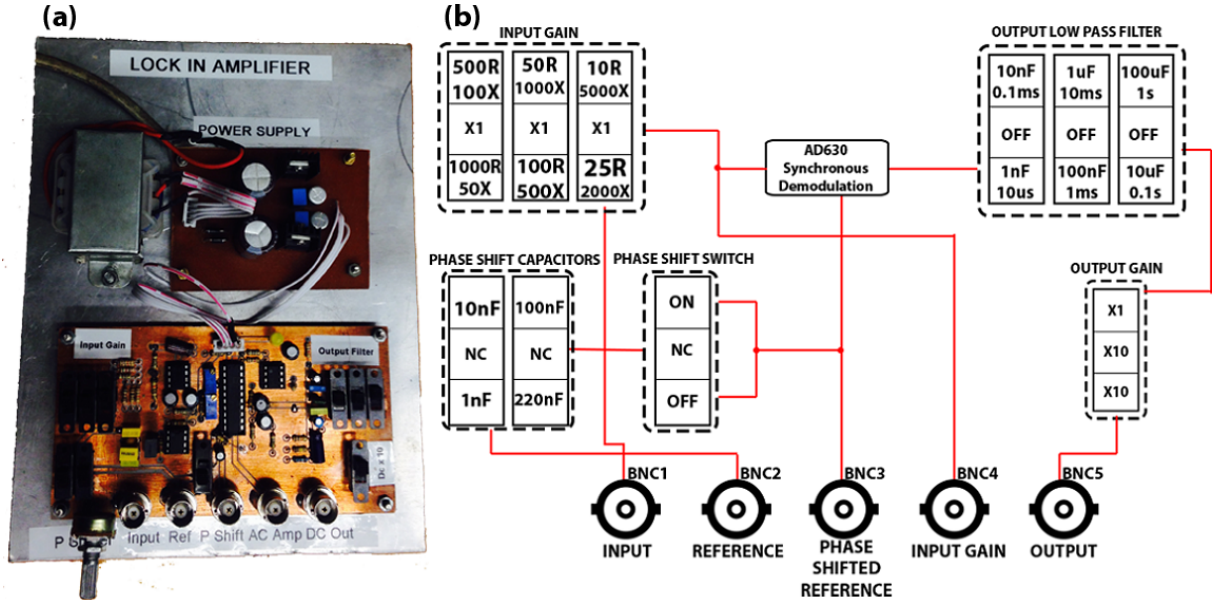


Figure 5: (a) Photograph of the instrument and (b) shows the schematic connections of the various input and output terminals with functional blocks of the instrument.

3.1.1 Phase Shift Switch

The phase shift in the reference signal can be turned on (Up) and off (Down) through the switch present in the “Phase Shift Switch” block. It is clear that turning the switch off will also disengage the phase shifter knob.

3.1.2 Phase Shift Adjustment

When the Phase Shift Switch is set on, the amount of the shift is given by

$$\phi = \pi - 2 \tan^{-1}(\omega RC)$$

The provided dial adjusts R and the jumper switches present in the block “Phase Shift Capacitors” change the C capacitance. The phase shifted reference can be measured on the BNC3 socket.

3.1.3 Input Gain

The AC input can be amplified to desirable level by using gain switches present in the “Input Gain” section and the amplified AC signal can be measured through the BNC4 Connector.

3.1.4 Output Low Pass Filter

These switches can be used to adjust the bandwidth (i.e. The 3 dB point) of the low pass filter applied to the output signal.

3.1.5 DC Gain

The DC gain switch amplifies the output signal by a factor of 10 (Down) or 1 (Up).

3.1.6 Reference

A square or sinusoidal wave of a known frequency is fed through this socket (labeled BNC2) which serves as the reference signal of the lock-in amplifier.

3.1.7 Input

The actual input signal to be analysed is connected on this socket which is labeled as BNC1 Connector.

3.1.8 DC Output

This is the ultimate output of the lock-in amplifier which has passed through all the stages with adjusted parameters. Normally, it should show a DC signal. However, if the signal shows some oscillating components, the low-pass filter should be adjusted.

4 Using PhysLock in an Optical Experiment: verifying Malus's law

To test our PhysLock in an optical setup, we used the configuration shown in Figure 5. An optical beam produced by a laser is passed through an optical chopper, which periodically interrupts the light beam with a frequency defined by the chopper's controller. This interrupted beam passes through the polarizer and the analyzer and is finally detected on a photodiode. The photodiode converts this interrupted optical signal into an electrical current which is converted to proportional voltage using a current-to-voltage amplifier.

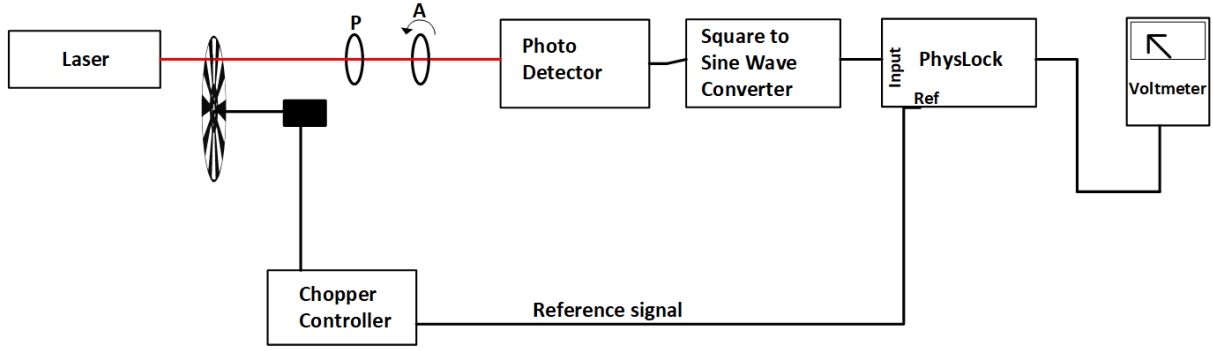


Figure 6: Schematic diagram of the experiment to verify the Malus's law where P represents the polarizer and A represents the analyzer.

The rectangular signal is converted into a sinusoidal signal by passing it through rectangular to sine wave converter. This ensures that the high frequency components (on the edges of square transitions) are removed. Remember that **PhysLock** shows optical performance at frequencies below 1 KHz. Finally, this signal along with a reference signal, taken from the chopper reference, is used to measure the DC value of that reference signal. Figure 7 shows the experimental curve which agrees almost perfectly with the theoretical prediction of the square of cosine relationship. In our experiment, we fixed the orientation of the polarizer while rotated the angle θ of the analyzer.

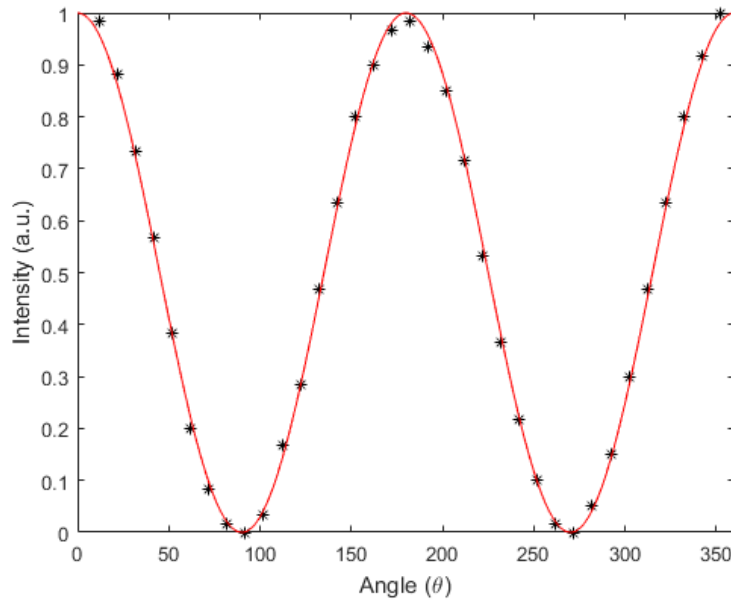


Figure 7: Intensity of an optical beam as a function of angle between two crossed polarizers, curve fitted on square of cosine, which satisfies Malus's law.

References

- [1] <https://www.analog.com/media/en/technical-documentation/data-sheets/ad630.pdf>

Experimental Analysis of Superconductivity and Quantum Interference

Emaan Sohail, Muhammad Shiraz Ahmad and Muhammad Sabieh Anwar*
Syed Babar Ali School of Science and Engineering, LUMS

12th July, 2019

Josephson effect is the flow of current without a potential drop across an insulator, with the ability to expel magnetic flux from its region. Superconducting QUantum Interference Devices (SQUIDs) are based on this effect to take sensitive measurements at quantum level. In this experiment, we study the variation of current, voltage and magnetic flux using a High-Temperature SQUID (HTS) in different configurations. We aim to observe the DC and AC Josephson and Meissner effects, study the temperature-resistance relation of the SQUID, and use the SQUID as a flux detector via flux locked loop circuits.

KEYWORDS:

Superconductivity · Josephson Effect · Flux Quantization · Critical Current · Flux Locked Loop · Meissner effect ·

*No part of this document can be re-used without explicit permission of Muhammad Sabieh Anwar.

Contents

1	Theoretical Introduction	3
1.1	Superconductivity	3
1.1.1	Cooper Pairs and Tunneling	3
1.1.2	Flux Quantization	4
1.1.3	Josephson Junctions	4
1.2	Operation of the SQUID	5
1.2.1	Framework of Josephson Junctions–The Meissner Effect	5
1.2.2	Quantum Interference	7
2	Apparatus and Functioning of the SQUID	7
2.1	Probe	7
2.2	Functionality of Mr.SQUID® electronic box	8
3	Experiments Performed using the SQUID	9
3.1	Calculating Resistance of the SQUID at room temperature	9
3.2	Observing the DC Josephson Effect	10
3.3	Observing the AC Josephson Effect	11
3.4	Observing the Voltage response across the SQUID in applied Magnetic Field	13
3.5	Additional Parameters of the SQUID coils	14
3.5.1	Modulation Depth	15
3.5.2	McCumber Parameter	15
3.5.3	Mutual Inductance	15
3.6	Relation between Temperature and Resistance of the SQUID	16
3.7	Analog Flux Locked Loop Circuit as a Flux Detector	17
3.8	Digital Flux Locked Loop	22
4	Appendices	29

1 Theoretical Introduction

This section provides theoretical details for the underlying phenomena on the basis of which the experiments are performed.

1.1 Superconductivity

Superconductivity is the phenomena when electrical resistance of a conductor is zero, and the conductor is capable of eliminating magnetic flux from its region.

1.1.1 Cooper Pairs and Tunneling

Certain materials exhibit the property of conducting electricity in resistance-less environments when cooled down below certain temperature ranges. This effect comes about as the result of pairing up of electrons in the material, which possess opposite spins and directions of motion, but the same speed. The movement of both electrons create a disturbance in the positive lattice of the material. The displacement caused by either electron becomes a cause of attraction for the other. This results in coupling between them into a pair. This development of attraction can also be depicted as the exchange of a "*phonon*"¹ between the pair (see Figure 1). Cooper pairs are named after the phenomenon's discoverer, Leonard Cooper[2]. Since the electrons in a pair show a coherence in their state, they share a common wave-function.

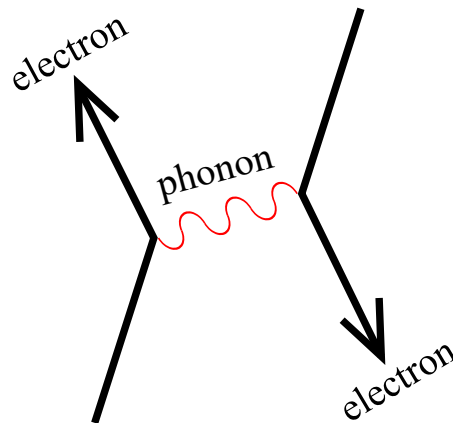


Figure 1: Feynman Diagram for Electron Coupling

The aspect which makes these Cooper pairs even more peculiar, is their ability to tunnel through high potential energy barriers, keeping the current flow alive, unlike the electrical conductivity at non-cryogenic temperatures[3].

¹Quantum of vibrational mechanical energy[1].

1.1.2 Flux Quantization

In quantum mechanics, a *fluxon* or ϕ_o is the quantum unit for magnetic flux. One fluxon has the value of approximately 2.07×10^{-15} Wb. Magnetic flux can exist in the SQUID as multiples of magnetic flux quantum, as long as it is in a superconducting state. The reaction of the superconducting phase to applied magnetic field (described in Section 1.2.1), manages to cause the expulsion of the extra magnetic flux (Meissner Effect).

1.1.3 Josephson Junctions

Josephson Junctions can be categorized into four types (see Figure 2). Namely, tunnel junction, separated by an insulating layer, proximity junction, separated by a normal metal, micro-bridge, with a constriction between two phases, and point contact junctions[10].

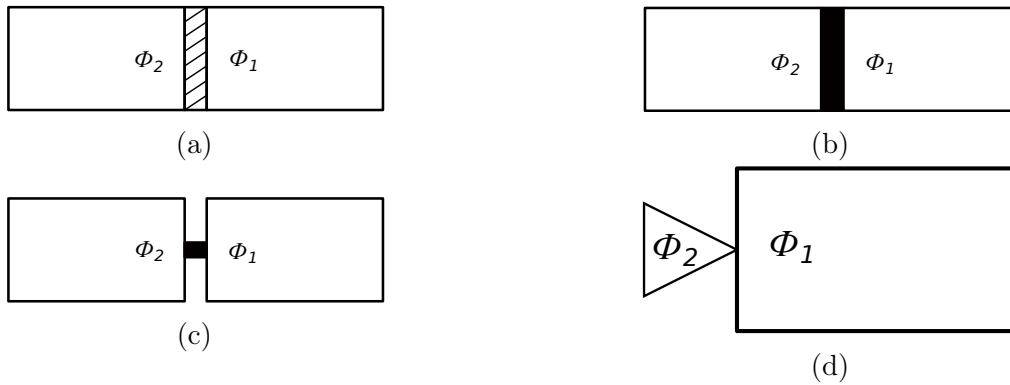


Figure 2: Types of Josephson Junctions showing (a) Insulating barrier of grain boundary or metallic compound, (b) Metal barrier, (c) Micro-junction, (d) Point Contact Junction. ϕ_1 and ϕ_2 are the wave-functions describing the different phases of the two superconductors, which do not differ in superconductive state.

However, the junction under discussion in the light of the SQUID is the insulating tunnel junction. This insulation can be a grain boundary². The gap between the two superconductors in the junction ranges from a distance of 10 Å to 50 Å. This configuration ensures lower energy ground state, which results in superconductivity. ϕ_1 and ϕ_2 in Figure 2a represent the respective phases on either side of the barrier. Below the critical temperature T_C , the temperature at which electrons enter a superconducting state, the resistance becomes zero and electrons flow with infinite conductivity. The maximum current which is allowed to flow without any resistance is known as the critical current I_C . Above the critical current, the junction becomes resistive.

The magnitude of the current through the tunnel depends on the phase difference between the junctions,

$$I = I_C \sin \Delta\phi, \quad (1)$$

²Grain boundary is a boundary between crystalline groups which inhibit electrical conductivity [12]

where I is the current through the junction, and $\Delta\phi$ is the difference between the two phases on either side of the junction. Since the two phases are coupled in the superconducting state, the difference in their time-dependent phases becomes zero,

$$\frac{d}{dt}\Delta\phi = 0,$$

making the current through the junction constant,

$$I = I_C.$$

This is known as the DC Josephson effect.

Looking through Josephson's second equation,

$$\frac{d}{dt}\Delta\phi = \frac{2e}{\hbar}V, \quad (2)$$

substituting equation 2 in equation 1 by taking the integral of equation 2, we get,

$$I = I_C \sin \left[\phi(0) - \left(\frac{4\pi e V t}{h} \right) \right], \quad (3)$$

where $\phi(0)$ is the superconducting phase at time $t = 0$. This tells us that with a fixed value of V , the I through the Josephson junction oscillates with the frequency,

$$f = \frac{2eV}{h}. \quad (4)$$

This oscillation of current at a fixed biased voltage is known as the AC Josephson effect.

1.2 Operation of the SQUID

The SQUID is a device which takes the advantage of quantum mechanical effects to act as a detector. It operates with a framework of coils in its chip. Thus, it is important to look at the design of the Josephson junctions.

1.2.1 Framework of Josephson Junctions—The Meissner Effect

The SQUID comprises of a loop with usually two Josephson Junctions, parallel to one another. Either of the junctions is equipped with capacitors and resistors as shown in Figure 3. The shunt resistances across the junctions facilitate controlled flow of current. There are two coils located outside the loop, which are responsible for application of magnetic flux on the SQUID when current passes through them (see Figure 3). I_{bias} is the applied current to the circuit, which divides into half when passing through each side of the loop. If $I_{bias} < I_C$, then the voltage V and the magnetic flux produced by it remain zero.

Once the current is raised above I_C , potential drop takes place across the junction. The quantum state of the system prefers to remain unchanged. Thus, in opposition to the magnetic field produced by the development of potential drop, an induced current known as the *screening*

current (I_S) is generated, which flows in a direction which favours the production of magnetic field needed to cancel out the initially generated flux (See Figure 3). This expulsion of the magnetic field is known as the Meissner effect.

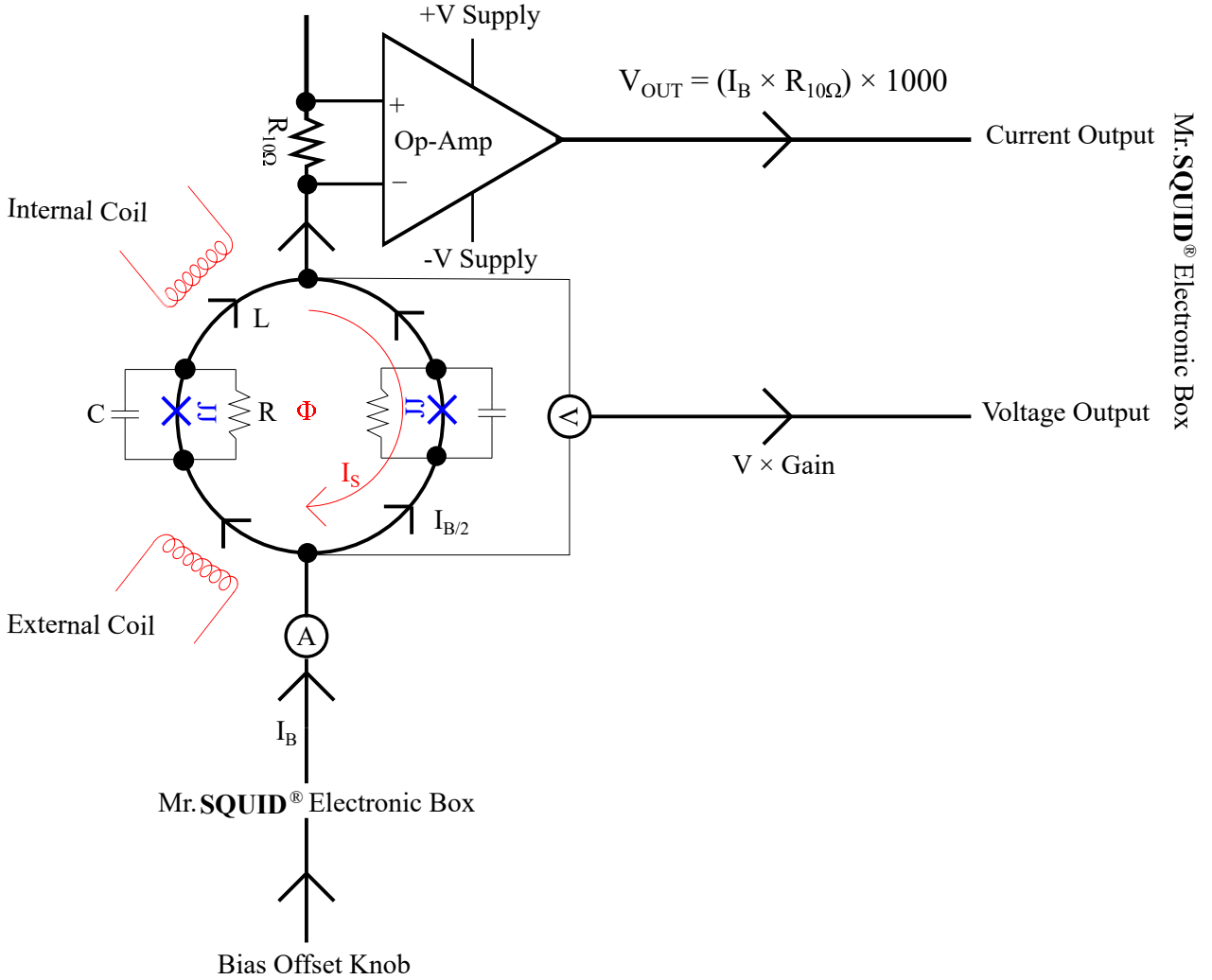


Figure 3: SQUID loop showing the two parallel Josephson Junctions (JJ), with capacitors (C), and resistors (R) across them. I_B is the biased current which divides into half ($I_{B/2}$) in either of the junctions. Internal and external modulation coils apply magnetic flux (ϕ), inducing the screening current (I_S). The self inductance of the loop (L) also contributes to the total flux (ϕ). An ammeter (A) in series and voltmeter (V) in parallel monitor the biased current and the voltage across a junction respectively. The output current is read as voltage across a resistor (R_{100}), which has been amplified by an operational amplifier (Op-Amp) by a factor of 1000.

Increasing the flux, increases the screening current in the loop, until half fluxon is reached. At this point, the screening current can not increase further, as it would increase the net current in the superconducting loop greater than the I_C , which would pull the system to a normal state. The energy state of the quantum system does not allow this, as expelling $\phi_o/2$ of flux is more energy consuming than keeping that flux in, and working to expel the extra flux following with the increase of magnetic field strength being applied. Consequently, the

screening current begins to decrease until it becomes zero. In order to remove the successive flux, it increases again, but in the opposite direction (See Figure 4a.).

Throughout this operation, the current through the SQUID remains constant, while the voltage varies with the applied flux periodically.

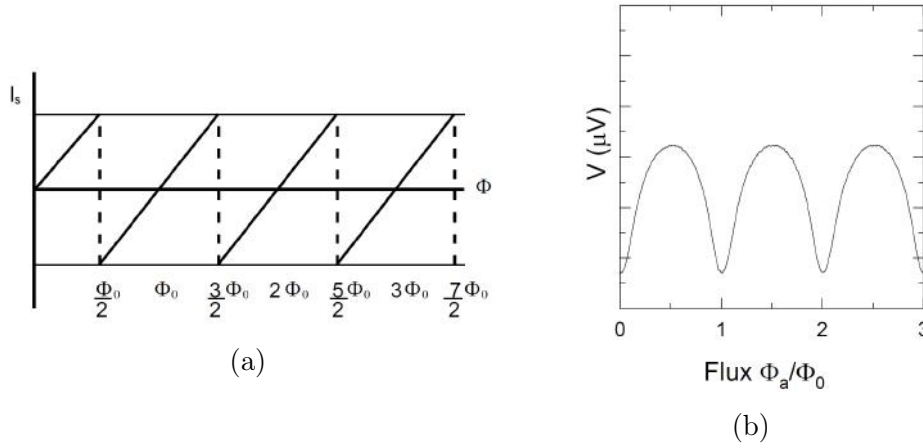


Figure 4: Behaviour of the current and voltage in the presence of magnetic field can be observed through these graphs. (a) Shows the rise and fall of screening current through the loop and resultant quantization of flux. (b) Shows the variation of voltage with applied magnetic flux at a constant biased current.

1.2.2 Quantum Interference

The passage of Cooper pairs through the gap, is analogous to the passage of coherent light waves through the double slits of Young's optical interference experiment. The wave-functions of the two light beams interfere on the screen, with periodic regions of high intensity light, and low intensity light. Likewise, when the wave-function of two superconductors interferes with current flow, the maxima and minima of the screening current depicts the interference pattern.

2 Apparatus and Functioning of the SQUID

In our experiments, we are using Mr.SQUID[®] device to study applications of the Josephson effect. The SQUID probe is equipped with an integrated circuit on which the Josephson junctions are embedded. For the High Temperature SQUID (HTS), Yttrium barium copper oxide (YBa₂Cu₃O₇) film is used to make the SQUID chip.

2.1 Probe

The chip of HTS is located on a probe, available with a DB-9 M/M connection at one end.



Figure 5: Mr.SQUID[®] probe.

2.2 Functionality of Mr.SQUID[®] electronic box

The current and voltages through the SQUID can be controlled using a control box which has various functions.



(a)



(b)

Figure 6: (a) Electronic box front view showing control knobs. (b) Back view displaying the connection pots.

Bias Offset Knob: Supplies DC current through the SQUID. Rotating the knob in either direction would trace out the current value at respective setting.

Sweep Output Knob: Supplies current through the SQUID back and forth about the DC offset value, which automates the manual function performed by the bias offset knob. Tuning

this knob clockwise traces out the Voltage–Current graph in the $V-I$ (see Figure 6a) mode. Whereas, in the $V-\phi$ mode, it applies oscillating magnetic field on the SQUID by passing current through the internal modulation coil.

Flux Bias Control Knob: In the $V-I$ mode, this knob applies magnetic field across the SQUID, by passing current through the internal modulation coil. Since the field is static, turning the knob periodically in either directions would trace out a curve in the $V-I$ mode. On the other hand, in the $V-\phi$ mode, it applies static magnetic field, which moves the $V-\phi$ curve right or left.

The following table summarizes the control knobs' functions in either mode:

<i>Control/Output</i>	<i>V-I Mode</i>	<i>V-Φ Mode</i>
<i>Sweep Output</i>	Sends current back and forth about a fixed DC value, through the SQUID loop. Sets the amplitude of the wave test signal.	Sends current through the internal modulation coil, producing oscillating magnetic field. Sets the amplitude of the wave test signal.
<i>Bias Offset</i>	Sets a DC value for the current in the SQUID loop.	Sets a DC value for the current in the SQUID loop.
<i>Flux Offset</i>	Sends DC current through the internal modulation coil, which generates flux applied to the SQUID loop.	Sets a DC value for the current in the internal modulation coil. This sets the static value for the applied magnetic flux.
<i>Current Output on Mr. SQUID[®] electronic box</i>	Total current through the SQUID loop.	Current through the internal modulation coil.
<i>Voltage Output</i>	Voltage across SQUID loop.	Voltage across SQUID loop.

Figure 7: Controls and outputs of Mr.SQUID[®] electronic box.

3 Experiments Performed using the SQUID

This section provides the details and outcomes of the experiments performed by availing the superconducting properties of the JJ junctions.

3.1 Calculating Resistance of the SQUID at room temperature

To conduct the experiment, SQUID probe is connected to the control box with a DB-9 M/M connector, to measure the resistance of the SQUID at room temperature (24 °C), from the slope of the $V-I$ curve.

The oscilloscope settings are configured to produce a linear $V-I$ curve, whose slope is determined to find the value of resistance. Refer to appendix (4) for the detailed procedure. The calculated resistance is 50 Ω (See Figure 8a).

3.2 Observing the DC Josephson Effect

In this section, we observe the superconducting state of Josephson Junctions by placing the SQUID probe in liquid nitrogen ($-196\text{ }^{\circ}\text{C}$), in an insulated dewar. After the phase transition, the critical current of the SQUID and its normal state resistance is calculated.

The apparatus is set with the probe connected to the electronic box and placed in liquid nitrogen. The opening of the dewar is blocked with a stuffed foam cover to inhibit the rapid evaporation of liquid nitrogen. The gradient of the V - I graph falls rapidly until the resistance becomes zero during the cooling of the SQUID³. Once adjustments are made on the scope, with both channels DC coupled, a graph showing the superconducting state of the SQUID is obtained (See Figure 8b). The horizontal line represents the current in the SQUID which flows without voltage (vertical shift zero). Once the horizontal line picks up gradient, it indicates the transition to normal state as a potential drop develops in the SQUID. The critical current is shown at the "knee" (Figure 8b). This critical current is maximized, by tuning the flux offset knob. The curve may have a vertical offset, which is characterized by horizontal region

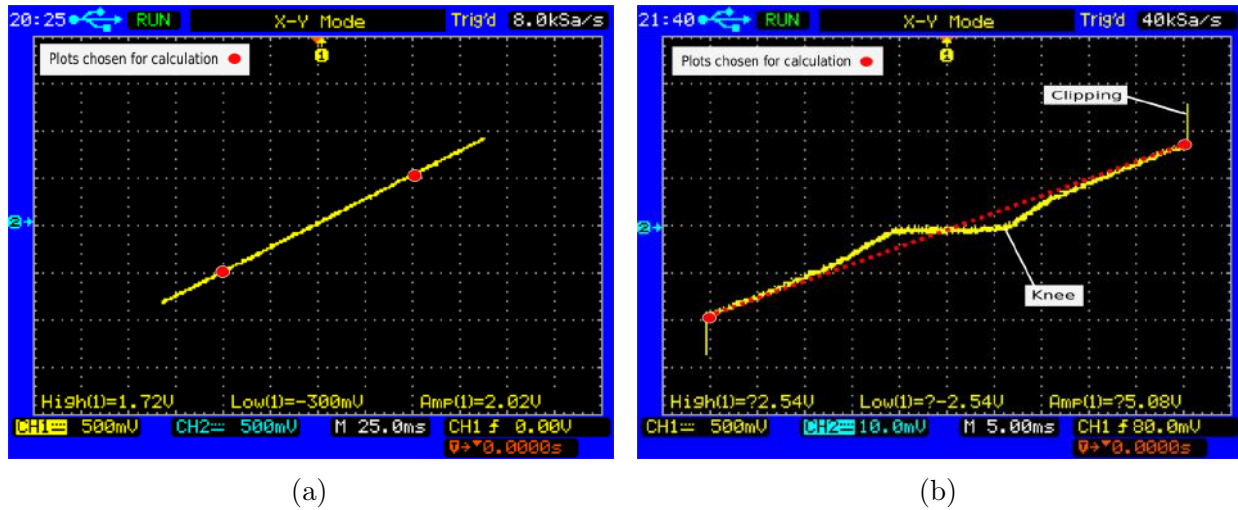


Figure 8: Drop of resistance to zero with drop in temperature. (a) Shows the V - I trace at room temperature in contrast to (b)'s curve showing a region of resistance-less current at 77 K. Horizontal line is the current which passes without a potential difference. The point on the "knee" shown, is the critical current above which normal state begins. The $R_N/2$ can be calculated by the slope of dotted red line shown.

not crossing the origin. This offset can be removed by adjusting the amplifier offset pot on the amplifier board inside the Mr.SQUID® electronic box (Figure 9)[15]. Once the suggested adjustments are made, the horizontal part of the curve can be read along Channel 1, till before the knee from the origin (either right or left). This represents the $2I_C$, as the SQUID has two parallel junctions and I_C is across a single junction, in a certain direction. As a result, the calculated I_C is $30\text{ }\mu\text{A}$.

The SQUID becomes resistive as soon as the current is raised above I_C . This normal state resistance is calculated by determining the slope joining the maximum points on either side

³The level of liquid nitrogen in the dewar must be enough that the probe is completely covered. This makes sure that the temperature of the SQUID remains constant and it remains in the superconducting phase.

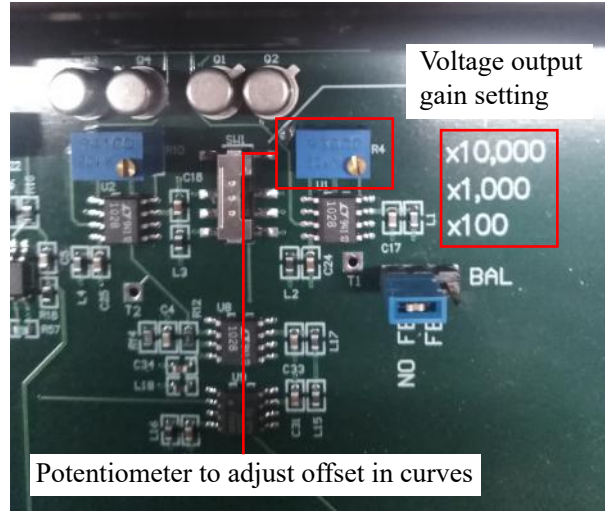


Figure 9: Offset adjustment can be made by changing the resistance of the potentiometer pointed in the figure. The gain factors in the box in the top right corner are the amplification factors for the voltage output (also see Figure 3).

of the curve as shown in Figure 8b. This is the resistance of one junction of the **SQUID**, and since the two junctions are parallel to one another, the resultant value for resistance will be twice the calculated slope. Taking in account the parameters, the calculated normal state resistance of the **SQUID** becomes $R_N \approx 1.44 \, \Omega$, with voltage gain factor of 100.

Thus, it can be concluded, that the current which flows through the **SQUID** below the critical temperature can remain without a potential difference till a certain current value (i.e. I_C), above which resistance and voltage appear. This is responsible for the characteristic shape of $V-I$ curve.

3.3 Observing the AC Josephson Effect

In experiment 3.2, we had observed the DC Josephson effect, in which the direct current crossed the insulating barrier, in the absence of magnetic flux and voltage. Here, we observe the effect of an applied AC voltage across the **SQUID** junctions, and the response of superconducting current to the constant voltage. A microwave source is used to cause the production of oscillating voltage.

The principle behind the AC Josephson effect was explained in section 1.1.3, where we saw that the current through **SQUID** oscillates according to the equation,

$$f = \frac{2eV}{h}.$$

This means that for applied voltage of $1 \, \mu\text{V}$, the current oscillates at $4.84 \times 10^8 \, \text{Hz}$.

To observe this phenomenon, we first set a frequency generator of range 2-4 GHz, with reference frequency of 12.8 MHz, which could be analyzed on a spectrum analyzer. The decibel to power ratio is set to 10 dBm which makes the DC voltage as approximately 2 V. The microwave generator is turned off and an N-BNC female cable with wires open at one

end is used as a wave transmitter. The central wire of the open end is used as an antenna by exposing 2-3 cm of its length, out of the coaxial cable.

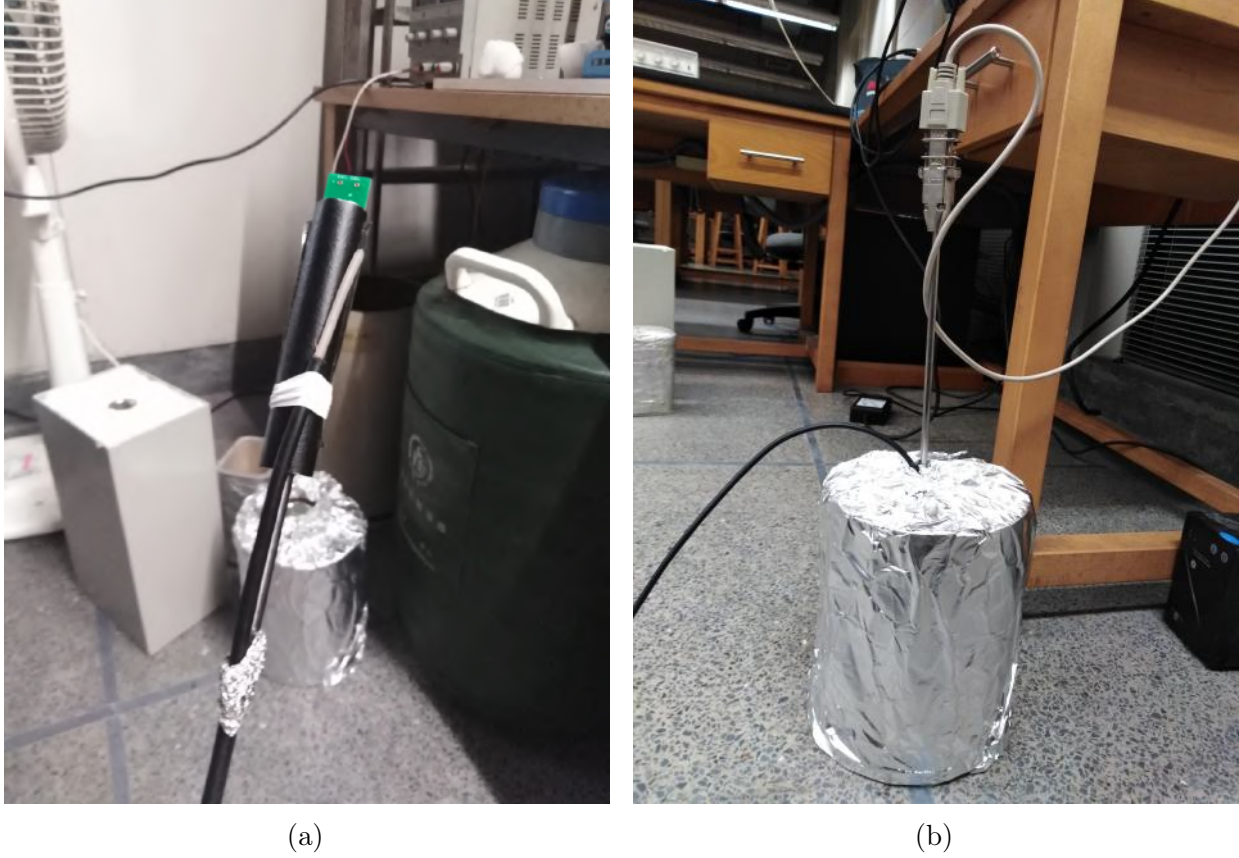


Figure 10: (a) Probe and the antenna from the microwave generator tied together to apply DC voltage when in superconducting state. (b) A non-metallic dewar covered in aluminum foil is used for this experiment, to prevent the internal reflections of the high frequency waves inside its walls.

The **SQUID** is then cooled to superconducting state to get a $V-I$ curve (Figure 11a). Then, a signal of the lowest frequency is sent through the antenna to the probe inside the dewar. The amplitude is gradually increased from the oscillator control box. Increasing the amplitude of the signal slowly decreases the critical current in the junction. This results in the ultimate diminishing of the I_C , until a slope appears. Once this happens, the amplitude of the voltage source is decreased back, until $1/2$ to $1/3$ of the original I_C is returned. At this set amplitude, the frequency of the wave signal is increased by 100 MHz at each step, until curves or steps on the $V-I$ curve start appearing. Figure 11 demonstrates the effect described.

The steps formed are known as the microwave induced Shapiro steps⁴. At each step the voltage remains constant but the current oscillates between two fixed values .

⁴Using a higher band voltage source can result in clearer and wider Shapiro steps.

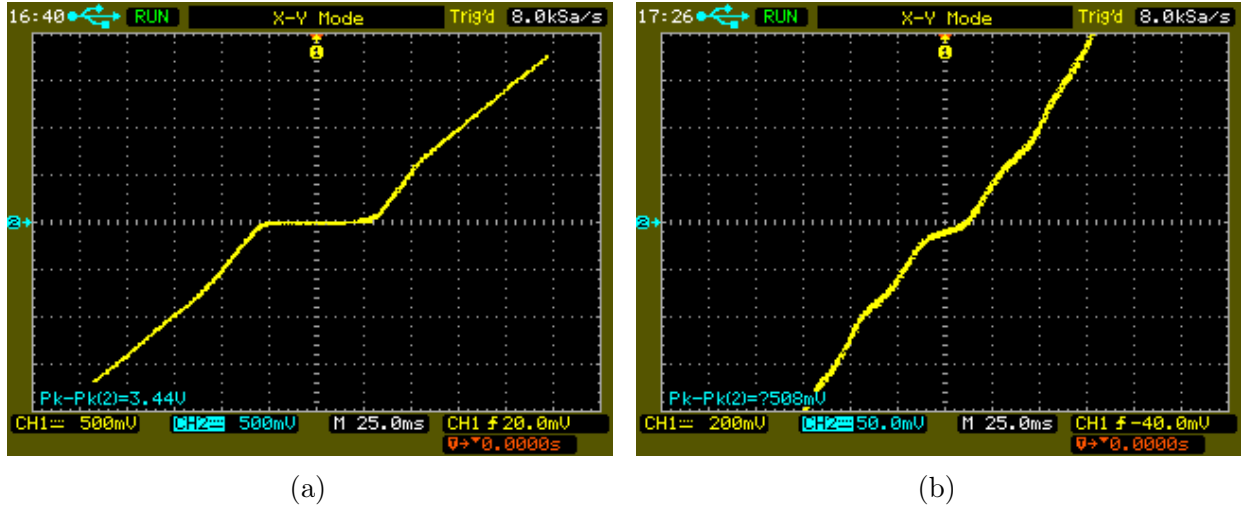


Figure 11: (a) $V-I$ Curve with critical current region covering two big divisions. (b) Curve with Shapiro steps and suppressed critical current.

3.4 Observing the Voltage response across the SQUID in applied Magnetic Field

In this observation, we observe the periodic variation of voltage when the SQUID loop is biased with a fixed current ($I_B > I_C$) and flux is generated by the internal modulation coil. In this analysis, the $V-\phi$ mode is used (refer to table in Figure 7).

Firstly, the $V-I$ graph is adjusted using the flux offset to get the critical current at its maximum, by tweaking the flux offset knob. This minuscule change in flux, generates screening currents in the SQUID loop, which add to the total current in the loop. Then, the position of the knee on the curve is noted and the sweep output knob is turned completely anticlockwise until a point appears on the origin of the scope's axes. Using the bias offset knob, the current through the SQUID is biased at a value slightly greater than the critical current (at the knee of the curve), setting a constant DC supply through the SQUID.

The flux offset is turned periodically clockwise and anti-clockwise. This knob passes current through the internal modulation coil which applies flux on the SQUID loop. Voltage is then induced in the loop which makes the point on the scope oscillate up and down. This oscillation traces out the periodic rise and fall of the voltage in the chip as the quantum system generates screening currents in reaction.

The manually modified flux in the latter step, can be observed by switching to the $V-\phi$ mode. In this mode, the horizontal axis represents the current linearly related to flux (ϕ_o), while the vertical axis yields the voltage. Channel 2 on the oscilloscope is AC coupled to observe the changing voltage levels⁵. Turning the sweep output clockwise, traces out a sinusoidal curve, due to the magnetic field applied through the internal modulation coil. This was also shown in Figure 4b.

From our curve, we can now calculate the modulation depth, ΔV , which is the peak-peak

⁵Channel 1 must remain in DC coupling mode.

voltage of the graph, or twice the amplitude of the curve⁶. The ΔV for our graph is $6.2 \mu\text{V}$, with voltage gain setting at 10,000 (Figure 12c).

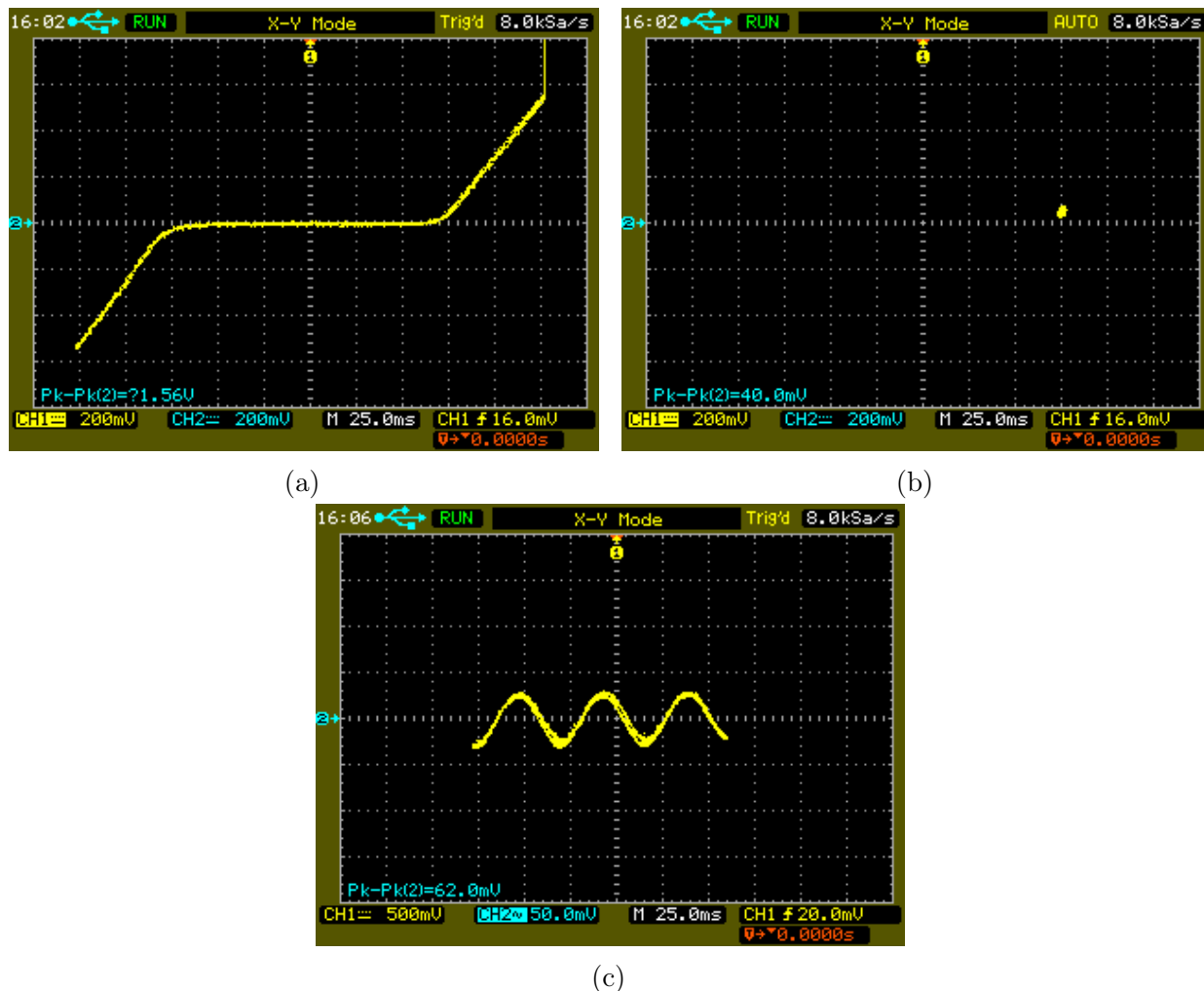


Figure 12: Steps followed to produce a $V-\phi$ curve. (a) Critical current adjusted to maximum with the flux offset knob. The sensitivity of the horizontal axis was increased improve the visibility. (b) Shows current biased slightly above the critical current, on the knee of the $V-I$ curve, (c) $V-\phi$ curve with modulation depth of $6.2 \mu\text{V}$.

3.5 Additional Parameters of the SQUID coils

We already calculated the values of I_C , R_N and ΔV of the SQUID. Now, we can use this data to calculate other meaningful parameters for our SQUID.

⁶In order to produce a clear $V-\phi$ curve, Channel 2's digital filter can be turned on (digital oscilloscope), or averaging could be done. See Figure 28b in section 4.

3.5.1 Modulation Depth

Modulation depth is the characteristic voltage of the **SQUID**. This voltage defines the maximum voltage which can be achieved by the **SQUID** when one quantum of magnetic flux is applied on it. It is calculated as following:

$$\begin{aligned} V &= I_C R_N \\ &= (30 \mu A)(1.12 \Omega) \\ &= 33.6 \mu V \end{aligned}$$

3.5.2 McCumber Parameter

"McCumber" or modulation parameter (β_L , where L denotes the total inductance of **SQUID**) is the factor that determines the extent to which magnetic fields can be shielded by the currents in the **SQUID**. It also defines the flux to voltage transfer ratio of the **SQUID**. There are two ways of calculating the β_L :

$$\beta_L = \frac{4I_C R_N}{\pi \Delta V} - 1 \quad (5)$$

$$= \frac{2I_C L}{\phi_o} \quad (6)$$

Using equation 5, the calculated value obtained is $\beta_L \approx 4.35$, while the equation 6 gives the result of $\beta_L \approx 2.12$ ($\beta_L \approx 1$ being the desirable value). This stark difference is the consequence of the thermal effects which no longer keep the thermal energies minuscule enough to make them comparable with the energy of a fluxon (ϕ_o/L). In addition, these thermal interruptions occur due to the relatively high critical temperature of of the **SQUID** used ($T_C \approx -183.15^\circ \text{C}$).

3.5.3 Mutual Inductance

The mutual inductance (M) of the **SQUID**, is the value that describes the current to flux relation. Inductance is the induction of voltage in a current carrying material, due to the development of magnetic flux with the changing current. Thus, it is a requisite to have this factor calculated. The **SQUID** loop's inductance is 100 pH, and the internal modulation coil has 35 pH. With our taken measurements in experiments 3.4 and 3.2, the mutual inductance of the external modulation coil can be calculated. M_{int} can be expressed as:

$$M = \frac{\phi_o}{\Delta I}$$

Thus, the our mutual inductance attained becomes 37.6 pH.

3.6 Relation between Temperature and Resistance of the SQUID

We had seen in experiment 3.2 that the resistance of the SQUID falls with decreasing temperature drastically. In this experiment, we study the rate with which the resistance of the SQUID drops with decreasing temperature. To execute the goal of this experiment, 1N4001–MIC Germanium diode is used as a temperature sensor. For this, it is necessary to find the relation between the voltage of the diode and the temperature. We did not use the thermocouple directly to measure the variance of resistance of the SQUID, as the thermocouple's range and reaction to the temperatures we are concerned with, are unsuitable. Thus, voltage calibration with temperature is done.

To begin with, the diode is connected with a resistor in series using the copper wires. This circuit is completed using BNC–Crocodile cable to connect the current source to the diode's wires. A thermocouple's connections are made with a separate multi-meter, and the temperature measurement mode is switched to °C. The thermocouple is bound with the diode using Teflon tape. This close positioning makes sure that the thermocouple and the diode are at the same temperature. The reading of diode's voltage at room temperature (20 °C) is then taken ⁷.

A heat gun is used to raise the temperature of the diode to take the corresponding voltage values for the potential difference across the diode. The temperature is raised till approximately 200 °C. This heat and trial method is done in order to test the proper voltage response of the diode to changing temperature⁸.

The diode attached with the thermocouple, is held above the opening of the dewar containing liquid nitrogen, and is very slowly lowered to take values for the voltage with decreasing temperature, until it is completely immersed in liquid nitrogen. The collected data is then used to plot a relation between the temperature and voltage of the diode (see appendix 4).

The diode is brought back to room temperature and fastened with Teflon tape behind the SQUID probe as shown in Figure 33 in appendix 4. Care must be taken that the tape is not made to cover the chip directly to prevent hindrance with its temperature response. The probe is covered with its mu-metal shield again and placed at the mouth of the opening of the dewar to lower it very slowly inside to make its temperature drop gradually; while taking the measurements of the resistances of the SQUID from the oscilloscope with changing temperature.

The voltages noted earlier for corresponding values of resistances of the SQUID, are used to find the equivalent temperatures from the graph shown in Figure 34. Consequently, the temperature values for the resistances can be acquired to study the variation (see graph 13).

⁷The temperature reading is confirmed using both the thermocouple and the temperature sensor of the lab.

⁸The readings are taken once both the temperature and the voltage values on the multi-meters become stable to decrease the extent of inaccuracy in the final results.

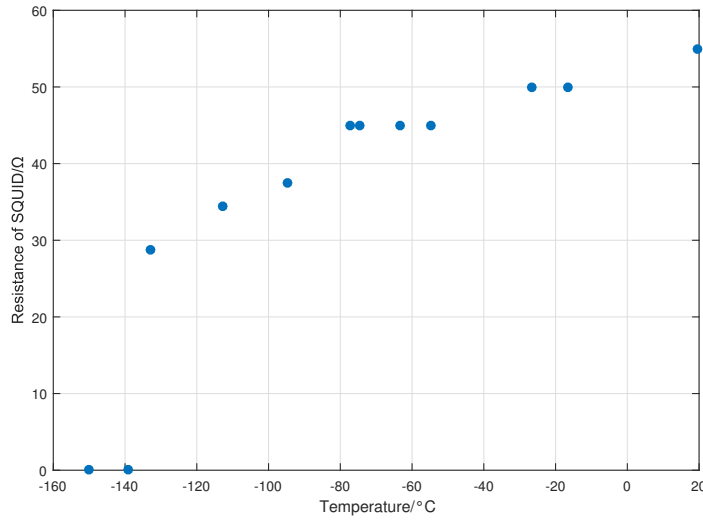


Figure 13: The graph shows that the resistance of the **SQUID** decreases at a slower rate initially until it reaches the T_C , at which it suddenly drops to zero (transition to superconducting state). The critical temperature is shown as -139°C . This is due to the limit of the type of thermocouple used which did not register temperature below -139°C , its saturation point, during the calibration of the diode. The temperature inside the dewar's environment drops at such a rate that the diode is unable to respond to the swift shift.

3.7 Analog Flux Locked Loop Circuit as a Flux Detector

In experiment 3.4, we applied magnetic flux using the internal modulation coil and studied the voltage response of **SQUID** loop. Now, we will see how the net magnetic field can be controlled with the feedback external coil. An analog flux locked loop circuit is used to lock magnetic flux in the **SQUID** loop by canceling out the effect of any magnetic flux applied to the **SQUID** coil by the internal modulation coil. It operates by taking input from the voltage output of the Mr.**SQUID**® electronic box. This voltage is the result of applied magnetic flux on the **SQUID**. The circuit amplifies and inverts this voltage, and the corresponding output current is led to the external coil, which generates feedback flux to cancel the applied flux.

The **FLL** circuit being used amplifies the input voltage by a factor of -10^9 . This means that the output of the Flux Locked Loop circuit would be ten times amplified but in opposite direction of the input signal. Figure 16a shows the **FLL** circuit's amplitude gain test in which a function generator is used to give input to the circuit, which is to be amplified and inverted. The peak-peak voltage of the input signal is seen as 1 V, whereas the amplified signal is 10 V.

To cater the amplification, the **FLL** circuit is given voltage by two 9 V transistor batteries. Test point one (TP1) on the circuit is the point at which the original voltage output from the electronic box can be observed on the oscilloscope. Whereas, test point two (TP2) displays the output of the **FLL** circuit. The amplifiers shown in Figure 14 carry out the process of amplifying the voltage to the desired value.

⁹Any other amplification factor could also be used depending on need.

This output voltage from the FLL is then fed into the external modulation coil. The corresponding current that passes produces magnetic flux which cancels the flux of internal modulation coil. Any further increase in applied flux is countered by the FLL to hold the SQUID in a flux "locked" condition.

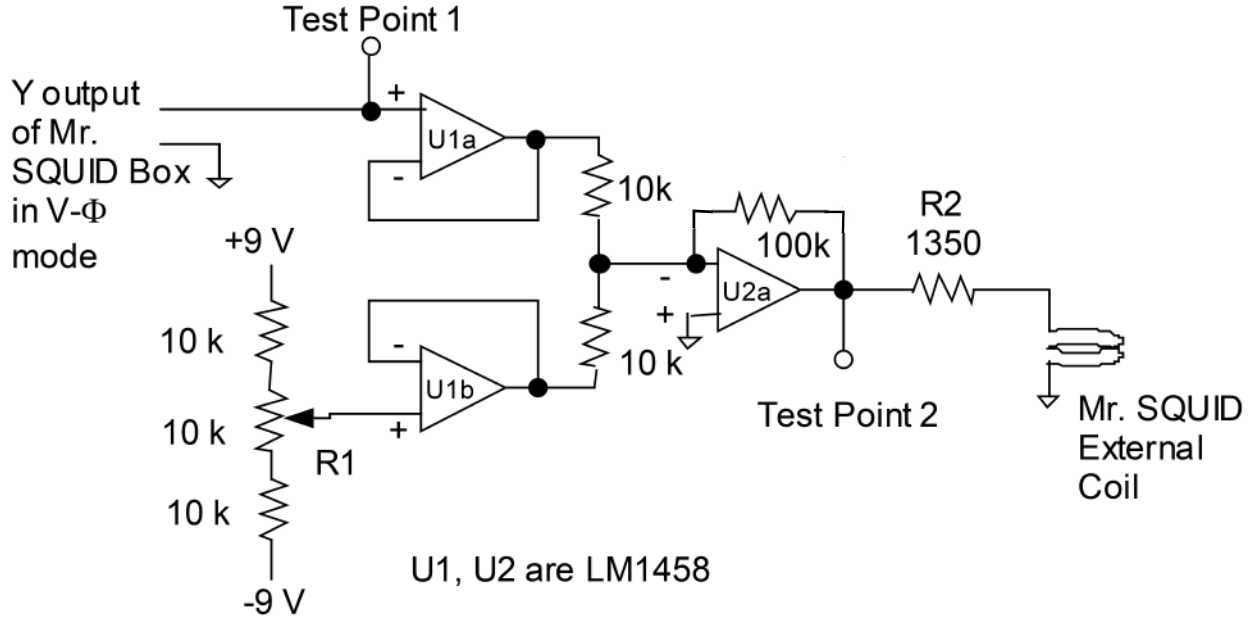


Figure 14: Circuit diagram for analog FLL showing a buffer amplifier, U1a, which isolates the input voltage from the electronic box. U1b isolates the +9 V and -9 V voltage supply. U2a is the gain amplifier which amplifies the voltage output of U1 by a factor of -10. R1 is a potentiometer and R2 a resistor of 1350 Ω resistance. Test points 1 and 2 can be tested to show input and output voltages of the circuit respectively.[13]

To begin with the experiment, the (FLL) circuit, is prepared on a soldered breadboard, whose schematic diagram is shown in Figure 14. Two copper wires are connected to the external coil's terminals on the probe, to take the coil's resistance in liquid nitrogen once the experiment has begun (Figure 15a). The measured value is 48.4 Ω .

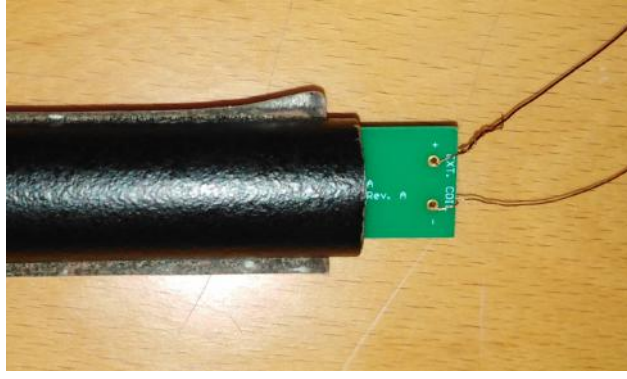
The SQUID probe is cooled after connecting it to the DB-9 connection at the back of the electronic box, with flux offset and bias offset knobs in the 12' o clock positions, while the sweep output completely counter clockwise. Nearby electronic devices are turned off to prevent RF interference. It is preferable to conduct this experiment in an isolated area where electromagnetic waves do not interfere with the signals detected by the SQUID¹⁰.

Since external coil is being used, a switch inside the Mr.SQUID® electronic box in "BUF" (buffered) position is turned to "DIR" (direct) position, to allow the direct connection between the external coil and a 100 mA fuse at position "F1". This is necessary as the current flowing to the external coil is directly controlled by the user, and can reach critical values which may cause the coil to melt (see Figure 15b).

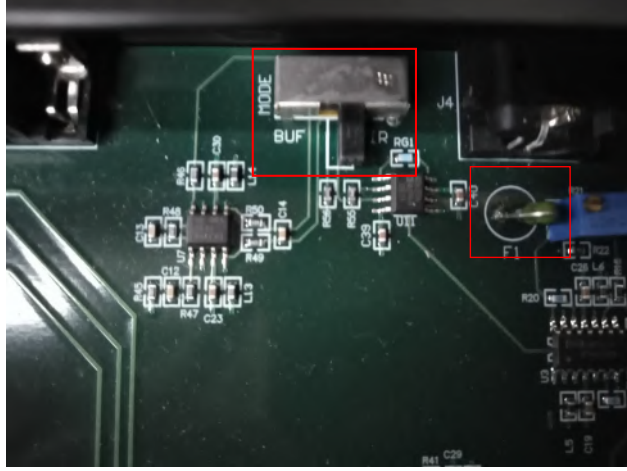
A $V-\phi$ curve is obtained as described in Section 3.4¹¹. The current is biased at $I_B = 32 \mu\text{A}$,

¹⁰Refer to section 4 for details about receiving clean and clear signals.

¹¹Gain factor of voltage output of Mr.SQUID® should be set at the default of $\times 10,000$ to produce clear



(a)



(b)

Figure 15: Prerequisites for the analog flux locked loop experiment. (a) Copper wires connected to terminals of the external coil, to take its resistance at 77 K. (b) Switch inside the electronic box switched to DIR position which creates a direct connection to the external coil through a 10 mA fuse. The BUF position creates a connection through a buffer amplifier with output ratio of $100 \mu\text{A}/\text{V}$.

when the $I_C = 25 \mu\text{A}$. The flux threading the loop by this current in the loop will be:

$$\begin{aligned}\phi_{SQ} &= M_{SQ} \times I_B, \\ &= 73 \text{ pH} \times 32 \mu\text{A}, \\ &\approx 2.34 \times 10^{-15} \text{ Wb}.\end{aligned}$$

The graph is adjusted by centering the curve symmetrically about the origin, in a single waveform, using the flux offset knob (setting the DC level of the flux) and the sweep output knob (setting the oscillating level of the flux) (16b). The horizontal axis in Figure 16b is used to calculate the current flowing through the internal modulation coil as $I_{int} = 45 \mu\text{A}$. Since the curve represents only one sine wave (one fluxon Φ_0), the cancellation needs $45 \mu\text{A}/\Phi_0$. With the mutual inductance of the internal modulation coil of 37.6 pH as calculated in 3.5,

$V-\phi$ curves.

the magnetic flux applied by the internal coil is¹²:

$$\begin{aligned}\phi_{int} &= M_{int} \times I_{int}, \\ &= 37.6 \text{ pH} \times 45 \text{ } \mu\text{A}, \\ &\approx 1.69 \times 10^{-15} \text{ Wb}.\end{aligned}$$

The voltage output of the electronic box is connected to the input of the FLL circuit. Testing probe is then used to observe the voltage changes on the oscilloscope, from test points 1 and 2. Since the output on TP1 is simply the **SQUID** voltage output, it remains same as before. TP2 signal is received as shown in Figure 16c. This amplified curve may also have a DC offset (can be observed by switching the Channel 2 to DC mode), which can be removed by adjusting the resistance of the potentiometer in the FLL circuit (see Figure 14). Once the offset is removed, the amplitude of the curve on either side of the vertical axis becomes equal.

So far, the external coil has remained disconnected from the FLL circuit. The voltage supply to the FLL is disconnected and the external coil's connection is made with the output of the FLL circuit using BNC–Crocodile cables. Test Point 1 at this point gives the regular V – ϕ curve as observed earlier (Figure 16b). This assures that the **SQUID** is still in a superconducting state with no flux trapping upon connection with the external coil.

In order to cancel the applied flux, the voltage source is reconnected to send current to the external coil. Consequently, the output from Test Point 1 (showing voltage output of the **SQUID**) would ideally show a horizontal straight line, as the voltage drop in the **SQUID** falls to zero (refer to Figure 16d). This line may however, not exactly be horizontal, owing to the incomplete cancellation of flux. When a fraction of the applied flux is left uncanceled, some voltage is still induced across the **SQUID** junctions due to the remnant flux. This would appear as a straight line with little slope (showing the rise in the vertical axis–voltage). TP2 signal shows the voltage given to the external coil (Figure 16e).

The current going to the external coil at the output of the FLL circuit is measured as $I_{ext} = 104 \text{ } \mu\text{A}$, which along with the coil's mutual inductance of 35 pH, gives the feedback flux as,

$$\begin{aligned}\phi_{ext} &= M_{ext} \times I_{ext}, \\ &= 35 \text{ pH} \times 104 \text{ } \mu\text{A}, \\ &\approx 3.64 \times 10^{-15} \text{ Wb}.\end{aligned}$$

The net flux held constant in the **SQUID** is,

$$\begin{aligned}\phi_{net} &= \phi_{SQ} + \phi_{int} - \phi_{ext}, \\ &= \phi_{total} - \phi_{ext}, \\ &= 2.336 \times 10^{-15} \text{ Wb} + 1.692 \times 10^{-15} \text{ Wb} - 3.64 \times 10^{-15} \text{ Wb}, \\ &= 4.028 \times 10^{-15} \text{ Wb} - 3.64 \times 10^{-15} \text{ Wb}, \\ &\approx 0.38 \times 10^{-15} \text{ Wb}.\end{aligned}$$

¹²The applied flux is not exactly equal to the value of a fluxon, as not all of the flux remains within the loop and may be lost to the surrounding region.

By studying the graphs in Figure 16, it can be concluded that the application of the feedback flux results in the linearization of the relation of voltage and magnetic flux. Increasing the applied flux any more would result in the increase in the potential difference across the SQUID loop.

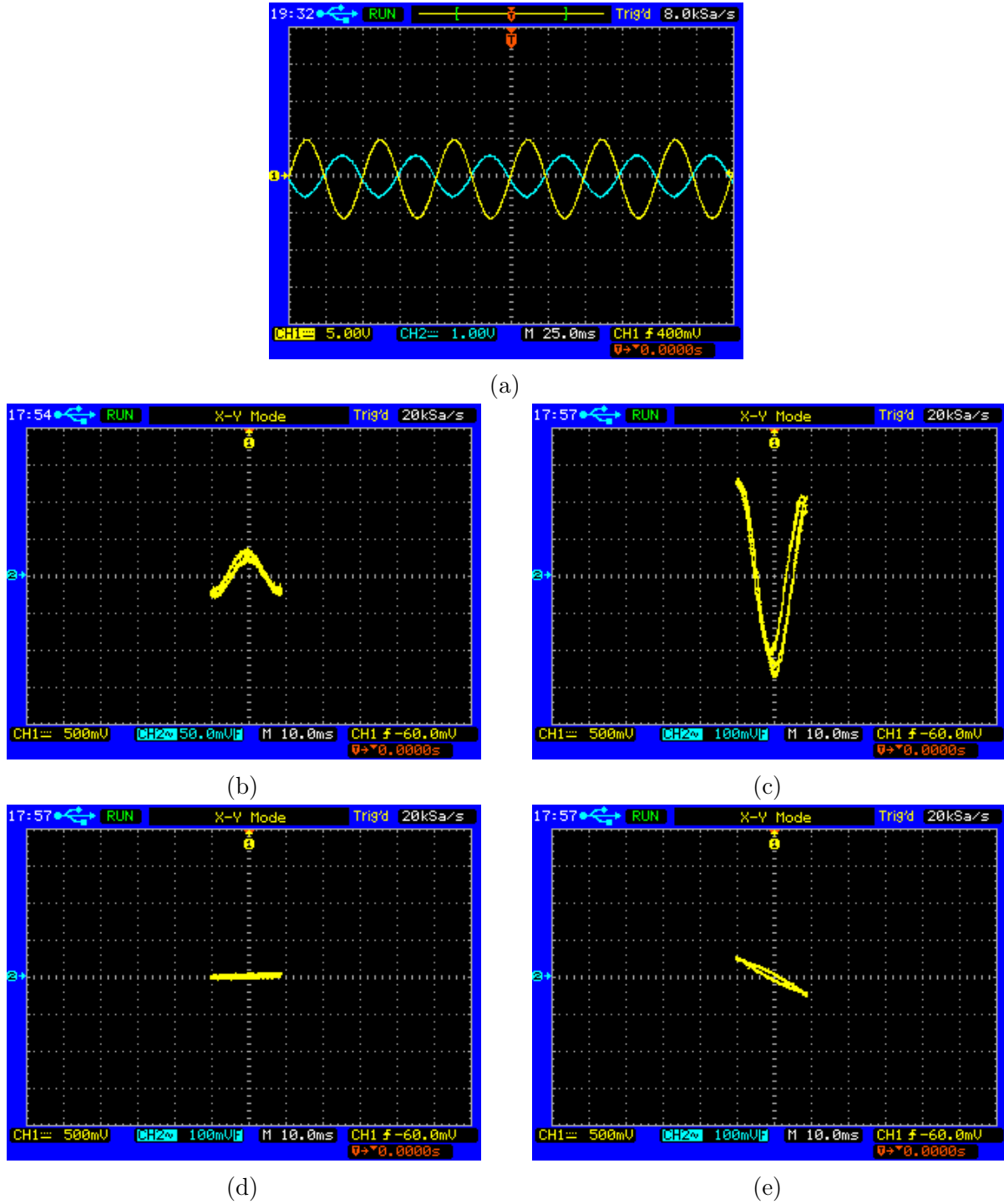
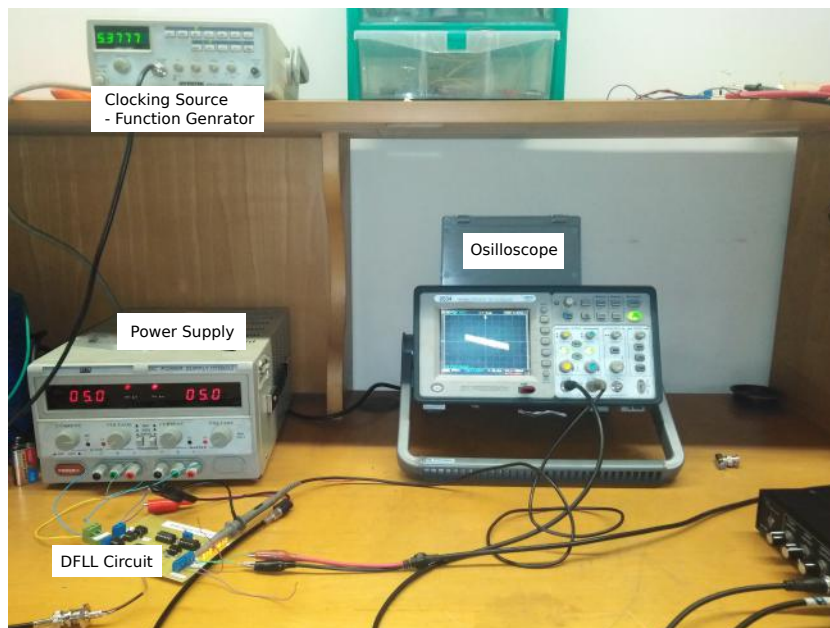


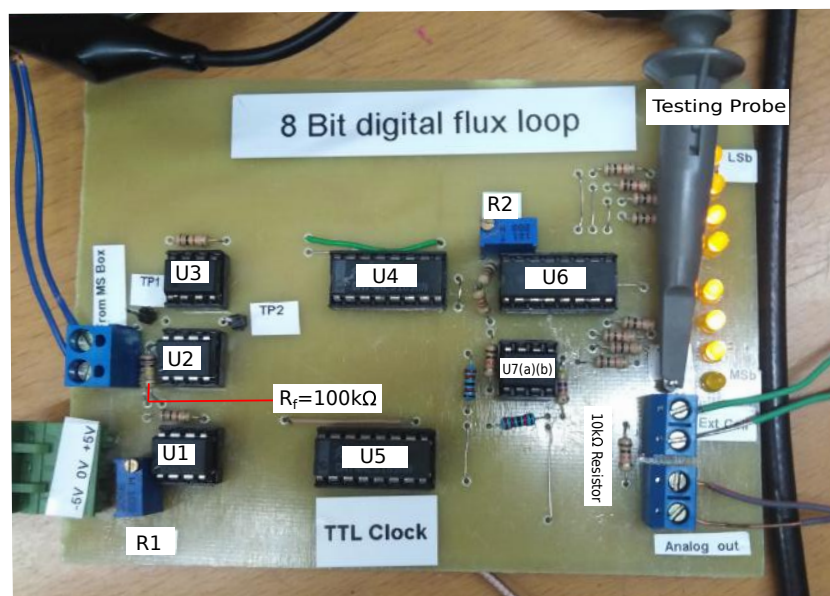
Figure 16: (a) Amplitude test with input signal from SQUID (blue—channel 2) and function generator's signal (yellow—channel 1). The peak to peak voltage of the input signal is seen as 1 V, whereas the amplified signal is 10 V.

3.8 Digital Flux Locked Loop

In this experiment we will perform the same task of flux cancellation using a FLL, as done in Section 3.7, but by using digital signals. This time, we will cancel the internal coil's flux by feeding the external coil with current through a circuit operated by binary operators using counters, amplifiers and comparators.



(a)



(b)

Figure 17: Digital Flux Locked Loop Experiment:(a) Experimental Setup(b) Circuit for 8-bit DFLL Circuit

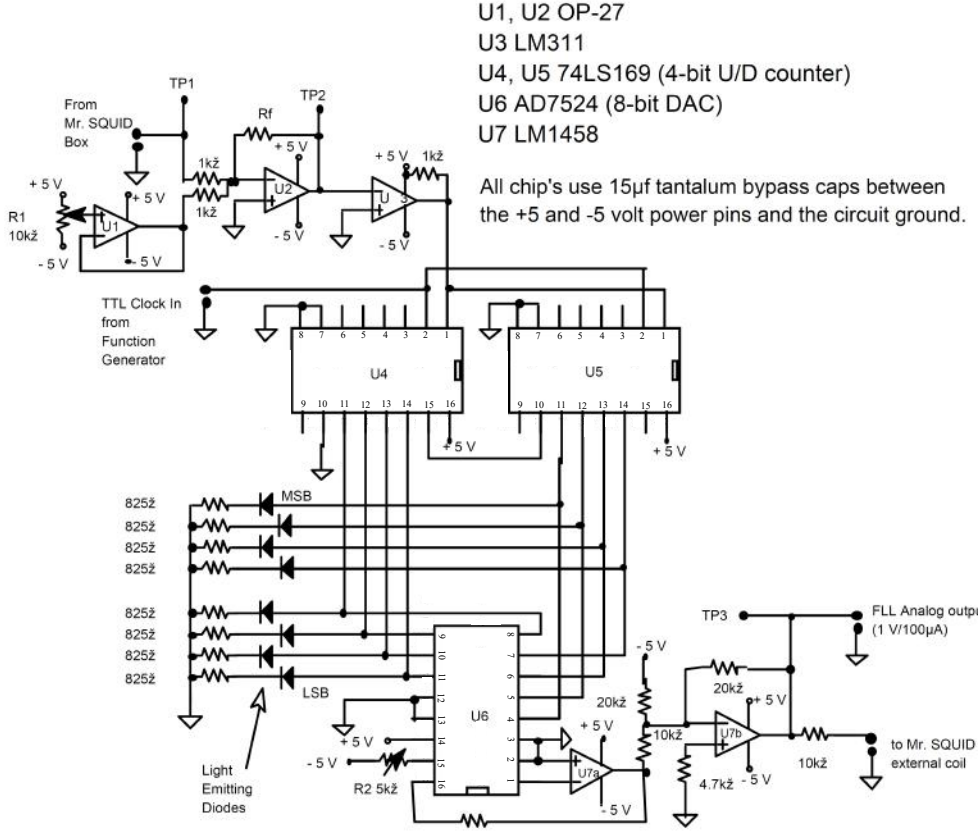


Figure 18: Circuit Diagram for 8-bit DFLF circuit. The circuit is equipped with operational amplifiers (op-amps), 4-bit up and down synchronous counters, and a digital to analog converter (DAC).

Theory of Operation:

Digital Flux Locked Loop (DFLL) works by taking input from the output voltage of the electronic box. This voltage is amplified and inverted by an op-amp (OP-27), U2, shown in Figure 18), by a factor of -100 . The gain factor can be changed by changing the resistance of feedback resistor R_f which is connected to pins 2 and 6 of amplifier U24. The gain also depends on the resistor connected to pin 2 (negative input) of U2, (i.e. OP-27),

$$\begin{aligned}
 Gain &= \frac{R_f}{R_{in}} \\
 &= \frac{100 \text{ k}\Omega}{1 \text{ k}\Omega} \\
 &= 100
 \end{aligned}$$

The amplification is aided by a voltage supply of +5 V and -5 V potential, with a common ground, which is buffered through another op-amp, U1 (OP-27). U1 isolates the output of the 10 kΩ potentiometer which is supplied by voltage. Its output is independent of the rest of the circuit's operation.

U3 (LM311) is a comparator, which compares the output voltage of the amplifier U2, with ground, and is capable of passing only two discrete signals, 0 V and 5 V, to the counters U4

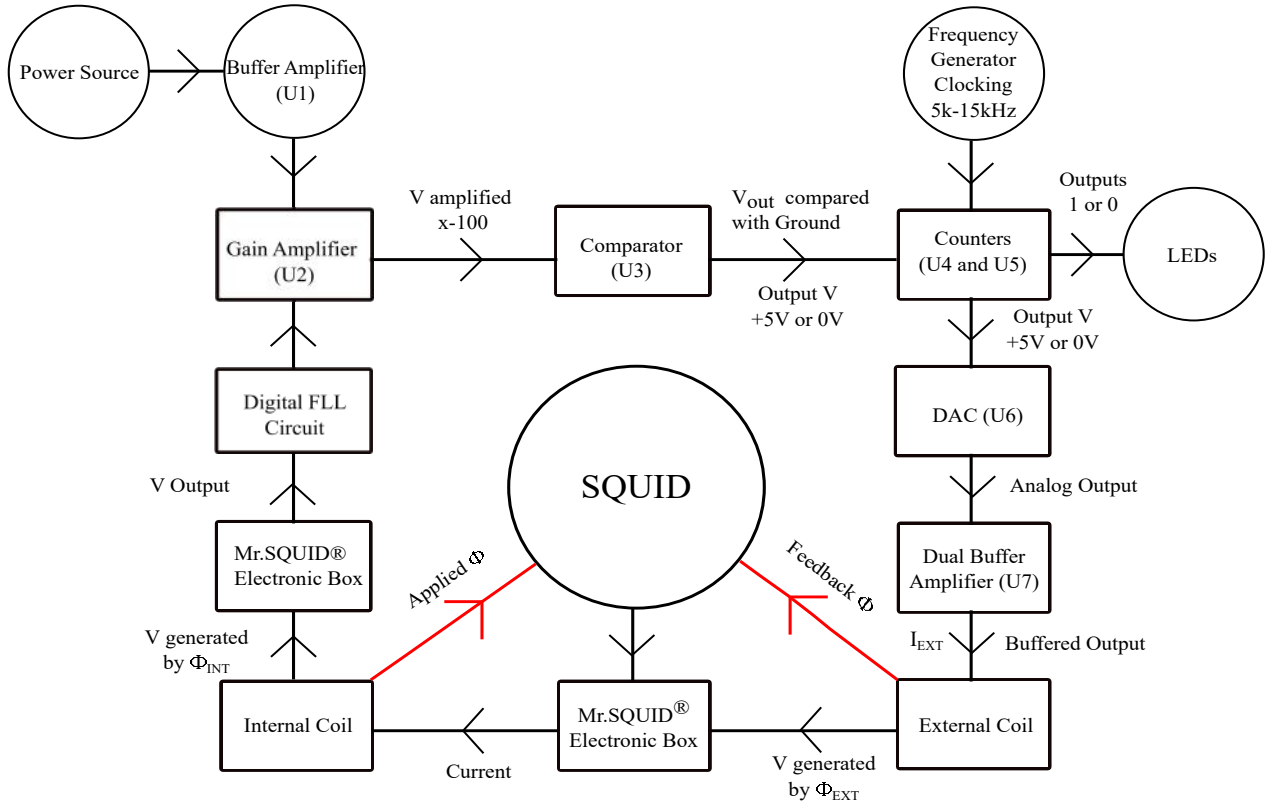


Figure 19: Schematic Representation of Digital Flux Locked Loop Experiment

and U5 (74LS169, 4-bit U/D counters)[4]. U3 passes 5 V, if its output is greater than 0 V, and passes 0 V otherwise. This is received by the counters as logical data.

The counters together work using Boolean Logic as 8-bit counters, and are continuously clocked by a function generator at a certain frequency. At each clock, they count the output of U3 as either 1 (for 5 V) or 0 (for 0 V). This is directly displayed on the 8 light emitting diodes (LED's) connected to the output pins 11 – 14 of either counter¹³.

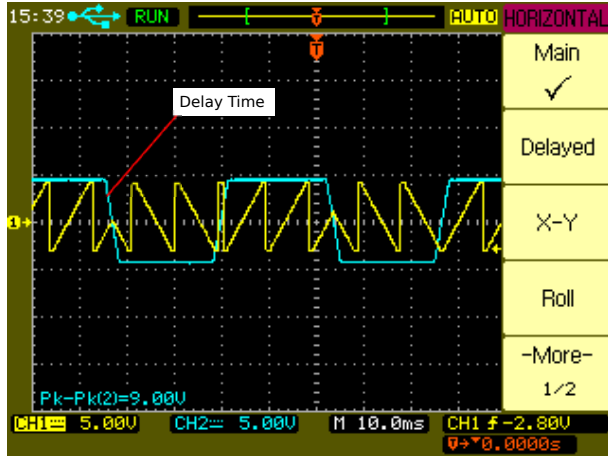
U4 then begins its count from 0 Least Significant Bit (0000) till 15 (1111), and repeats the increment from 0 to 15. U5 begins its count from 16 (binary 0001 1111) (continuation of the preceding 4-bit count by U4) till the Most Significant Bit, 128[11]. The cycle then repeats. The clock pattern is visible through the turning on (logical 1), and off (logical 0) of the LED's.

Next in the cycle is a DAC (U6, AD7524; 8-bit DAC)[5], which uses these logical outputs to display as analog signals. These appear as small steps on the analog output signal. The higher the clocking frequency, the smaller the appearance of step¹⁴. Ultimately, a dual operational amplifier, U7 (LM1458)), buffers (or isolates) the analog output of U6, to send current to the external coil.

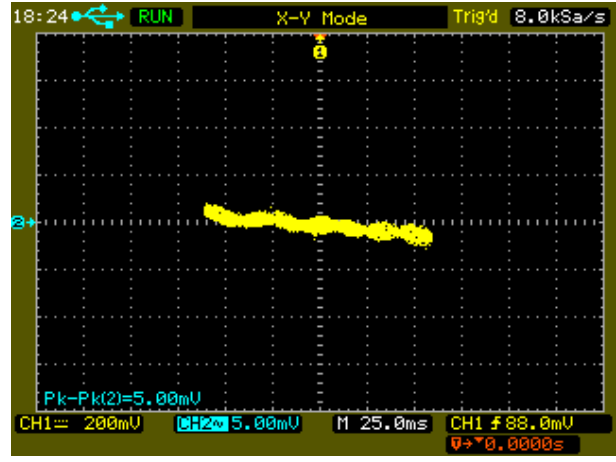
To conduct this loop, the circuit is connected to the power supply, with separate negative and positive potentials of 5 V, and a common ground between them. Before beginning the experiment, it is necessary to make sure that the output voltage of the circuit is 0 V, when

¹³See Figure 18 for pin configuration. Check the data sheet for the pin functions of LS169 4-bit counter cited under reference [4].

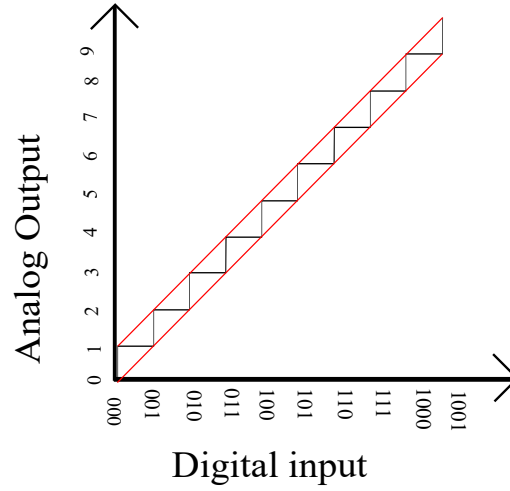
¹⁴A test circuit to test the working of the digital to analog converter can also be set (refer to Section 4).



(a)



(b)



(c)

Figure 20: (a) Output signal of counters in terms of 1's and 0's shown in main mode in blue. The slight slope of the wave indicates the delay time of the integrated circuits used. (b) Steps seen as slight curves due to increase sensitivity of the horizontal and vertical scales. (c) Digital signals to analog output

no input is given. Any offset has to be removed. The counters U4 and U5 are removed (to disconnect their output from the DAC input), and the DAC's (U6) pins 5 to 11 are connected to the circuit ground. These pins are the inputs of the converter[5]. Pin 4 of the converter is connected to the 5 V terminal, and voltage at TP3 (output) is measured using a voltmeter. In our case, it is a non-zero voltage, and was set to 0.000 V by adjusting the resistance of R2 resistor (Figure 18). The SQUID probe is cooled and the $V-\phi$ curve is obtained. The output voltage is connected to the input of the DFLL circuit and tested at Test Point 1 (Figure 22a). The current through the internal coil from the curve is calculated as 1.65×10^{-4} A, using the horizontal axis. This translates to $82.5 \mu\text{A}/\Phi_0$, since two sines are displayed. The applied

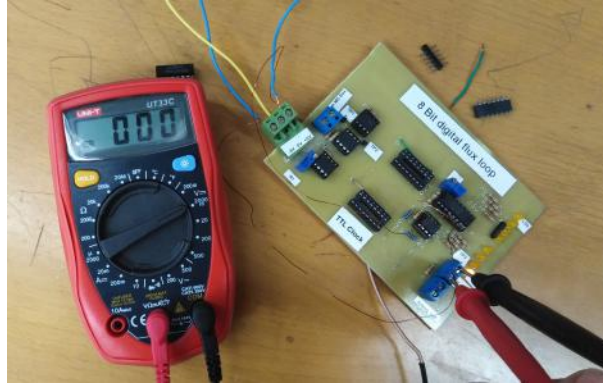


Figure 21: Output Voltage bias removed

flux from external coil was,

$$\begin{aligned}
 &= M_{int} \times I_{int}, \\
 &= 37.6 \text{ pH} \times 165 \text{ } \mu\text{A}, \\
 &\approx 6.20 \times 10^{-15} \text{ Wb}.
 \end{aligned}$$

This with the flux generated by the **SQUID** loop of $2.19 \times 10^{-15} \text{ Wb}$, with $I_B \approx 30 \text{ } \mu\text{A}$ becomes $8.394 \times 10^{-15} \text{ Wb}$.

The voltage supply is connected to the respective terminals to give the net voltage as 0 at the common terminal. The curve is then observed by testing on TP2 (amplified and inverted). This curve is adjusted by coupling the Channel 2 to DC mode, and adjusting the potentiometer (R1), to set equal amplitude on either side of the vertical axis (see Figure 22b).

The amplification factor calculated from the peak-peak voltages of curves 22a and (bottom left, written in blue) is calculated as approximately -107.5 . The power is disconnected, and the external coil connected to circuit output. A frequency generator with range of at least 5 kHz-15 kHz signal is used to connect its TTL (transistor-transistor logic) clock output to the counters' input using a BNC-BNC connection. The frequency is set to 5 kHz. The wave type was set to square wave. The power is reconnected and signal at TP2 resulted as a horizontal linear line indicating the cancellation of flux (Figure 22c). Signal at TP3 shows the output voltage given to the external coil to keep the flux constant inside the **SQUID**. The voltage across the external coil is -5.2 mV , which makes $I_{ext} \approx 107.4 \text{ } \mu\text{A}$. The calculated flux is,

$$\begin{aligned}
 \phi_{ext} &= M_{ext} \times I_{ext}, \\
 &= 35 \text{ pH} \times 107.4 \text{ } \mu\text{A}, \\
 &= 3.76 \times 10^{-15} \text{ Wb}.
 \end{aligned}$$

The net flux is,

$$\begin{aligned}
 \phi_{net} &= \phi_{SQ} + \phi_{int} - \phi_{ext}, \\
 &= \phi_{total} - \phi_{ext}, \\
 &= 8.39 \times 10^{-15} \text{ Wb} - 3.75 \times 10^{-15} \text{ Wb}, \\
 &\approx 4.64 \times 10^{-15} \text{ Wb}.
 \end{aligned}$$

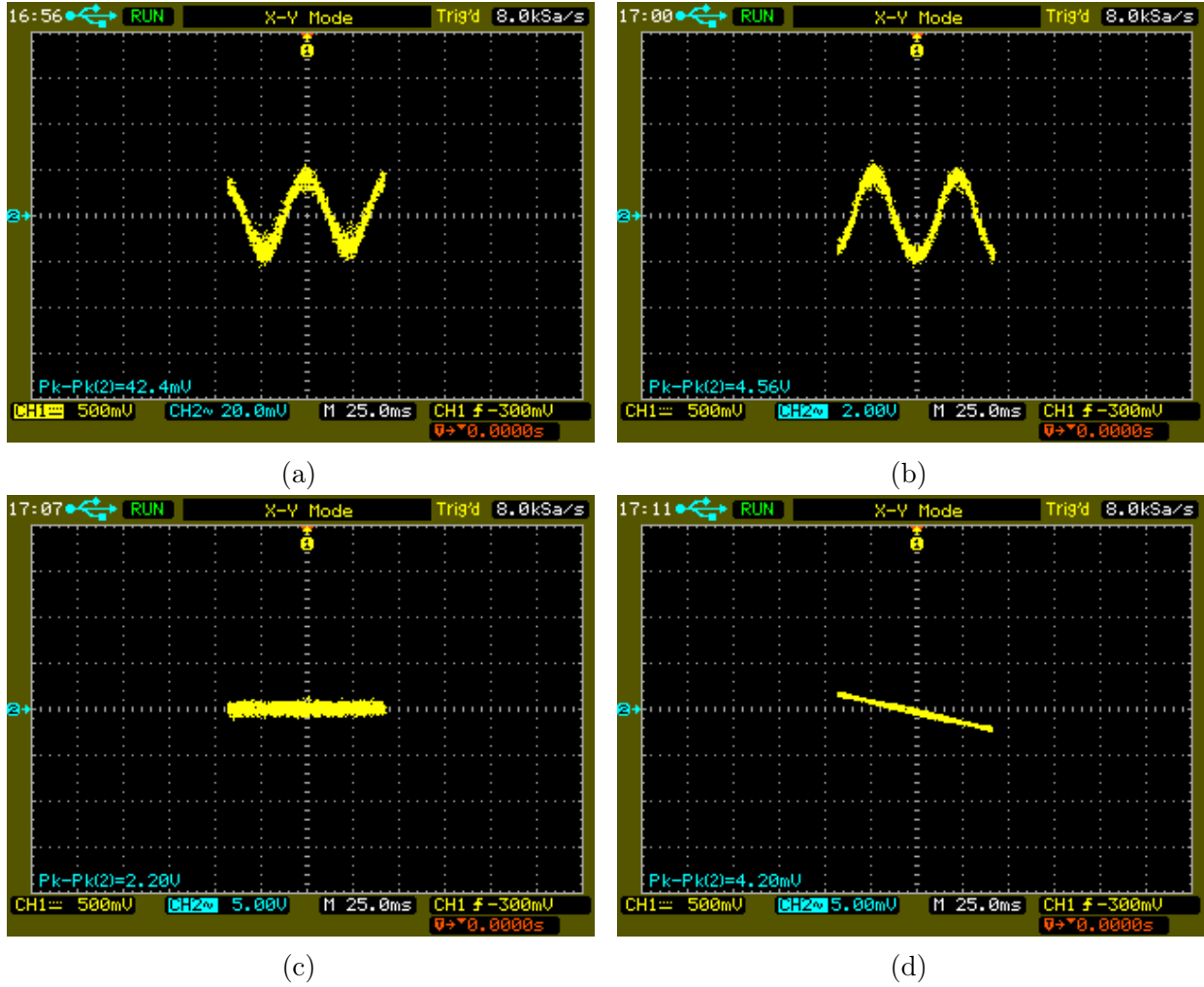


Figure 22: (a) TP1 showing FLL's input signal, (b) TP2 showing the inverted and amplified signal (factor -100). (c) TP2 shows the cancelled flux when digital counting begins (external coil connected) (d) TP3 showing the analog output being fed into the external coil.

This flux did not remain constant due to varying voltage output of the DFLL circuit, changing the current in the external coil. Analog voltage is calculated by taking the binary output on the LED's as inputs for the DAC and using the algorithm followed by the DAC,

$$V_{analog} = \frac{D}{2^n} V_{reference},$$

where $V_{reference}$ is the voltage at pin 15 of the DAC, and D is the input binary number [14],

$$\begin{aligned} V_{analog} &= \frac{1101 \ 1111}{2^8} (-3.52), \\ &= \frac{255}{256} (-3.52), \\ &\approx -3.51V. \end{aligned}$$

The analog output measured is -1.53 V, which continues to fluctuate one or two volts about this value. This means that our digital and analog results vary due to the uncertainties created from the fluctuating counting cycles.

Acknowledgments

We acknowledge the Physlab team for insightful discussions and help, including Muhammad Shafique for his contribution in the making of circuits for this experiment. Special thanks to Khadim Mehmood, Hafiz Muhammad Rizwan, and Muhammad Ayyaz Mehmood for the making of shielded dewar. We also pay gratitude to Ali Hassan for his assistance in lab resources. Emaan Sohail would like to acknowledge Dr. Athar Osama and Pakistan Innovation Foundation for facilitating this programme.

4 Appendices

Troubleshooting the Problems faced in the Project

This section describes the obstacles faced in the performance of the experiments, and the corrective actions taken to solve them.

Radio Frequency Interference and Noise

Given its high sensitivity, the SQUID is able to detect unwanted signals from the environment, which may dominate over the signals we want to observe; and put disruptive effects on our outputs. For this reason, it is suggested to turn off all the nearby electronic devices, especially the wireless technology. The effects may include noisy signals like the ones received by us in Figure 23a , or suppressed amplitude of the $V-\phi$ curve (Figure 23b). This may result in the flattening of the curve as a result of quantization error. Quantization error occurs when the noise of the electronics with the radio frequency interference from environment is greater than the wanted output signal. Increase in noise may be the result of low quality BNC-BNC cable usage or the usage of testing probes with high resistances. Checking the terminal to terminal resistances of the cables should be done before experiment.

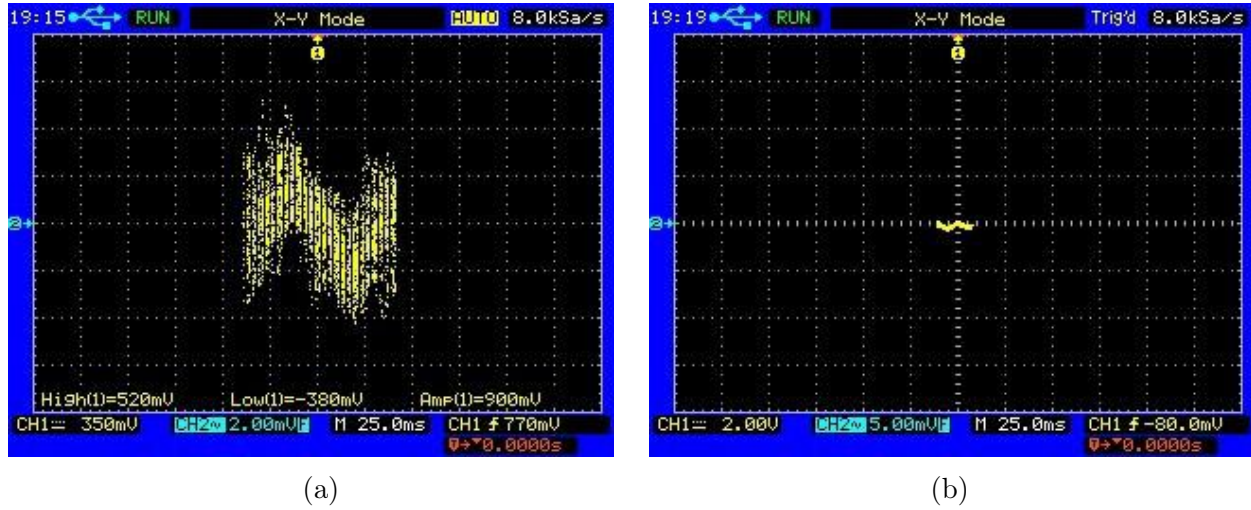


Figure 23: Possible Effects of External Environment on the $V-I$ Graphs. (a) RF interference (b) $V-I$ Curve with decreased amplitude

To carry out a smooth experiment, we looked for isolated places to conduct the experiment to obtain desirable $V-\phi$ curves. This quest for interference free environment led to the conclusive action of making a Faraday shield for our SQUID probe. However, before making one, it is reasonable to explore suitable areas for experimentation to identify the sources of disruption in the results.

- *FLL Experiment in the Basement of SSE building, LUMS*
Basements are rather dormant in terms of cellular and wireless network usage, along

with working machinery. Thus, they can serve as ideal locations to qualitatively test curves. As predicted, the results were relatively better (see Figure 26a). The apparatus was set up as shown:



Figure 24: Apparatus Set up in Basement: The distance between the apparatus and the SQUID had been kept at its maximum.

- *Cold Room*

A cold room enclosed within metal walls and doors, with the temperature of 9°C temperature was thought of a good location to suppress the incoming interference. However, the room did not shield the signals; in fact the interference came with time intervals in the form of pulses, indicating oscillating interference signals (see Figure 26b).

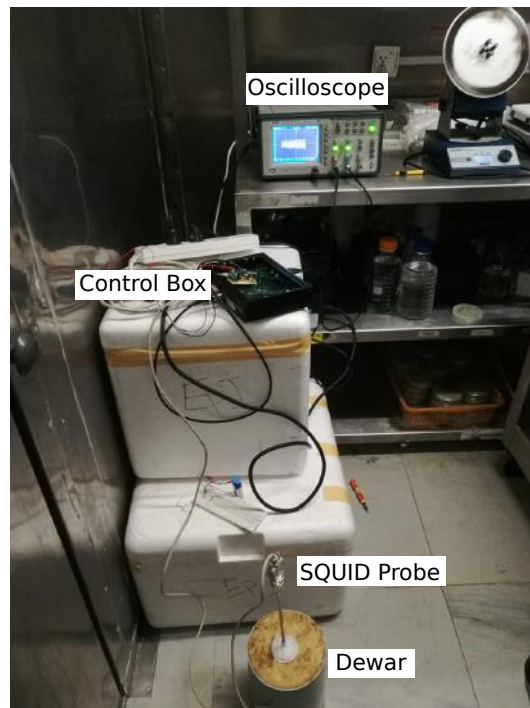


Figure 25: Experimental set up in the cold room. The metallic walls can be seen.

- *Annex*

This place is a detached part of the main building bordered by a metal cage. It could shield from waves with larger wavelengths. However, from the results, we conclude that outdoor locations are not an ideal location. The $V-I$ curve traced can be seen in Figure 26c.

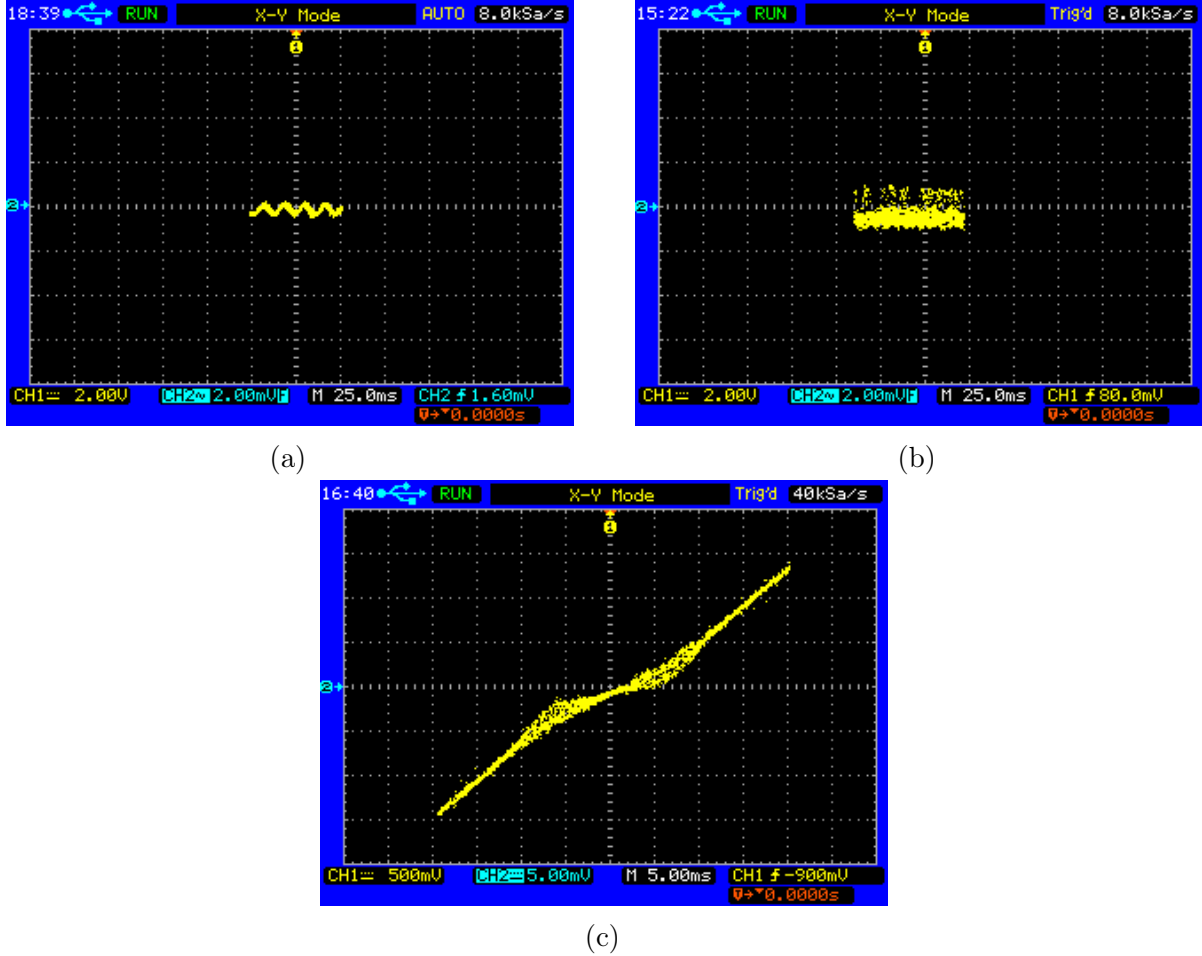


Figure 26: Results obtained at different locations to check for RF interference. (a) Relatively clear $V-\phi$ curve produced in basement. (b) Increased RF interference in a refrigerated cold room (-9°C). (c) $V-I$ curve unstable in annex.

- *Degaussing*

Another cause for suppressed $V-\phi$ curves could be flux trapping inside the SQUID probe, which is a frequent circumstance. A flux may remain trapped within the SQUID if its shield is magnetized. In such situations, it may get challenging to identify the cause for flat $V-\phi$ curves. This can be dealt by demagnetizing the magnetic shield of the probe (See appendix 4).

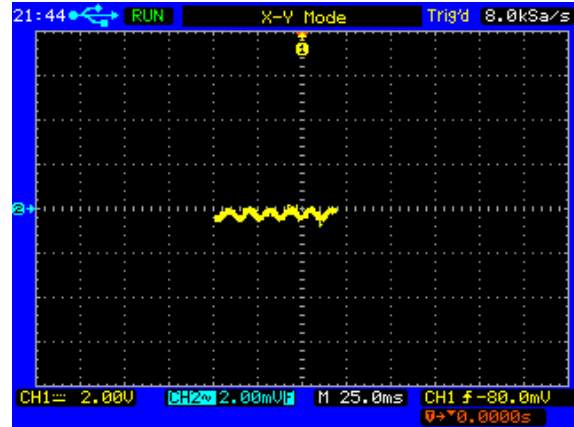
- *Faraday Shield*

A Faraday shield or cage is a metallic covering which blocks the interference by electromagnetic waves. The waves' wavelengths are larger than the penetration gaps in the metal of the shield or cage which does not let them pass through. The waves

surrounding the shield, cause the electrons in the metal to be repelled by their own oscillating electrons. This keeps the waves outside the inner regime metal container [6]. This cancels the effect of the radiations striking the shield. Non-magnetic conductors provide better shielding. The skin depth of the conductor (distance covered by the EM wave before it is attenuated by metal surface) must also be smaller than the metal layer's thickness[16]. This prohibits its penetration. Since wireless network frequencies range from 2.4 GHz to 300 GHz, and the fact that skin depth decreases with increasing frequencies, a metal layer of few millimeters could easily be used as an effective shield. Within the range of frequencies mentioned, the wavelengths of the radiation range from 10 cm to 1 mm (1mm being at highest frequency). This concludes that the holes of any effective Faraday cage must not be wider than 1 cm. Yet, A non-metallic dewar can be wrapped with aluminum foil to suppress interference (see Figure 10b), or a shield could be made. Several prototypes were made keeping in consideration the requirements of a Faraday shield. It concluded in the assembly of a dewar made of metal.



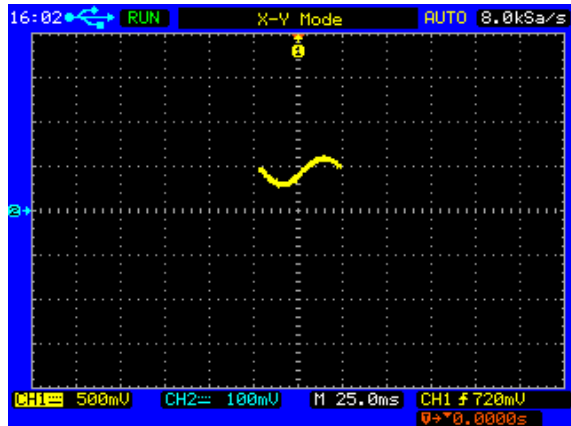
(a)



(b)



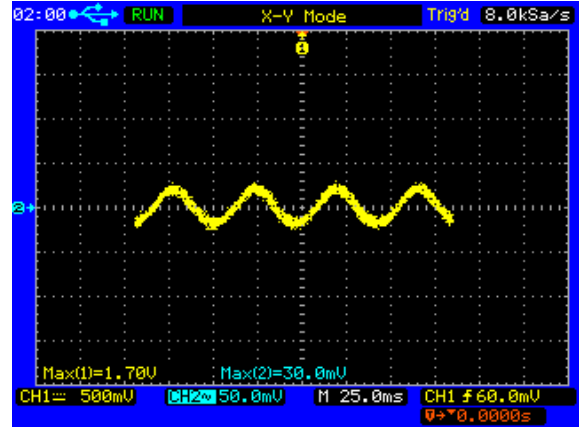
(c)



(d)



(e)

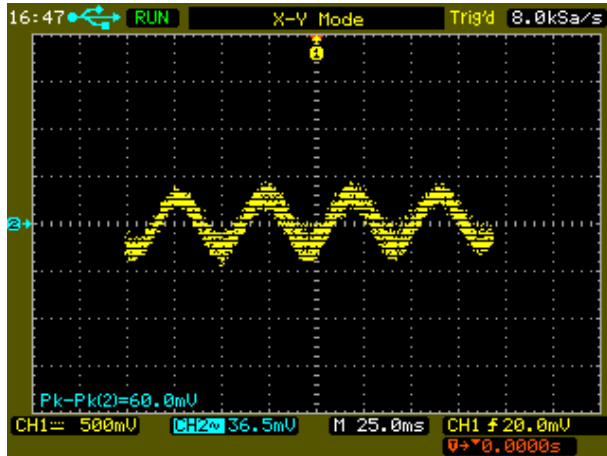


(f)

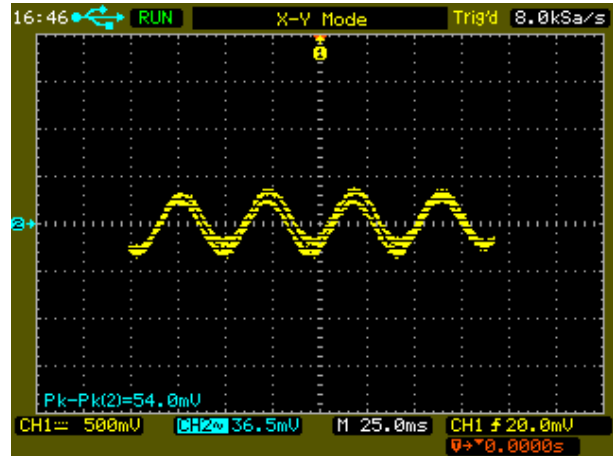
Figure 27: First Prototype: (a) Dewar made of thick metallic sheet. (b) Relative increase in amplitude of the $V-\phi$. Second Prototype: (c) The dewar from (a) placed in a metallic box, with insulation. (d) Increased amplitude. Third Prototype: (g) Effective insulation to increase durability of liquid nitrogen. (h) The amplitude of curve suppressed with removal of a layer of metal sheet from dewar.

- *Use of Digital Filter*

The output on oscilloscope can be made clear from noise, by turning on the digital filter, which takes average signals within certain random signals, which get cancelled.



(a)



(b)

Figure 28: (a) $V-\phi$ curve without channel 2 digital filter. (b) $V-\phi$ curve with channel 2 digital filter.

Testing the working of the IC, DAC (AD7524), of digital flux locked loop circuit

For experiments like DFLL) in section 3.8, the IC's being used may show symptoms of being faulty by getting overheated, or not performing their function. This can be countered by the use of temporary circuits made on breadboards to independently test the working. To deal

with the situation, the circuit was set up using the schematic diagram in Figure 18, by giving the DAC inputs (originally received from counters) through pins 5 – 11¹⁵, as either +5 V (representing logical 1) or –5 V (representing logical 0). The inputs on these pins were varied, and there corresponding outputs on pins 14 and 15 were read for correct changes.

Testing the SQUID electronic box

In order to test the Mr.SQUID[®] electronic box, 10 Ω ($\times 1$) and 20 Ω ($\times 1$) resistors can be used to calculate resistances. The confirmation of known data through the calculations would ensure that the electronic box carries out its function correctly. The oscilloscope and Mr.SQUID[®] electronic box are connected to the power supply, and $V-I$ mode is turned on the electronic box, while X-Y mode on the scope. The 10 Ω resistor is connected to a spare DB-9 male connector as shown in Figure 29b, which is then plugged into the DB-9 female connection¹⁶ on the back of the electronic box.

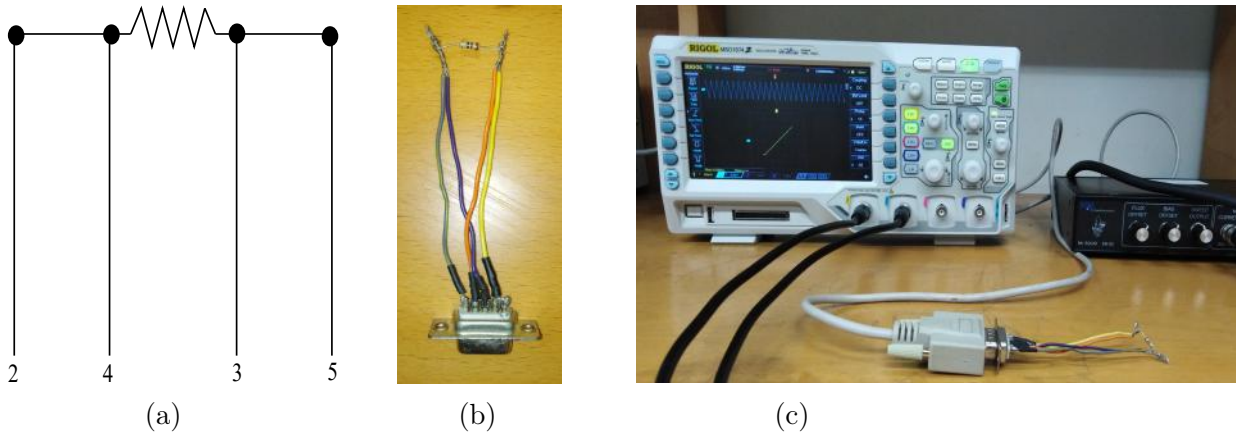


Figure 29: (a), (b) Resistor connected to DB-9 male connector. Pins 2 and 4 are connected to one terminal of the resistor, and pins 3 and 5 are connected to the other terminal of the connector.

Both Channel 1 (horizontal axis connected to the current output on electronic box) and Channel 2 (vertical axis connected to voltage output) on the scope are DC coupled to generate a voltage-current graph.

The plots shown in Figure 30a, are used to calculate the gradient of the graph, which gives the value of resistance connected. The coordinates of the plots can be read using the scaling options shown in Figure 30a, where the Channel 1 and 2 indicate 1 V/division and 100 mV/division respectively¹⁷. The gain for voltage output is $\times 100$ ¹⁸.

¹⁵Check data sheet for AD7524 under the reference [7]

¹⁶Check pin configuration for DB-9 male connector under reference [8].

¹⁷In order to directly calculate the change in voltage and current, "cursor" or "measure" options on a digital scope can be used, which directly gave the shifts in axes (see Figures 31).

¹⁸The voltages received from the SQUID are too small, and need to be amplified for the ease of display and calculation. Therefore, a default amplification factor of $\times 10,000$ is set for the voltage output of Mr.SQUID[®] electronic box. This factor may however be switched to $\times 100$ or $\times 1000$ from the circuit board shown in

The following value accurately gives the answer of $10\ \Omega$:

$$\begin{aligned}
 \text{Resistance} &= \frac{\text{Voltage}}{\text{Current}} \\
 &= \frac{\text{Voltage from Channel 2 Gain}_V}{\text{Voltage from Channel 1}/10,000\Omega} \\
 &= \frac{2\text{ V} - (-2\text{ V})/100}{200\text{ mV} - (-200\text{ mV})/10,000\ \Omega} \\
 &= 10\ \Omega
 \end{aligned}$$

This is repeated for a parallel combination for $10\ \Omega$ and $20\ \Omega$ resistors(Figure 30b). The ohmmeter is used to confirm the resistances calculated.

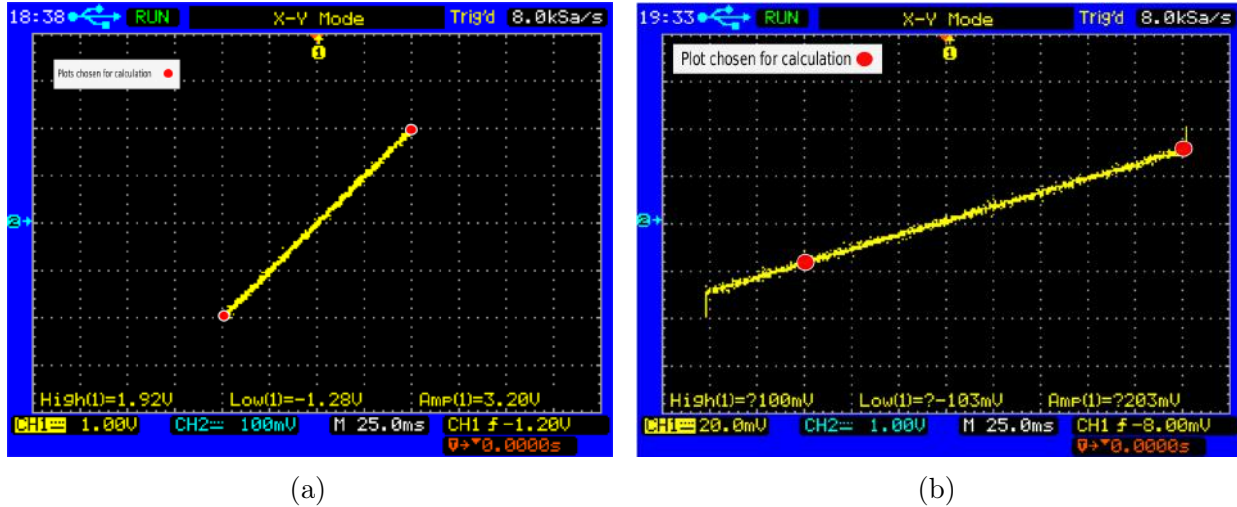


Figure 30: (a) V - I graph for a $10\ \Omega$ resistor. (b) $20\ \Omega$ and $10\ \Omega$ in parallel

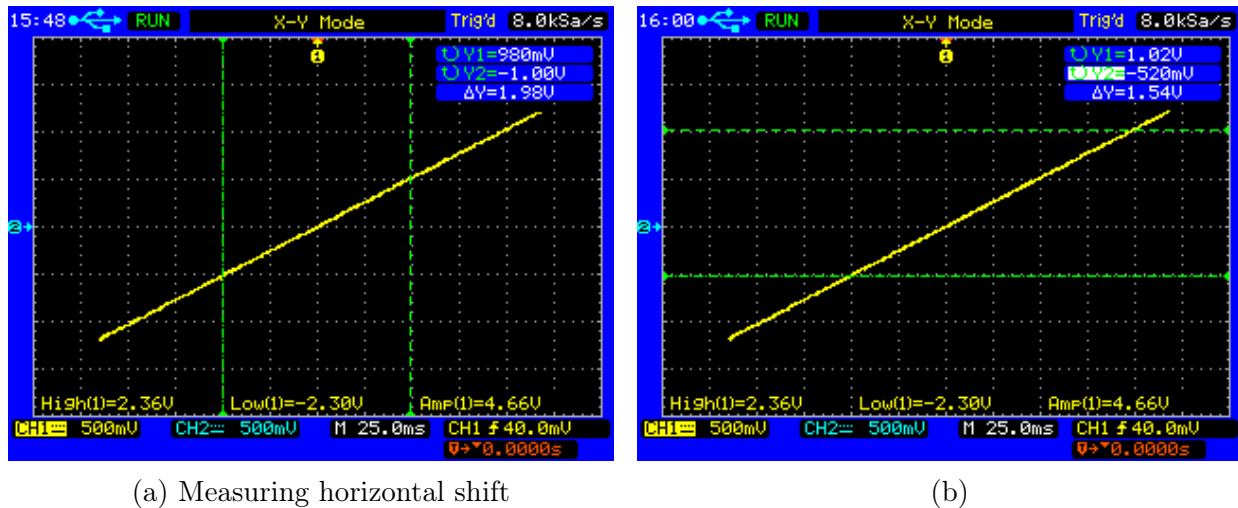


Figure 31: Using cursor to take measurements. (a) Measuring horizontal shift (b) Measuring vertical shift.

Figure 9 as per user's choice. The current output from the electronic box, is a conversion to voltage across a $10,000\Omega$ resistor and needs to be reconverted to current by dividing it with $10,000\Omega$. The scaling factor can further be adjusted using the "Probe" factor in the oscilloscope's channel settings.

Demagnetization of the SQUID 's magnetic shield

The magnetic shield of the SQUID can also become magnetised when frequently exposed to magnetic fields. Thus, in order to assure safe experimentation to detect sensitive signals, the shield was degaussed. This was done by placing the shield in a solenoid and passing alternating current through it which generates constantly changing magnetic field. This changes the ordered alignment of the magnetic domains inside the shield. The AC voltage is first increased to a certain value in the solenoid, and is then slowly decreased until it is zero.

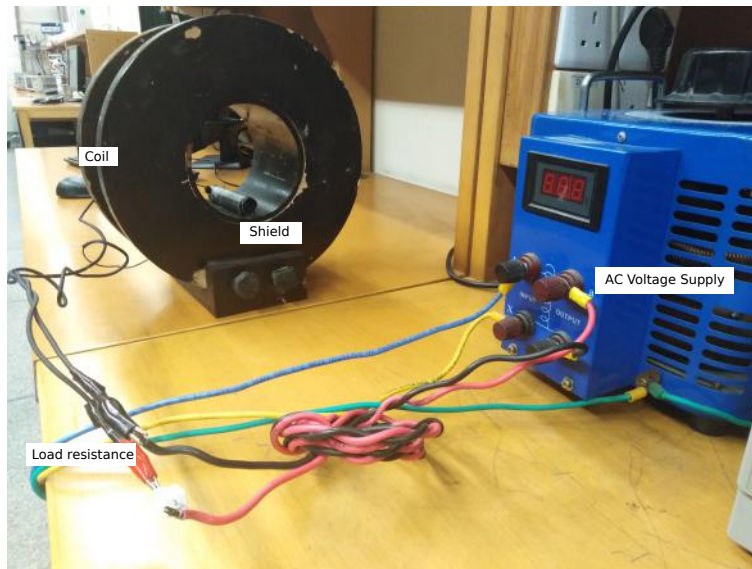
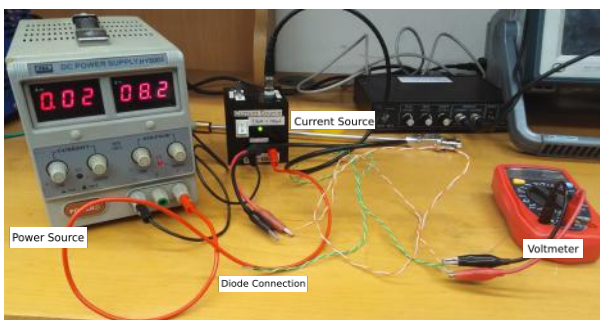


Figure 32: Demagnetising Shield

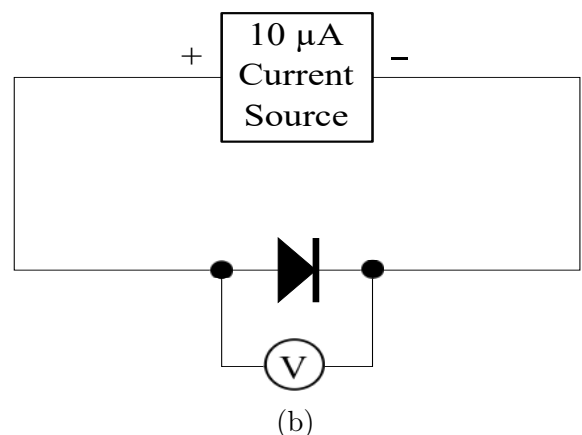
Figures and Diagrams

Refer to the respective experiments to view complete procedures for the following figures.

Temperature–Voltage Relation of Diode



(a)



(b)



(c)

Figure 33: (a) Diode connected with a $10 \mu\text{A}$ current source. (b) Circuit diagram for taking potential drop across the diode. (c) Diode fastened with the SQUID probe.

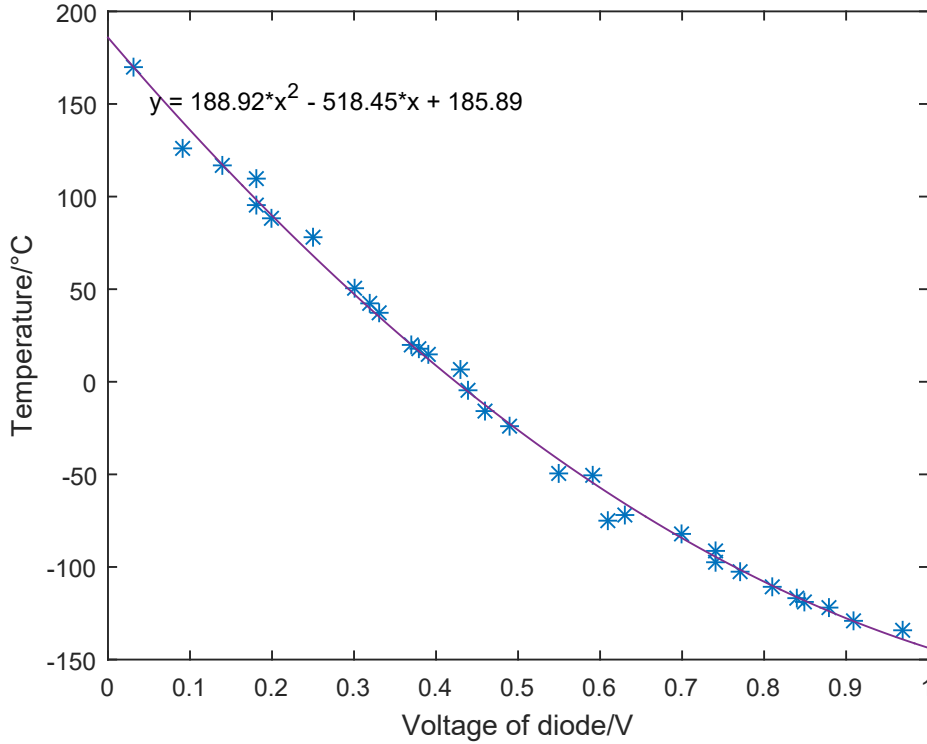


Figure 34: Plot for the voltage across 1N4001–MIC Germanium diode with changing Temperature

The voltage across 1N4001–MIC Germanium diode is taken as it is increased to 200°C , brought back to room temperature, until it is cooled to -196°C . This data is then plotted. A quadratic equation is obtained to define the relation by the curve fitting of the plot:

$$y = 188.92x^2 - 518.45x + 185.89. \quad (7)$$

References

- [1] URL: <https://www.britannica.com/science/phonon>.
- [2] URL: https://en.wikipedia.org/wiki/Cooper_pair.

- [3] URL: [https://chem.libretexts.org/Bookshelves/Physical_and_Theoretical_Chemistry_Textbook_Maps/Supplemental_Modules_\(Physical_and_Theoretical_Chemistry\)/Quantum_Mechanics/02._Fundamental_Concepts_of_Quantum_Mechanics/Tunneling](https://chem.libretexts.org/Bookshelves/Physical_and_Theoretical_Chemistry_Textbook_Maps/Supplemental_Modules_(Physical_and_Theoretical_Chemistry)/Quantum_Mechanics/02._Fundamental_Concepts_of_Quantum_Mechanics/Tunneling).
- [4] URL: <http://www.ti.com/lit/ds/symlink/sn54s169.pdf>.
- [5] URL: <https://www.analog.com/media/en/technical-documentation/data-sheets/AD7524.pdf>.
- [6] URL: <http://hyperphysics.phy-astr.gsu.edu/hbase/Solids/coop.html#c2>.
- [7] URL: <https://www.analog.com/media/en/technical-documentation/data-sheets/AD7524.pdf>.
- [8] URL: <https://www.db9-pinout.com/>.
- [9] 2019. URL: <https://www.pasternack.com/t-calculator-skin-depth.aspx>.
- [10] Saurabh Basu. *IIT Guwahati*. URL: <https://www.youtube.com/watch?v=i7cETh3AXQg&t=97s>.
- [11] Sourav Gupta. *Synchronous Counter*. August 21, 2018. URL: <https://circuitdigest.com/tutorial/synchronous-counter>.
- [12] Numakura Hiroshi. *Physical Metallurgy*. 2014. URL: <https://www.sciencedirect.com/book/9780444537706>.
- [13] *Mr. SQUID® User's Guide - Version 6.4, STAR Cryoelectronics*. 6th ed. 2003, p. 121.
- [14] Tim Wilmshurst Rob Toulson. *Fast and Effective Embedded Systems Design*.
- [15] About STARCryo et al. *Mr. SQUID FAQs | STAR Cryoelectronics*. URL: <https://starcryo.com/mr-squid-faqs/>.
- [16] Mac Van Valkenburg and Wendy Middleton. *Reference Data for Engineers, 9th Edition*.

See discussions, stats, and author profiles for this publication at: <https://www.researchgate.net/publication/325190728>

Orbital Angular Momentum Generation and Detection

Preprint · May 2018

DOI: 10.13140/RG.2.2.21594.03525/1

CITATIONS

0

READS

268

1 author:



Muhammad Shiraz Ahmad

Lahore University of Management Sciences

6 PUBLICATIONS 0 CITATIONS

SEE PROFILE

Some of the authors of this publication are also working on these related projects:



Estimating Quality of Apples Using A Polarization Based Sensor [View project](#)



Measurement of Verdet Constant of different Materials by Faraday Rotation [View project](#)

Optical communication system based on *LASER* beams carrying *Orbital angular momentum*.

M.SHIRAZ AHMAD

Department of Physics, Syed Babar Ali School of Science and Engineering (SBASSE), Lahore University of Management Sciences (LUMS), Opposite Sector U, D.H.A., Lahore 54792, Pakistan

Compiled May 7, 2018

LASER beam can be structured in a way that Its wave-fronts are twisted in a helical form. This twisted light carries orbital angular momentum (OAM) independent of polarization state. A wide range of modes of OAM can be multiplex into a single beam and also can be de-multiplexed to isolate them, hence OAM can be used in optical communication systems. In this paper, we have discussed methodologies to generate OAM modes, multiplex, transmit through an optical fiber and then de-multiplex them to recover all modes again. © 2018 Optical Society of America

OCIS codes:

<https://dx.doi.org/10.13140/RG.2.2.21594.03525>

1. INTRODUCTION

As no any optical instrument support infinite band-width of frequencies of beam¹. Science is almost reached on its upper limit of scientific revolution. With daily base increase of Internet, mobile phone users, needs are also being increasing. Many new methods have been developed like multi core fiber (to fulfill needs) in which every core supports some band-width. This problem of limited bandwidths can be resolved by shifting our communication system on Orbital Angular Momentum (OAM) of light beams. As light beam can carry infinite OAM states² theoretically, if we denote signal with ℓ we can increase band width of signals to $\ell = \infty$ theoretically, hence if we will be able to do that task, problems that are caused due to limitation on bandwidth will be resolved.

In this paper, we have provided brief review on basics, some famous ways to generate and detect OAM, limitations and future scope.

2. OPTICAL ANGULAR MOMENTUM

Light beam carries angular momentum (AM). Total angular momentum is superposition of Spin and Orbital AM [1]. Orbital angular momentum (OAM) can be further divided into two categories, i. e external OAM and internal OAM. External OAM is origin dependent which means at any point, if we want to measure OAM, simply we take cross product of center of beam with its total linear angular momentum³. Our main interest in this

paper has remained in internal OAM as it is origin independent [3].

As beam of light contains sinusoidally varying Electric and Magnetic field components. Net energy transferred is represented by poynting vector $\vec{P} = \frac{1}{\mu_0} \vec{E} \times \vec{B}$ where μ_0 is vacuum permittivity, \vec{E} and \vec{B} are electric and magnetic field vectors⁴.

In case of plane wave fronts⁴, \vec{P} remains parallel to beam axes, but beam can also be generated in such a way that \vec{P} no longer remains parallel to beam axis, but circulates around beam axis, making helical shape, such beam is also called optical vortex. These beams with optical vortex are shown in Fig. 3 (2a-2g)⁵ Such beams with azimuthal dependence of phase fronts actually contain Orbital Angular Momentum[4]. Azimuthal dependence can be defined by $\exp(-i\ell\phi)$, where ℓ is integer (which characterize *Helical Modes* that can have any value (positive or negative)) whos positive values belong to right circulation and negative values belongs to left circulation.

$\ell = 0$ characterizes normal EM beam whose phase fronts or wave fronts are plane surfaces, this can be seen in Fig. 2a, where as intensity profile of such beam can be seen in Fig. 3a. In same way, $\ell = \pm 1$ characterizes single helical surface with Step Length = λ (Helical pattern can be seen in Fig. 2b with intensity profile Fig. 3b which belongs to $\ell = +1$ and Fig. 2c belongs to $\ell = -1$). Theoretically, We can make as much modes we want by setting values of ℓ with Step Length = $|\ell|\lambda$, here ℓ is

⁴Either light beam is linearly polarized or circularly polarized \vec{P} , independent of polarization

⁵Do not confuse yourself with shape of circularly polarized light and OAM, since both looks same. In circularly polarized light, Electric and Magnetic field vectors rotate around propagation vector, where as in OAM with nonzero ℓ , Poynting vector circulates around beam propagation.

¹Commonly different instruments support different limited band width

²OAM is independent of frequency, single frequency can also have infinite modes theoretically

³Quantum Mechanical picture can be seen [2]

called topological charge of optical vortex, ϕ is azimuthal coordinate of beam cross section. *OAM* modes with different values of topological charge and their intensity profiles are shown in Fig. 3 and Fig. 4 respectively.⁶

3. PRODUCTION OF OAM STATES

OAM modes with $\ell = \pm 1$ exist in nature, higher modes do not exist naturally but can be generated using artificial ways. Some popular ways to generate these modes includes using Spiral Phase Plates, Diffraction Grating, Spatial Light Modulators etc.

A. Spiral Phase Plates

These can be of plastic or some transparent medium whose thickness increases azimuthally. Plane phase front after passes through it, changes into twisted ones (As shown in Fig. 1). Thickness of such *Spiral Phase Plates*[5] are designed according to formula $T = (\ell\lambda)/(n-1)$, where T is change in thickness between thinnest and thickest part of plate, during moving around 360 degree in azimuthal angle. Some difficulties can be caused, if we try to generate *OAM* using *Spiral Phase Plates* as these plates only support wavelength for which they are designed for. Moreover they are expensive and are not adjustable.

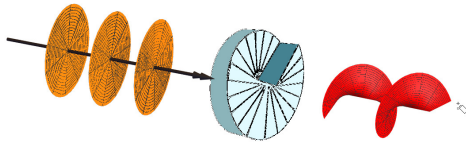


Fig. 1. Light beam of $\ell = 0$ after passing through Spiral Phase Plate, converted into *OAM* $\ell = +1$

B. Diffraction Grating

parallel lines of diffraction grating produce $\ell = 0$ lines, and if we design diffraction grating with middle part fork like (Ref. Fig. 4b), then different modes can be generated, where as ℓ of *OAM* increases as number of lines on fork dislocation increases.

C. Spatial Light Modulator(SLM)

It is a device which is used to modulate phase and intensity of beam, hence *OAM* modes can be generated. A program designed in Matlab[6] can be used to generate holograms (for specific topological charge) in *.bmp format and can be loaded in SLM[7], high quality beams can easily be generated[8]. Fig. 4a belongs to $\ell = 0$, hence effects no change on plane wave front, Fig. 4b belongs to $\ell = 1$ and converts Fig. 2a to Fig. 2b, In the same way Fig. 4c belongs to $\ell = 2$ and converts Fig. 2a to Fig. 2d and Fig. 4d belongs to $\ell = 3$ and converts Fig. 2a to Fig. 2f. Another thing to note here is that if we pass again these beams with newly generated *OAM* with same holograms, we recover back old phase fronts.

⁶In this paper, plots up-to $\ell = \pm 3$ are mentioned along their intensity profiles of phase fronts, further modes can also be easily drawn by careful analysis of Step Length = $|\ell|\lambda$ and using Mathematica Codes mentioned in APPENDIX.

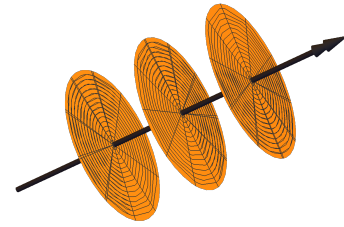


Fig. 2a. Phase front with $\ell = 0$, Arrow is showing direction of propagation of beam and flat surface is showing that this beam has Zero *OAM*

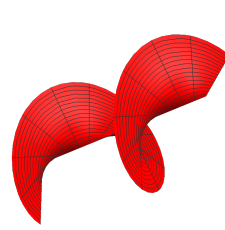


Fig. 2b. Phase front with $\ell = +1$, as there is one curved (clockwise) phase front, so It has +1 *OAM*

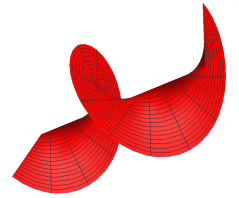


Fig. 2c. Phase front with $\ell = -1$, as there is one curved (anticlockwise) phase front, so It has -1 *OAM*

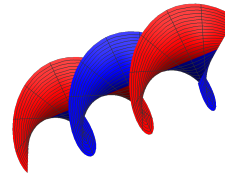


Fig. 2d. Phase front with $\ell = +2$, as there two curved (clockwise) surfaces, so It has +2 *OAM*

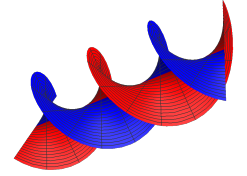


Fig. 2e. Phase front with $\ell = -2$, as there two curved (anticlockwise) surfaces, so It has -2 *OAM*

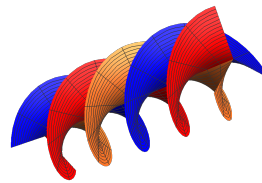


Fig. 2f. Phase front with $\ell = +3$, as there two curved (clockwise) surfaces, so It has +3 *OAM*

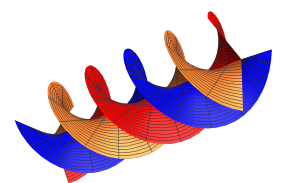


Fig. 2g. Phase front with $\ell = -3$ as there two curved (anticlockwise) surfaces, so It has -3 *OAM*

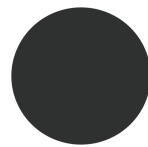


Fig. 3a.
 $\ell = 0$

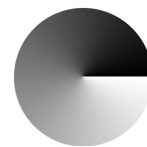


Fig. 3b.
 $\ell = +1$

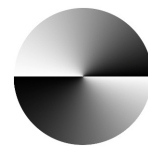


Fig. 3c.
 $\ell = +2$



Fig. 3d.
 $\ell = +3$

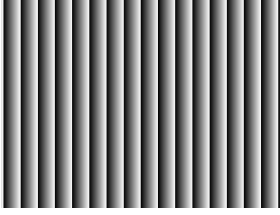


Fig. 4a

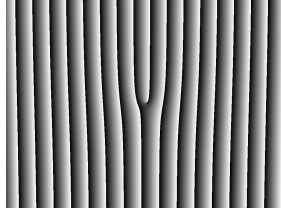


Fig. 4b

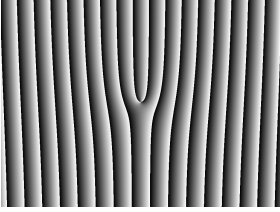


Fig. 4c

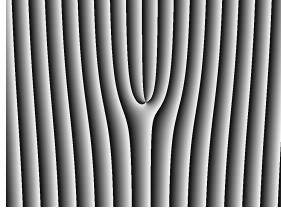


Fig. 4d

D. Diffractive holographic filters

Computer generated holographic filters is modern technique to generate and isolate OAM components. Holographic pictures printed on transparent paper with high resolution also can do required work, hence we can print shapes of Fig. 2 to generate OAM. Further details can be seen in Ref. [5].

Although Fig. 3a-3d are phase fronts of different OAM modes, but holograms of that shape can also generate OAM.

4. DETECTION OF OAM STATES

As Spin of light beam can easily be measured⁷ by converting it into s and p components and then measuring, but OAM can not be measured in that way. Some techniques have been discovered to do that task. Most easiest way to measure OAM value is by using Maczander Interferometry.

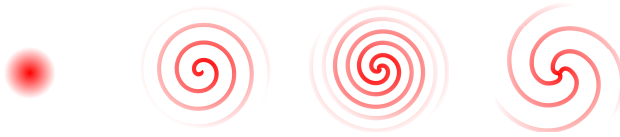


Fig. 5a.
 $\ell = 0$

Fig. 5b.
 $\ell = +1$

Fig. 5c.
 $\ell = +2$

Fig. 5d.
 $\ell = +3$

Fig.5 Interference pattern of Maczander Interferometry, when beam carrying OAM is interfered with wave having plane wave-front.

Beam containing OAM is interfered with beam having plane phase front ($\ell = 0$) and then interference pattern is observed on screen. This interference shows spiral patterns (As shown in Fig. 5) which starts from center and slowly goes away with circulating. Number of lines starting from center determines value of OAM ℓ . In case of absence of OAM (or $\ell = 0$), dark spot appears as shown in Fig. 5a, If we interfere beam of values $\ell = 1, 2, 3$ with plane waves, we get interference patterns like Fig. 5b, 5c, 5d. we are not going in detail separating all modes from single beam, but It can be seen in Ref.[9]

⁷Circularly polarized light contains spin. Spin can have only two possible values, hence right and left circularly polarized light contains these two values

5. OPTICAL COMMUNICATION SYSTEM BASED ON OAM

It is possible to use OAM in our optical communication system to replace conventional system in which different signals are being transferred in different frequency modes. It is experimentally tested to generate multi OAM modes, multiplex and transfer through conventional multi-mode fiber successfully over 2.6-km without loss of any information. [10].

In paper [11] it is tested to send up to 100 modes using single hologram. Since this stream is under development we can hope that soon OAM based communication system will be possible to replace total communication system of world but currently it is under development.

6. APPENDIX

A. MATHEMATICA CODES

Mathematica Code. 1 (for Fig. 2a)

```
1 Show[ParametricPlot3D[{0, u Sin[t + 2 \[Pi]/3],
2   u Cos[t + 2 \[Pi]/3]}, {t, 0, 10}, {u, 0, 0.3},
3   Boxed -> False, Axes -> False],
4   ParametricPlot3D[{0.3, u Sin[t + 4 \[Pi]/3],
5     u Cos[t + 4 \[Pi]/3]}, {t, 0, 10}, {u, 0, 0.3},
6     Boxed -> False, Axes -> False],
7     ParametricPlot3D[{0.6, u Sin[t + 6 \[Pi]/3],
8       u Cos[t + 6 \[Pi]/3]}, {t, 0, 10}, {u, 0, 0.3},
9       Boxed -> False, Axes -> False],
10      ParametricPlot3D[{t, 0, 0}, {t, 0, 3}, {u, 0, 1},
11        Boxed -> False, Axes -> False] /. Line[pts_]
12      :> Arrow[Tube[pts, .01], {0, -.4}]]
```

Mathematica Code. 2 (for Fig. 2b)

```
1 Show[ParametricPlot3D[{t/3, u Sin[t + 1 \[Pi]],
2   u Cos[t + \[Pi]]}, {t, 0, 10}, {u, 0, 1},
3   ViewPoint -> {Pi, -Pi, -2}, PlotTheme ->
4   "Scientific", Boxed -> False, Axes -> False,
5   MeshShading -> {{Red, Red}, {Red, Red}}]]
```

Mathematica Code. 3 (for Fig. 2c)

```
1 Show[ParametricPlot3D[{-t/3, -u Sin[t + 1 \[Pi]],
2   -u Cos[t + \[Pi]]}, {t, 0, 10}, {u, 0, 1},
3   ViewPoint -> {Pi, -Pi, -2}, PlotTheme ->
4   "Scientific", Boxed -> False, Axes -> False,
5   MeshShading -> {{Red, Red}, {Red, Red}}]]
```

Mathematica Code. 4 (for Fig. 2d)

```
1 Show[ParametricPlot3D[{t/2, u Sin[t + 1 \[Pi]],
2   u Cos[t + \[Pi]]}, {t, 0, 10}, {u, 0, 1},
3   ViewPoint -> {Pi, -Pi, -2}, PlotTheme ->
4   "Scientific", Boxed -> False, Axes -> False,
5   MeshShading -> {{Red, Red}, {Red, Red}}],
6   ParametricPlot3D[{t/2, u Sin[t + 2 \[Pi]],
7     u Cos[t + 2 \[Pi]]}, {t, 0, 10}, {u, 0, 1},
8     ViewPoint -> {Pi, -Pi, -2}, PlotTheme ->
9     "Scientific", Boxed -> False, Axes -> False,
10      MeshShading -> {{Blue, Blue}, {Blue, Blue}}]]
```

Mathematica Code. 5 (for Fig. 2e)

```
1 Show[ParametricPlot3D[{-t/2, -u Sin[t + 1 \[Pi]],
2   -u Cos[t + \[Pi]]}, {t, 0, 10}, {u, 0, 1},
3   ViewPoint -> {Pi, -Pi, -2}, PlotTheme ->
4   "Scientific", Boxed -> False, Axes -> False,
5   MeshShading -> {{Red, Red}, {Red, Red}}],
6   ParametricPlot3D[{-t/2, -u Sin[t + 2 \[Pi]],
7     -u Cos[t + 2 \[Pi]]}, {t, 0, 10}, {u, 0, 1},
8     ViewPoint -> {Pi, -Pi, -2}, PlotTheme ->
9     "Scientific", Boxed -> False, Axes -> False,
10      MeshShading -> {{Blue, Blue}, {Blue, Blue}}]]
```

Mathematica Code. 6 (for Fig. 2f)


```

1 Show[ParametricPlot3D[{t/2, u Sin[t + 2 \[Pi]/3],
2   u Cos[t + 2 \[Pi]/3]}, {t, 0, 10}, {u, 0, 1},
3   ViewPoint -> {Pi, -Pi, -2}, PlotTheme ->
4   "Scientific", Boxed -> False, Axes -> False,
5   MeshShading -> {{Red, Red}, {Red, Red}}],
6   ParametricPlot3D[{t/2, u Sin[t + 4 \[Pi]/3],
7   u Cos[t + 4 \[Pi]/3]}, {t, 0, 10}, {u, 0, 1},
8   ViewPoint -> {Pi, -Pi, -2}, PlotTheme ->
9   "Scientific", Boxed -> False, Axes -> False,
10  MeshShading -> {{Blue, Blue}, {Blue, Blue}}],
11  ParametricPlot3D[{t/2, u Sin[t + 6 \[Pi]/3],
12  u Cos[t + 6 \[Pi]/3]}, {t, 0, 10}, {u, 0, 1},
13  ViewPoint -> {Pi, -Pi, -2}, PlotTheme ->
14  "Scientific", Boxed -> False, Axes -> False],
15  MeshShading -> {{Green, Green}, {Green, Green}}]

```

Mathematica Code. 7 (for Fig. 2g)

```

1 Show[ParametricPlot3D[{-t/2, -u Sin[t + 2 \[Pi]/3],
2   -u Cos[t + 2 \[Pi]/3]}, {t, 0, 10}, {u, 0, 1},
3   ViewPoint -> {Pi, -Pi, -2}, PlotTheme ->
4   "Scientific", Boxed -> False, Axes -> False,
5   MeshShading -> {{Red, Red}, {Red, Red}}],
6   ParametricPlot3D[{-t/2, -u Sin[t + 4 \[Pi]/3],
7   -u Cos[t + 4 \[Pi]/3]}, {t, 0, 10}, {u, 0, 1},
8   ViewPoint -> {Pi, -Pi, -2}, PlotTheme ->
9   "Scientific", Boxed -> False, Axes -> False,
10  MeshShading -> {{Blue, Blue}, {Blue, Blue}}],
11  ParametricPlot3D[{-t/2, -u Sin[t + 6 \[Pi]/3],
12  -u Cos[t + 6 \[Pi]/3]}, {t, 0, 10}, {u, 0, 1},
13  ViewPoint -> {Pi, -Pi, -2}, PlotTheme ->
14  "Scientific", Boxed -> False, Axes -> False],
15  MeshShading -> {{Green, Green}, {Green, Green}}]

```

B. GENERATION AND DETECTION OF $\ell = +1$

In summarizing, If we start with OAM $\ell = +1$ value, it will be easy to understand above all. Let we want to generate beam carrying OAM ℓ value 1, starting with LASER which produces $HG_{(0,0)}$ ⁸. Now, we can produce $\ell = +1$ mode either by passing it through **Spatial Phase Plate** or hologram that look like Fig. 4b. We can also generate this mode by **Spatial Light Modulator**, by generating *. bmp image for $\ell = +1$ from code mentioned in Ref. [6] and loading it into SLM. Phase front of that beam will look like Fig. 2b and Its intersection will look like Fig. 3b. Now, we want to measure value of ℓ , we will have to interfere it with beam of plane phase front (Which look like Fig. 2a) using Maczander Interferometry arrangement, and we will obtain interference pattern like Fig. 5a.

REFERENCES

1. L. Allen, M. W. Beijersbergen, R. J. C. Spreeuw, and J. P. Woerdman, Phys. Rev. A **45**, 8185 (1992).
2. S. J. van Enk and G. Nienhuis, Europhys. Lett. (EPL) **25**, 497 (1994).
3. M. Padgett, J. Courtial, and L. Allen, Phys. Today **57**, 35 (2004).
4. Optical Society, "OSA Publishing," <http://www.osapublishing.org>.
5. F. A. Starikov, G. G. Kochemasov, S. M. Kulikov, A. N. Manachinsky, N. V. Maslov, A. V. Ogorodnikov, S. A. Sukharev, V. P. Aksenov, I. V. Izmailov, F. Y. Kanev, V. V. Atuchin, and I. S. Soldatenkov, Opt. Lett. **32**, 2291 (2007).
6. E. Galvez, "Forked diffraction pattern," <http://departments.colgate.edu/physics/research/optics/oamgp/ForkedDiffractionGrating.txt> (2016).
7. D. King-smith, "Creating laguerre-gaussian modes using a spatial light modulator," .
8. N. Matsumoto, T. Ando, T. Inoue, Y. Ohtake, N. Fukuchi, and T. Hara, J. Opt. Soc. Am. A **25**, 1642 (2008).
9. J. Jin, J. Luo, X. Zhang, H. Gao, X. Li, M. Pu, P. Gao, Z. Zhao, and X. Luo, Sci. Reports **6**, 24286 (2016).

⁸Normal Laser sources that can be found in optics Lab's generate these modes having $\ell = 0$ (Plane phase fronts)

10. L. Zhu, A. Wang, S. Chen, J. Liu, Q. Mo, C. Du, and J. Wang, Opt. express **25**, 25637 (2017).
11. A. Trichili, C. Rosales-Guzmán, A. Dudley, B. Ndagano, A. Ben Salem, M. Zghal, and A. Forbes, Sci. Reports **6**, 27674 (2016).

See discussions, stats, and author profiles for this publication at: <https://www.researchgate.net/publication/329554976>

Reflection and Transmission of Light from MultilayerFilms: An easy approach, using MATLAB

Preprint · December 2018

DOI: 10.13140/RG.2.2.18069.58081

CITATIONS

0

READS

50

1 author:



[Muhammad Shiraz Ahmad](#)

Lahore University of Management Sciences

4 PUBLICATIONS 0 CITATIONS

SEE PROFILE

Some of the authors of this publication are also working on these related projects:



Calculation of optical reflection and transmission coefficients of a multi-layer system using Matlab [View project](#)



Measurement of Verdet Constant of different Materials by Faraday Rotation [View project](#)

Reflection and Transmission of Light from Multilayer Films: An easy approach, using MATLAB

M.SHIRAZ AHMAD^{*1}

¹Department of Physics, Syed Babar Ali School of Science and Engineering (SBASSE), Lahore University of Management Sciences (LUMS), Opposite Sector U, D.H.A., Lahore 54792, Pakistan

Compiled December 10, 2018

When optical beam hits a multilayered system of different refractive indices, it gets reflected, refracted, and absorbed in a way that can be derived from the Fresnel equations. But, with increasing number of layers, math becomes complicated. We have designed a MATLAB algorithm underlying the transfer-matrix method for the calculation of the optical properties of multilayered system and have verified it with experimental observations. © 2018 Optical Society of America

OCIS codes: .

<http://dx.doi.org/10.1364/ao.XX.XXXXXX>

1. INTRODUCTION

The optical beam passing through the interface of different refractive indices, changes its direction towards/away normal to the interface, and the changed direction can be calculated mathematically using refractive indices making that interface. To understand this, we can consider an example illustrated in Figure 1. Assuming n_2 to be sand. If a car enters into a region with higher refractive index at oblique angle, its right front wheel enters into an area of n_2 earlier than the left front wheel, hence starts facing lossy force earlier, causing a change in direction towards the normal. Same intuition can help to predict diverted optical path of optical beam.

But if a linearly polarized light faces an interface of higher refractive index it gets refracted and reflected. The direction of beam propagation (\vec{k}) is shown in figure 2 and sinusoidal waves shows that the oscillation of electric field is perpendicular to the direction of wave propagation. Optical beam is characterized as p -polarized, if electric field oscillations are perpendicular to the plane formed by incident, reflected and transmitted beam, and p if oscillations are in the same plane. The direction of reflected and transmitted beams can be calculated by using Snell's Law and intensities can be computed via Fresnel coefficients as:

$$r_p = \frac{n_2 \cos \theta_1 - n_1 \cos \theta_2}{n_2 \cos \theta_1 + n_1 \cos \theta_2}, \quad (1)$$

$$r_s = \frac{n_1 \cos \theta_1 - n_2 \cos \theta_2}{n_1 \cos \theta_1 + n_2 \cos \theta_2}, \quad (2)$$

$$t_p = \frac{2n_1 \cos \theta_1}{n_2 \cos \theta_1 + n_1 \cos \theta_2}, \quad (3)$$

$$t_s = \frac{2n_1 \cos \theta_1}{n_1 \cos \theta_1 + n_2 \cos \theta_2}. \quad (4)$$

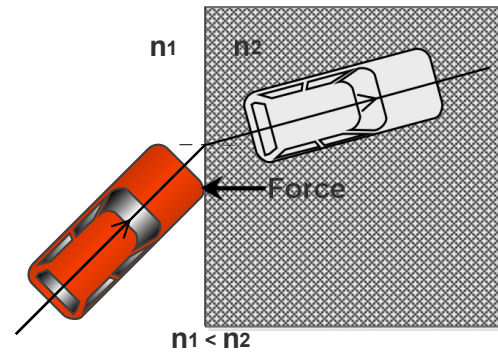


Fig. 1. Car entering into sand (intuition)

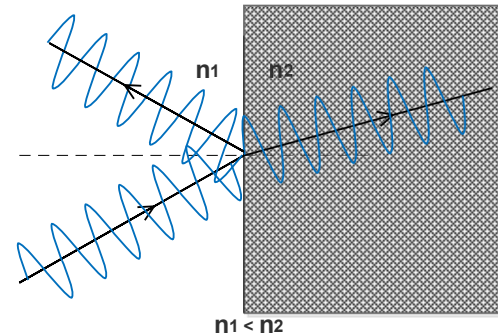


Fig. 2. Refraction of optical beam at the interface between two media of different refractive indices

These coefficients can easily be used on single interface, but for multilayered system, matrix transformation method is more useful.

A. Matrix Method

Suppose we have a multilayered system[1] having N refractive indices stacked together making $N - 1$ interfaces with refractive index n_j , impedance Z_j , thickness d_j for layer j . Also the layer 0 is semi-infinite with $Z = -\infty$ and layer N is being treated semi-infinite with $Z = \infty$ and phase change is ϕ_j .

$$\begin{pmatrix} E_{j-1} \\ H_{j-1} \end{pmatrix} = \begin{pmatrix} \cos \phi_j & i \sin \phi_j / Z_j \\ Z_j i \sin \phi_j & \sin \phi_j \end{pmatrix} \begin{pmatrix} E_j \\ H_j \end{pmatrix} \quad (5)$$

Eq. (5) relates amplitudes in one layer to the next adjacent layer and therefore repeated application of transfer matrix allows us to propagate waves from one side of the multilayer system to the other using

$$\begin{pmatrix} E_1 \\ H_1 \end{pmatrix} = \prod_{j=2}^{N-1} \begin{pmatrix} \cos \phi_j & i \sin \phi_j / Z_j \\ Z_j i \sin \phi_j & \sin \phi_j \end{pmatrix} \begin{pmatrix} E_N \\ H_N \end{pmatrix}. \quad (6)$$

And the characteristic matrix[2] for the entire system will be

$$M = \begin{pmatrix} m_{11} & m_{12} \\ m_{21} & m_{22} \end{pmatrix} = \prod_{j=1}^{N-1} \begin{pmatrix} \cos \phi_j & i \sin \phi_j / Z_j \\ Z_j i \sin \phi_j & \sin \phi_j \end{pmatrix}. \quad (7)$$

Here, $Z_j = \sqrt{\frac{\epsilon_0}{\mu_0}} n_j \cos \theta_j$ and by applying the boundary conditions for figure (3), we have

$$Z_0 = \sqrt{\frac{\epsilon_0}{\mu_0}} n_0 \cos \theta_i \quad \text{and} \quad Z_N = \sqrt{\frac{\epsilon_0}{\mu_0}} n_N \cos \theta_t. \quad (8)$$

Consequently,

$$r = \frac{Z_1 m_{11} + Z_1 Z_N m_{12} - m_{21} - Z_N m_{22}}{Z_1 m_{11} + Z_1 Z_N m_{12} + m_{21} + Z_N m_{22}} \quad (9)$$

$$t = \frac{2Z_1}{Z_1 m_{11} + Z_1 Z_N m_{12} + m_{21} + Z_N m_{22}} \quad (10)$$

To find r or t for any configuration of multilayered system, we only need to compute the characteristic matrices for each film, multiply them and substitute resulting matrix elements into the Eqs. (9) and (10).

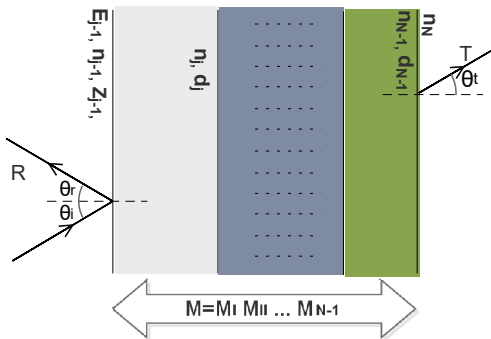


Fig. 3. Propagation of optical beam through a multilayer structure consisting of the materials with different indices of refraction.

To find reflection and transmission coefficients, we have

$$R = rr' \quad \text{and} \quad T = tt', \quad (11)$$

where r' and t' are the complex conjugates of r and t .

2. ALGORITHM

We implement the matrix transformation method via MATLAB. Syntax of such function is

$$[\theta_{\text{incident}}, R_s, R_p, T_s, T_p] = \text{MultiLayerFilm}(n_{1 \rightarrow N}, d_{2 \rightarrow K}, \theta_{\text{incident}}, \lambda.)$$

Here *MultiLayerFilm* is the MATLAB function whose algorithm is shown in algorithm (1), $n_{1 \rightarrow N}, d_{2 \rightarrow K}, \theta_{\text{incident}}, \lambda$ are input arguments and function gives output values.

Algorithm 1. *MultiLayerFilm*($n_{1 \rightarrow N}, d_{2 \rightarrow K}, \theta_{\text{Incident}}, \text{Lambda}$)

```

1: for  $\theta_i := \theta_{\text{Incident}}^*$  do
2:    $\theta_{i \rightarrow N} = \text{SneilsLaw}(n_{1 \rightarrow N}, \theta_i)$ 
3:    $\phi_{2 \rightarrow K} = n_{2 \rightarrow K} d_{2 \rightarrow K} \frac{2\pi}{\lambda}$  ▷ here  $K = N - 1$ 
4:    $Z_s = \sqrt{\frac{\epsilon_0}{\mu_0}} n_{1 \rightarrow N} \cos \theta_{1 \rightarrow N}$ 
5:    $m_s = \text{Matrix}(\phi_{2 \rightarrow K}, Z_s)$ 
6:    $[R_s, T_s] = \text{RT}(m_s, Z_{s1}, Z_{sN})$ 
7:    $Z_p = \sqrt{\frac{\epsilon_0}{\mu_0}} n_{1 \rightarrow N} / \cos \theta_{1 \rightarrow N}$ 
8:    $m_p = \text{Matrix}(\phi_{2 \rightarrow K}, Z_p)$ 
9:    $[R_p, T_p] = \text{RT}(m_p, Z_{p1}, Z_{pN})$ 
10: End.
11:  $\text{rtplot}(\theta_{\text{Incident}}^*, R_s, R_p, T_s, T_p)$ 

```

* θ_{Incident} is an array.

User defined functions are in boldface.

Let we have two layers of thickness 1 mm and 0.2 mm separated with distance of 0.3 mm having refractive indices 1.4, 1.5, wavelength 1547 nm. Now we want to find R_s, R_p, T_s, T_p for incident angles from 0° to 90° with the following function.

```

1 % n (Glass) = 1.4441
2 % n (Borosilicate Glass) = 1.5007
3 % d (Glass) = 1mm
4 % d (Air) = 0.302 mm
5 % d (Borosilicate Glass) = 2.228 mm
6 [Incident, RS, RP, TS, TP] = ...
7   MultiLayerFilm([1 1.47 1.5007 1], [1e-3 0.302e-3
   2.228e-3], 0:90, 1547e-9);

```

This generate arrays Incident, RS, RP, TS, TP corresponding to $\theta_{\text{incident}}, R_s, R_p, T_s, T_p$, as shown in figure 4

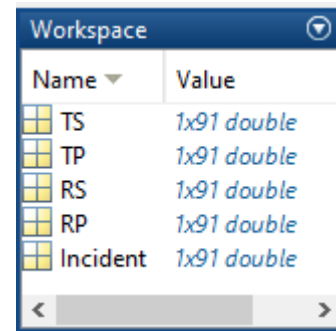


Fig. 4. Workspace of MATLAB showing output values of function *MultiLayerFilm*.

3. EXPERIMENTAL SETUP

Experimental setup is shown in Figure 7. We used two transparent materials of thickness 1 mm, 2.288 mm having refractive indices 1.47, 1.5007 (at $\lambda = 1547$ nm) with separation of 0.302 mm and placed on a rotating table. Optical power sensor that can be rotated along the table to measure transmitted/reflected beam. Actual setup is shown in Figure 6 and measured reflection and transmission coefficients for θ_i from 1° to 90° and measured corresponding transmission and reflection power amplitudes, for both s and p polarized optical beams.

4. RESULTS AND DISCUSSION

Figure 5 show results of our experimentally measured transmission/reflection intensities, measured for different incident angles θ_i ($0^\circ \rightarrow 90^\circ$). Here lines represent theoretical plots generated by algorithm (1) and stars represent experimental measurements which exactly matches to the observations based on MATLAB algorithm.

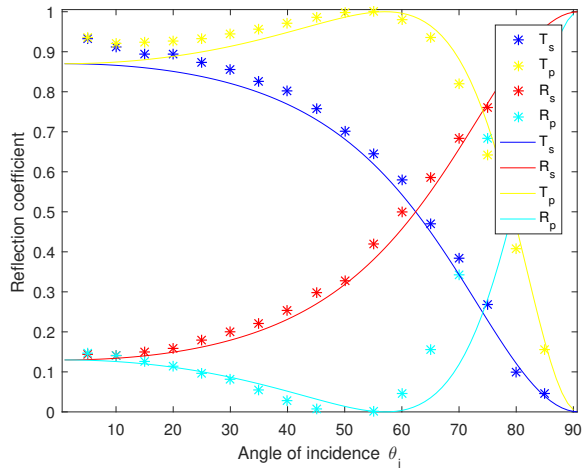


Fig. 5. Power coefficients, lines show theoretical and stars show experimental results.

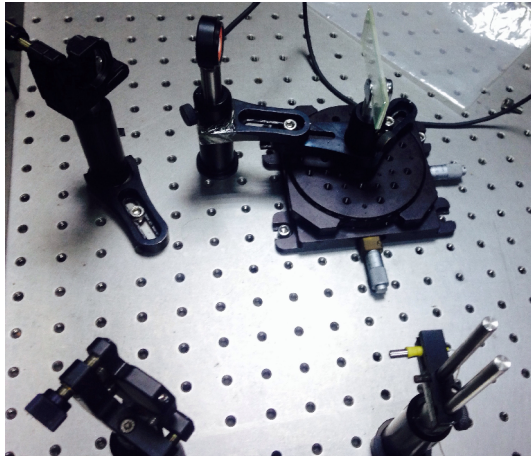


Fig. 6. Screen shot of experimental setup

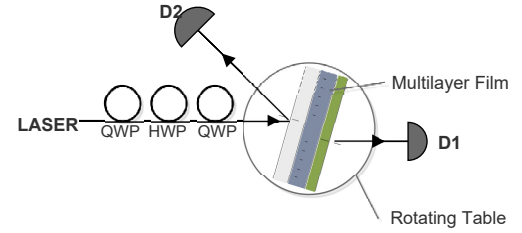


Fig. 7. Schematic diagram of experimental setup.

5. APPENDIX

A. MATLAB Functions

A.1. MultiLayerFilm

```

1 function [Incident,RS,RP,TS,TP] = MultiLayerFilm(n,d,
    Incident,Lambda)
2 BOUNDARY = length(n)-1;
3 INC=Incident;
4 for INCIDENCE=Incident
5 %% Calculation of angles on boundaries starting from
    first
6 Theta=SnellsLaw(n,INCIDENCE);
7 %%
8 Phi(2:BOUNDARY) = n(2:BOUNDARY).*d(1:BOUNDARY-1).*(2.*pi
    ./ (Lambda));
9 Z_s = (2.6544e-3).*n(1:BOUNDARY+1).*cosd(Theta(1:
    BOUNDARY+1));
10 Z_p = (2.6544e-3).*n(1:BOUNDARY+1)./cosd(Theta(1:
    BOUNDARY+1));
11 m1=Matrix(Phi,Z_s);
12 [R_s(INCIDENCE+1),T_s(INCIDENCE+1)]=R_T(m1,Z_s(1),Z_s(
    BOUNDARY+1));
13 m2=Matrix(Phi,Z_p);
14 [R_p(INCIDENCE+1),T_p(INCIDENCE+1)]=R_T(m2,Z_p(1),Z_p(
    BOUNDARY+1));
15 end
16 RS=R_s; RP=R_p; TS=T_s; TP=T_p;
17 rtplot(Incident,R_s,R_p,T_s,T_p);
18 end

```

A.2. Matrix

```

1 function m = Matrix(Phi,Z)
2 Limit=length(Phi);
3 M1=[1 0;0 1];
4 for j=2:Limit
5     M{j} = [cosd(Phi(j)) (1i*sind(Phi(j)))/Z(j) ; 1i*Z
        (j)*sind(Phi(j)) cosd(Phi(j))];
6     M1=M1*M{j};
7 end
8 m=M1;
9 end

```

A.3. R_T

```

1 function [R,T] = R_T(m,Z_o,Z_s)
2 r=(Z_o*m(1,1)+Z_o*Z_s*m(1,2)-m(2,1)-Z_s*m(2,2))/...
3     (Z_o*m(1,1)+Z_o*Z_s*m(1,2)+m(2,1)+Z_s*m
4     (2,2));
5 t=(2*Z_o)/...

```

```

5      (Z_o*m(1,1)+Z_o*Z_s*m(1,2)+m(2,1)+Z_s*m
6      (2,2));
7  T=abs(t.*t');
7  R=abs(r.*r');
8  end

```

A.4. norm2unity

```

1  function norm = norm2unity(input)
2  norm=(input-min(input))/(max(input)-min(input))
3  end

```

A.5. rtplot

```

1  function Output = rtplot(Incident,R_s,R_p,T_s,T_p)
2  Incident=Incident+1;
3  plot(Incident,T_s,'r');
4  hold on
5  plot(Incident,R_s,'r');
6  hold on
7  plot(Incident,T_p,'b');
8  plot(Incident,abs(R_p),'b');
9  hold off
10 % [K,I] = min(R_p);
11 % X_b=I.*(ones(1,length(Incident)));
12 % plot(X_b,R_p,'--');
13 end

```

A.6. SnellsLaw

```

1  function angles = SnellsLaw(n, incident)
2  Theta=zeros(1,length(n));
3  Theta(1)=incident;
4  for j=2:length(n)
5      Theta(j) = asind((n(j-1)/n(j))*sind(Theta(j-1)));
6  end
7  angles=Theta;
8  end

```

REFERENCES

1. A. Zangwill and A. Zangwill, *Modern electrodynamics* (Cambridge University Press, 2018), p. 604–607.
2. E. Hecht and E. Hecht, 9. *Interference* (Pearson Education, 2017), p. 441–446.

See discussions, stats, and author profiles for this publication at: <https://www.researchgate.net/publication/329075570>

Measurement of Verdet Constant by Faraday Rotation

Experiment Findings · December 2017

DOI: 10.13140/RG.2.2.34028.41608

CITATIONS

0

READS

828

3 authors, including:



Muhammad Junaid Arshad

Lahore University of Management Sciences

6 PUBLICATIONS 0 CITATIONS

[SEE PROFILE](#)



Muhammad Shiraz Ahmad

Lahore University of Management Sciences

6 PUBLICATIONS 0 CITATIONS

[SEE PROFILE](#)

Some of the authors of this publication are also working on these related projects:



Quantized Vortices in Superconductors [View project](#)



Estimating Quality of Apples Using A Polarization Based Sensor [View project](#)

Measurement of Verdet Constant of different Materials by Faraday Rotation

First Semester Project for MS Physics

Fall 2017
December 14, 2017

Submitted by: Rizwan Abbas 2017-12-0004
 Muhammad Junaid Arshad 2017-12-0005
 Muhammad Shiraz Ahmed 2017-12-0006
Submitted to: Dr. Muhammad Faryad

Department of Physics Syed Babar Ali School of Science and Engineering
Lahore University of Management Sciences, Lahore.

1 Introduction to the Faraday Rotation

In 1845, Michael Faraday discovered the first magneto-optical effect called as “Faraday rotation effect” or “Faraday effect”, which defines the connection between magnetism and light. He was able to rotate the polarization of light when he applied the magnetic field in the same direction as the direction of the light. This effect, known as the Faraday Rotation or Faraday Effect, only occurs when light passes through transparent dielectrics materials, materials which can change the direction of polarized light are called birefringent material. Following figure shows that when a plane polarized light passing through the material of length d which is oriented in the direction of magnetic field the plane of polarized light gets rotated by an angle θ . Faraday effect is caused by left and right circularly polarized waves propagating at slightly different speed, a property known as circularly birefringence. A

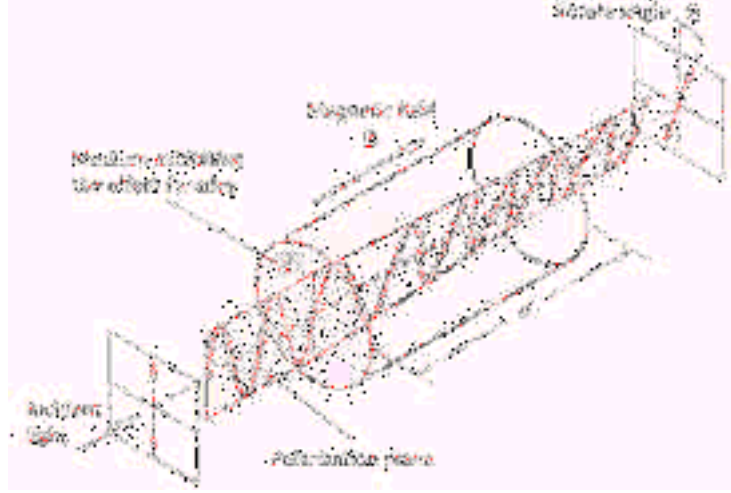


Figure 1: Plane of polarization of light is rotated under the action of magnetic field [1].

linearly polarized light that is seen to rotate in Faraday effect can be seen as consisting of superposition of RCP and LCP light. In circularly polarized light the direction of electric field rotates at the frequency of light either clockwise or counter clockwise. Direction of polarization rotation depends on the properties of the material [3].

2 Birefringence

In an optically anisotropic material the light passing through the material deviates at a specific angle. For example the light passing through the material perpendicular to the optical axis the components of light which are perpendicular to the optical axis show ordinary refractive index and the component of light which are parallel to the optical axis shows some extra-ordinary refractive index due to this difference of refractive index the speed of light change and plane of polarization of light is changed by an angle this is the basic reason of rotation of light when passing through birefringence material. According to Snell's law ,the ray that does not deviate in spite of normal incident is called extra-ordinary ray and has the opposite polarization.

$$\Delta n = n_e - n_o$$

Its significance is that the optical materials can cut to impose specific change in polarization of incident beams e.g half-wave plates are cut to impose $\frac{\pi}{2}$ phase shift. When linearly polarized light travels in a birefringence crystal the phase difference impose on two com-

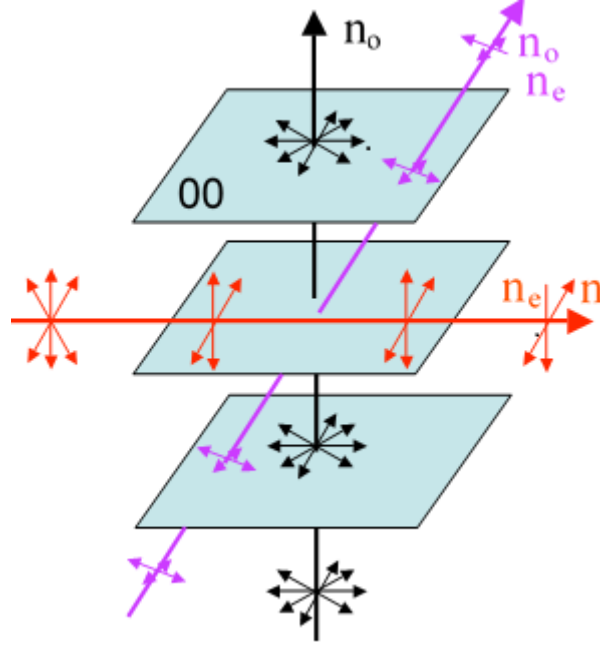


Figure 2: Light passing through the birefringence materials

ponents of light depends on birefringence, crystal thickness L and free space wavelength λ :

$$\Phi_l = \frac{2\pi L}{\lambda} n_l \quad (1)$$

$$\Phi_r = \frac{2\pi L}{\lambda} n_r \quad (2)$$

3 Faraday Magneto-Optic Effect

A non-conducting cylinder of length d is placed in a uniform external magnetic field \vec{B} parallel to its axis, as shown in the above figure. A linearly polarized electromagnetic wave with electric field $\vec{E} = E_i \exp\{i(kz - \omega t)\}$ is incident on one end of the cylinder, where $\omega = 2\pi f$ is the angular frequency of the wave and $k = \frac{\omega}{c}$ is the wave number in vacuum and c is the speed of light. We are going to deduce the small angle $\Delta\phi$ by which the plane of polarization of the transmitted wave is rotated with respect to that of the incident.

3.1 Microscopic Analysis For a Polarizable Gaseous Medium

We first give an analysis for a gaseous medium in which the index of refraction is near unity. Here, we ignore any magnetization of the medium. The sense of the analysis is that there is a different index of refraction for left-handed and right-handed circularly polarized waves that are propagating parallel to the external magnetic field. Then, the left- and right-handed components of a linearly polarized wave possess a phase difference as they traverse in the medium, such that the direction of linear polarization changes with time and distance.

We follow the usual microscopic analysis of the index of refraction of a polarizable medium by deducing the electric dipole moment $\vec{P} = -e\vec{x}$ on an electron of charge $-e$ and mass m that is bound to the origin by a spring of constant $k = m\omega_o^2$ under the influence of the external magnetic field $\vec{B}_o = \vec{H}_o = H_o\hat{z}$ and a weak electromagnetic wave with (transverse) electric field $E_\omega \exp\{i(kz - \omega t)\}$ and $B_\omega = E_\omega \leq B_o$. We suppose that the velocity of the electron in this field is small compared to the speed of light, so that the magnetic field of the wave does not influence the motion of the electron. Then, the equation of motion of the electron is given by:

$$m\ddot{x} = -m\omega_o^2 x - e \left(E_\omega \exp\{i(kz - \omega t)\} + \frac{\vec{v}}{c} \times H_o\hat{z} \right) \quad (3)$$

We consider that the electron is close to the rest i.e. origin and we take the ‘ z ’ as constant now we take the trial solution $x = x_o \exp\{i(kz - \omega t)\}$ putting this into equation number (3) we get:

$$(\omega_o^2 - \omega^2) \vec{x}_o = \frac{\omega_e H_o}{mc} \vec{x}_o \times \hat{z} \quad (4)$$

This shows that the displacement of electron is in xy plane. For any vector \vec{A} that is transverse to the z -axis can be written as:

$$\begin{aligned} \vec{A} &= A_x \hat{x} + A_y \hat{y} \\ \vec{A} &= A_x \left(\frac{\hat{x} + i\hat{y}}{2} + \frac{\hat{x} - i\hat{y}}{2} \right) \\ \vec{A} &= A_- \hat{e}_+ + A_+ \hat{e}_- \end{aligned}$$

where

$$\begin{aligned} A_+ &= \frac{A_x + iA_y}{\sqrt{2}} \\ A_- &= \frac{A_x - iA_y}{\sqrt{2}} \\ \hat{e}_+ &= \frac{x + iy}{\sqrt{2}} \\ \hat{e}_- &= \frac{x - iy}{\sqrt{2}} \end{aligned}$$

thus equation (4) can be written as

$$(\omega_o^2 - \omega^2)(x_o - \hat{e}_+ + x_o - \hat{e}_-) + \frac{\omega e H_o}{mc}(x_o \hat{e}_+ - x_o \hat{e}_-) = -\frac{e}{m}E_{\omega-}\hat{e}_+ + E_{\omega+}\hat{e}_- \quad (5)$$

$$\omega_H = \frac{eH_o}{mc} \quad (6)$$

This is the Larmor frequency of an electron in the static magnetic field \vec{H}_o . The equation of motion in the \hat{e}_{\pm} basis does not mix the x-components (which is the reason we use these basis), so we taking dot product with \hat{e}_{\pm} of equation (5) we have:

$$\begin{aligned} x_{o+} &= -\frac{e}{m} \cdot \frac{E_{\omega+}}{\omega_o^2 - \omega^2 - \omega\omega_H} \\ x_{o-} &= -\frac{e}{m} \cdot \frac{E_{\omega-}}{\omega_o^2 + \omega^2 - \omega\omega_H} \end{aligned}$$

The resulting electric polarization P_w of the medium, with the number density N of electrons is:

$$\vec{P}_w = -Ne\vec{x}\vec{P}_w = -Ne(x_- \hat{e}_+ + x_+ \hat{e}_-) \vec{P}_w = P_w \hat{e}_+ + P_w \hat{e}_-$$

where

$$P = \frac{Ne^2}{m} \cdot \frac{E_w \exp\{i(kz - \omega t)\}}{\omega_o^2 + \omega^2 - \omega\omega_H}$$

we introduce two dielectric constant

$$\begin{aligned} \hat{e}_+ &= 1 + \frac{4\pi Ne^2}{m(\omega_o^2 - \omega^2 - \omega\omega_H)} \\ \hat{e}_- &= 1 + \frac{4\pi Ne^2}{m(\omega_o^2 + \omega^2 - \omega\omega_H)} \end{aligned}$$

now let us take $\omega_p = \sqrt{\frac{4\pi N e^2}{m}}$ which is the plasma frequency of the medium corresponding to the dielectric constants:

$$n_{\pm} = \sqrt{\hat{e}_{\pm}} \quad (7)$$

The wave $E_{\omega-} = E_o(\vec{x} + i\vec{y}) \exp\{i(k_-z - \omega t)\}$ is designated as left handed circularly polarized, and we see that in typical media the velocity of this wave is smaller than that of the right-handed circularly polarized wave $E_{\omega+} = E_o(\vec{x} - i\vec{y}) \exp\{i(k_+z - \omega t)\}$. Here we have the relation $\Delta n = n_+ - n_-$. Since the indices of refraction are different for the LCP and RCP waves inside the medium it follows that the speed, wavelength and wave number will also be different inside the medium. If we assume that the refractive index for left and right circularly light then the phase of the RCP component will be smaller than the phase of LCP component inside the medium of length L .

$$\begin{aligned} \Delta\phi &= \frac{\omega L}{C} \cdot (n_r - n_l) \\ \Delta\phi &= \frac{\omega L}{C} \cdot (\Delta n) \end{aligned}$$

and $\Delta n = n_+ - n_-$ is

$$\begin{aligned} n_{\pm} &= 1 + \frac{\omega_p^2}{2(\omega_o^2 - \omega^2 \pm \omega\omega_H)} \\ \Delta n &= \frac{\omega\omega_H\omega_p^2}{(\omega_o^2 - \omega^2)^2 - \omega^2\omega_H^2} \end{aligned} \quad (8)$$

now equation (1) can be written as by substitution of equation (5), we have

$$\Delta\phi = \frac{e}{2mc^2} \cdot \frac{\omega^2\omega_p^2}{(\omega_o^2 - \omega^2)^2 - \omega^2\omega_H^2} \cdot H_o L \quad (9)$$

where $\frac{\omega^2\omega_p^2}{(\omega_o^2 - \omega^2)^2 - \omega^2\omega_H^2}$ is called the Verdet constant. This change in angle of the polarization of the wave is the Faraday rotation and it is denoted by V .

$$V = \frac{\omega^2\omega_p^2}{(\omega_o^2 - \omega^2)^2 - \omega^2\omega_H^2} \quad (10)$$

3.2 Microscopic Analysis for a Magnetic Medium

Classical models for magnetic media are less satisfactory than those for dielectric media. Here we give a model for the Faraday effect in magnetic media which is fairly plausible, following Becquerel [5]. We suppose that the bulk magnetization density $M = N\mu$ of the (nonconducting) medium is due to a distribution of individual magnetic moments μ at N sites per unit volume. These magnetic moments have fixed locations inside the medium, but the direction of the moment is affected by a magnetic field, $\frac{d\vec{L}}{dt} = \vec{\tau}$ which is equal to $\vec{\mu} \times \vec{B}$, where

$$\vec{L} = -\frac{\vec{\mu}}{\Gamma}$$

is the angular momentum associated with a magnetic moment μ .

$$\frac{d\vec{\mu}}{dt} = \omega_H \times \vec{\mu}$$

Which implies that the magnetic moment $\vec{\mu}$ precesses about the direction of \vec{B} with angular velocity:

$$\begin{aligned}\omega_H &= \frac{eH}{2mc} \cdot \hat{H}(\text{orbital}) \\ \omega_H &= \frac{eH}{mc} \cdot \hat{H}(\text{spin})\end{aligned}$$

The precession occurs even when the moment is exactly parallel or anti parallel to the external field \vec{H} . We now consider the interaction of the magnetic medium with an optical wave that propagates along the z-axis. As we decompose this wave into left- and right-handed circularly polarized components,

$$E_\omega = E_{w-} \exp\{i(k_- z - \omega t)\} \hat{e}_+ + E_{w+} \exp\{i(k_+ z - \omega t)\} \hat{e}_- \quad (11)$$

The electric field vector of the left-handed component $E_{w-} \exp\{i(k_- z - \omega t)\} \hat{e}_+$ rotates with angular velocity $\omega_- \hat{z}$ at a fixed value of z while that of the right-handed component rotates with angular velocity $\omega_+ \hat{z}$. We argue that because of the precession the component of field rotate at different angular velocities,

$$\begin{aligned}\omega_+ &= \omega + \omega_H \\ \omega_- &= \omega - \omega_H\end{aligned}$$

relative to the electronic structure of the medium, so that the index of refraction for these component are

$$n_+ = n(\omega) + \omega_H \frac{dn}{d\omega}$$

$$n_- = n(\omega) - \omega_H \frac{dn}{d\omega}$$

Now taking the difference of the refractive index we have

$$\Delta n = n_+ - n_-$$

$$\Delta n = 2\omega_H \frac{dn_\omega}{d\omega}$$

Then the wave entered the medium at $z = 0$ with linear polarization in the x-direction. The wave at $z = L$ is linearly polarized at angle

$$\Delta\phi = \frac{\Delta n \omega L}{2c}$$

$$\Delta\phi = \frac{\omega \omega_H}{c} \cdot \frac{dn}{d\omega} \cdot L$$

$$\Delta\phi = -\Gamma \frac{\lambda}{c} \cdot \frac{dn}{d\lambda} \cdot H_o$$

$$V = -\Gamma \frac{\lambda}{c} \cdot \frac{dn}{d\lambda} \tag{12}$$

$$V = -\frac{e}{2mc^2} \cdot \lambda \cdot \frac{dn}{d\lambda} (orbital) \tag{13}$$

$$V = -\frac{e}{mc^2} \cdot \lambda \cdot \frac{dn}{d\lambda} (spin) \tag{14}$$

Here V is the Verdet constant of the medium. Note that $\frac{dn}{d\lambda}$ is negative for typical optical materials. The Verdet constant for some diamagnetic materials is reasonably close to the form of above for orbital magnetization [6]. The Verdet constant for many diamagnetic materials is closer to 1/2 of the orbital prediction [7]. The largest Verdet constants are obtained with glassy materials doped with para-magnetic ions [8], for which, however, equa. (13) and (14) are not a particularly good description of Verdet constant.

3.3 Experimental setup

In this section we take a look at the experimental setup used in this project. The actual picture of the setup is also shown in the next section but this is the schematic of the setup. Here we see we have unpolarized light coming out of laser then using the polarizer we polarize it and then allowing it to go through the Helmholtz (Physics already explained) we collect the final light on Photodetector.

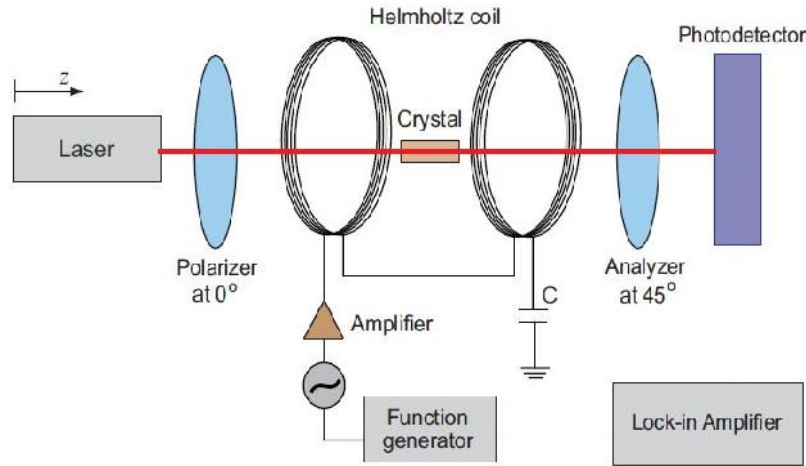


Figure 3: Schematic illustration of experimental setup for Faraday rotation [2].

The use of function generator was to provide ac signal at the resonating frequency of around 800 kHz. Where lock-in Amplifier was used to measure the small alternating component of our signal.

4 Results and Conclusions

Here we use a modified method to measuring the Verdet constant for Water, Air , Sugar solution and Iso-propanol at a wavelength of 405 nm. We use gaussmeter to measure the magnetic field inside the coils. We plot the measured value of current as a function of magnetic field for different substances as shown in figures below. As the magnetic field \vec{B} between Helmholtz coils is not constant but is a function of position so we tried to maintain our sample in the center of two coils where usually the magnetic field of the Helmholtz coils is uniform.

4.1 Verdet constant of water

In the first part we measured the i_{dc} the dc component of the signal. For this part the magnetic field was turned off but the water in the sample container was in its place at the center of the coils. Further details of performing this activity are already given in the lab manual so skipping that part we get to the next task that is to measure the alternating component of our signal. For this part magnetic field was turned on and at the fixed value of 90 G we recorded the change in i_{ac} by varying the angle of analyzer in steps of 10° . Then using the data we made a plot of i_{ac} Vs θ as in shown in Fig. 5 which shows the maximum rotation at an angle of 45° . Next we fixed the analyzer at the maximum rotation angle i.e. 45° with respect to polarizer. Then by increasing magnetic field in steps of 10 G we recorded the value for i_{ac} from lock-in amplifier (reason and process for using lock-in amplifier are given in student manual). Then finally we plotted the i_{ac} Vs B and using the least square fit (straight line fit) from the slope of the graph using the equation $\theta_{rms} = V B_{rms} d$ (for uniform magnetic field) we get $V = (8.8 \pm 0.9) \times 10^{-6} \text{ rad G}^{-1} \text{ cm}^{-1}$. We calculated the uncertainty in our measurement of Verdet constant using error analysis techniques learned in first few lectures.

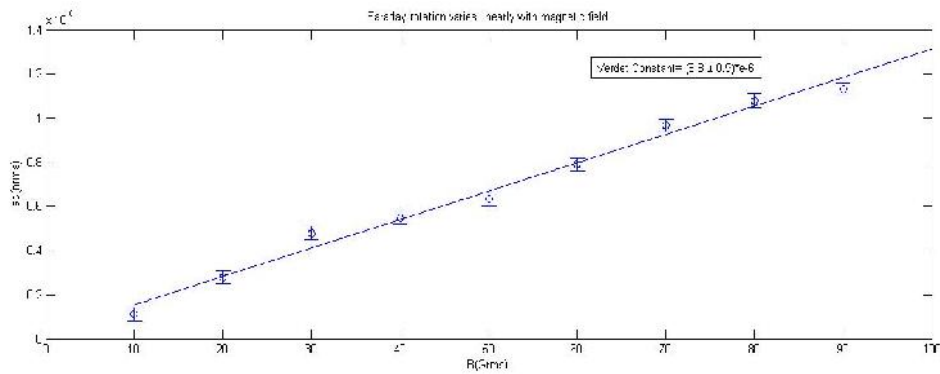


Figure 4: Verdet constant of water

```

1 x=[10:10:90];
2 y=[0.1113, 0.2791, .4802, 0.5501, 0.6327 , 0.79109, 0.9674, 1.0787,
   1.1311 ].*1e-9;
3 e=[0.03, 0.03, 0.03, 0.03, 0.03, 0.03, 0.03, 0.03, 0.03].*1e-9
4 plot(x,y,'o')
5 hold on
6 errorbar(x,y,e,'o');
7 hold on

```

```

8 a=lsqcurvefit(@line123,[1 1],x,y);
9 x1=10:0.01:110;
10 y1=line123(a,x1);
11 plot(x1,y1);
12 title('Faraday rotation varies linearly with magnetic field');
13 xlabel('B(Grms)');
14 ylabel('iac(nrms)');
15
16 %% Slope calculation
17 l=0;
18 m=0;
19 xmean=mean(x);
20 for c=1:1:9
21     l=l+(y(c).*(x(c)-xmean));
22     m=m+(x(c)-xmean).^2;
23 end
24 slope=l/m
25
26 %% Uncertainty in slope
27 uiny=0.03e-9
28 uinslope= uiny*(sqrt(9/m))
29
30 %% calculation of verdet constant
31 v=slope/(169.16e-9*(sqrt(2))^2*4.285)
32 uinv=sqrt((uinslope/(169.16e-9*(sqrt(2))^2*4.285))^2+((v*(0.003e-9))/
    169.16e-9)^2+ ((v*(0.2)/4.285)^2))

```

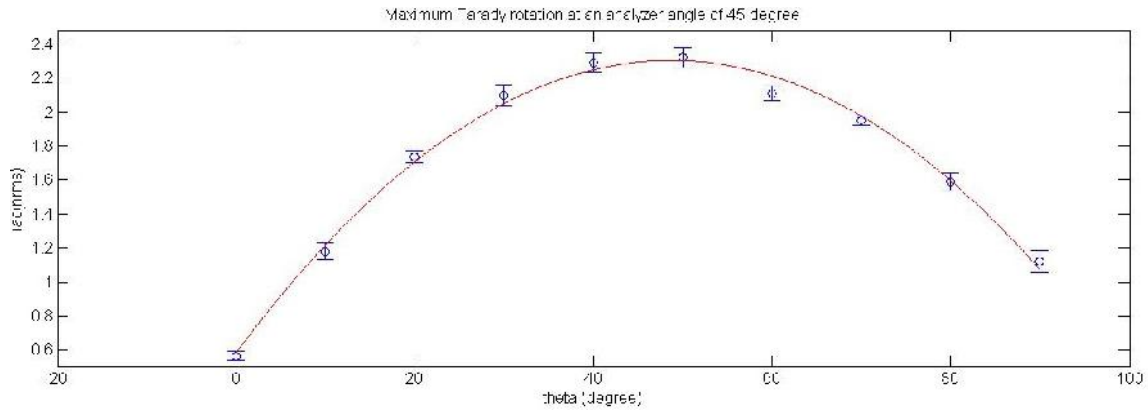


Figure 5: Faraday rotation varies with analyzer angle

```

1 x=[0:10:90];
2 y=[0.5636, 1.1812, 1.7371, 2.0993, 2.2907, 2.3221, 2.1121, 1.9521,
    1.5921,1.1223]
3 e=[0.013, 0.024, 0.017, 0.031, 0.027, 0.029, 0.022, 0.014, 0.025,
    0.03].*2
4 plot(x,y,'o')
5 hold on
6 errorbar(x,y,e,'o');
7 hold on
8 a=lsqcurvefit(@quad123,[1 1 1],x,y);
9 x1=0:0.01:90;
10 y1=quad123(a,x1);
11 plot(x1,y1,'r');
12 title('Maximum Farady rotation at an analyzer angle of 45 degree');
13 xlabel('theta');
14 ylabel('iac(nrms)');
15 axis tight

```

4.2 Verdet constant for air

Similarly in the foot steps of our above discussed method we tried to measure the Verdet constant of Air but with slight modifications to our experimental setup. For this part there was no sample placed at the center of the coils instead what we did was to place two iron plates on either side of the coils and made small hole in them just about the size of laser

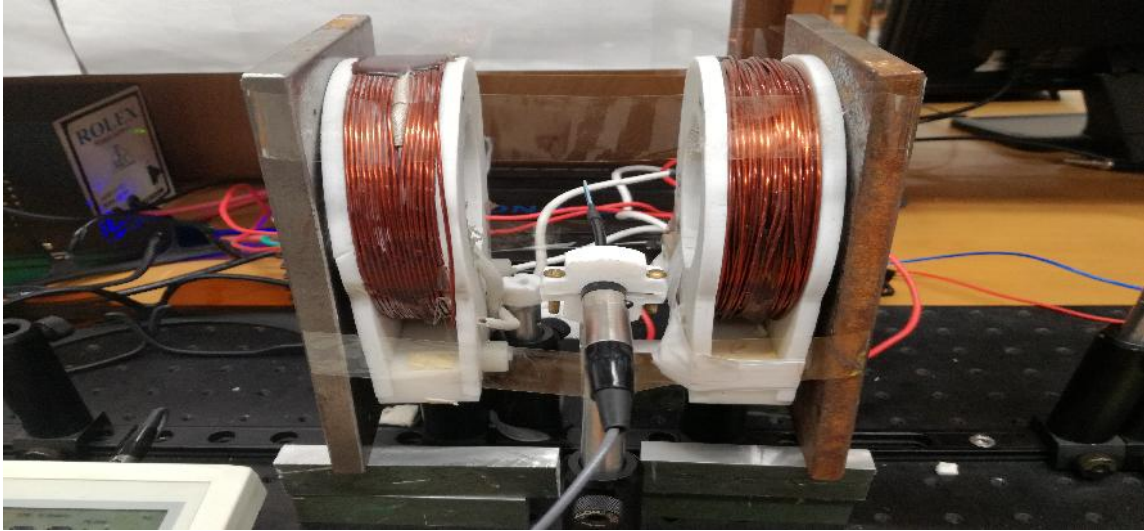


Figure 6: Modification to minimize the effect of Magnetic field away from coils

light to allow the light to pass through them. The main reason for using these iron plates was to make sure that only the air in between the coils is under the influence of magnetic field so that we can have the rough estimate of the sample length (air under consideration). SUGGESTION: By doing this we realized that this addition of iron bars could be made a part of the original step because in this experiment as we require magnetic field to be only limited near the sample and not far away i.e. we don't want the field to extend to photo diode, polarizer or analyzer because this might in turn make our calculation wrong since the application of field on those elements of experimental setup might in turn generate more Faraday rotation if those things are dielectric in nature. Finally doing the same experimental procedure first we measured the i_{dc} and afterwards measured i_{ac} and then the plot of i_{dc} Vs θ as shown in Fig. 11 again shows the maximum rotation at angle of 45° . Then finally we plotted the i_{ac} Vs B then using the least square fit (straight line fit) from the slope of the graph using the equation $\theta_{rms} = V B_{rms} d$ (for uniform magnetic field) we found out $V = (1.01 \pm 0.03) \times 10^{-6} \text{ rad } G^{-1} \text{ cm}^{-1}$. We calculated the uncertainty in our measurement of Verdet constant using error analysis techniques learned in first few lectures of this graduate lab course.



Figure 7: Magnetic field near coils

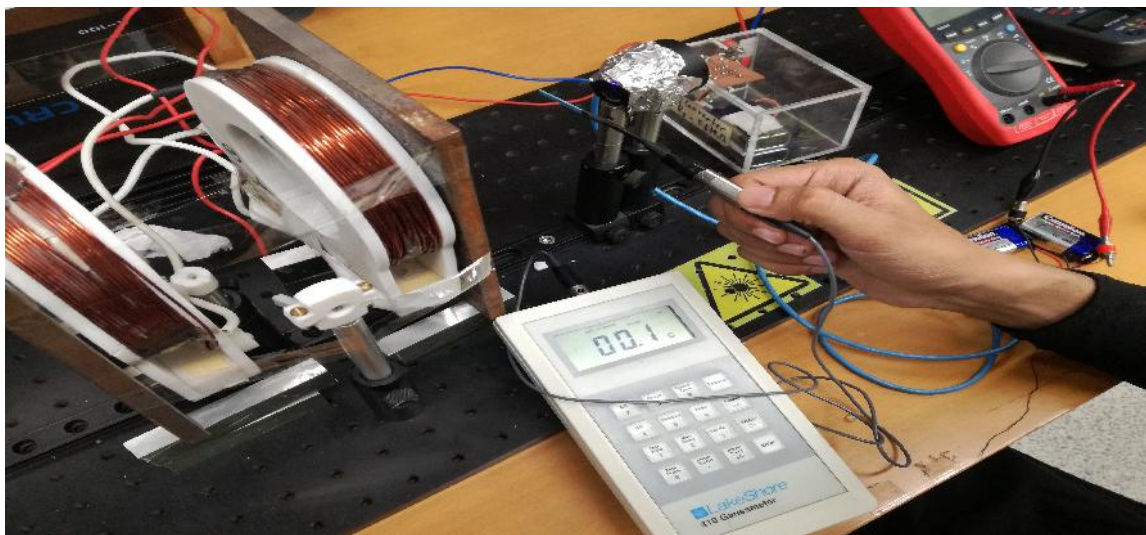


Figure 8: Magnetic field near the Photo diode

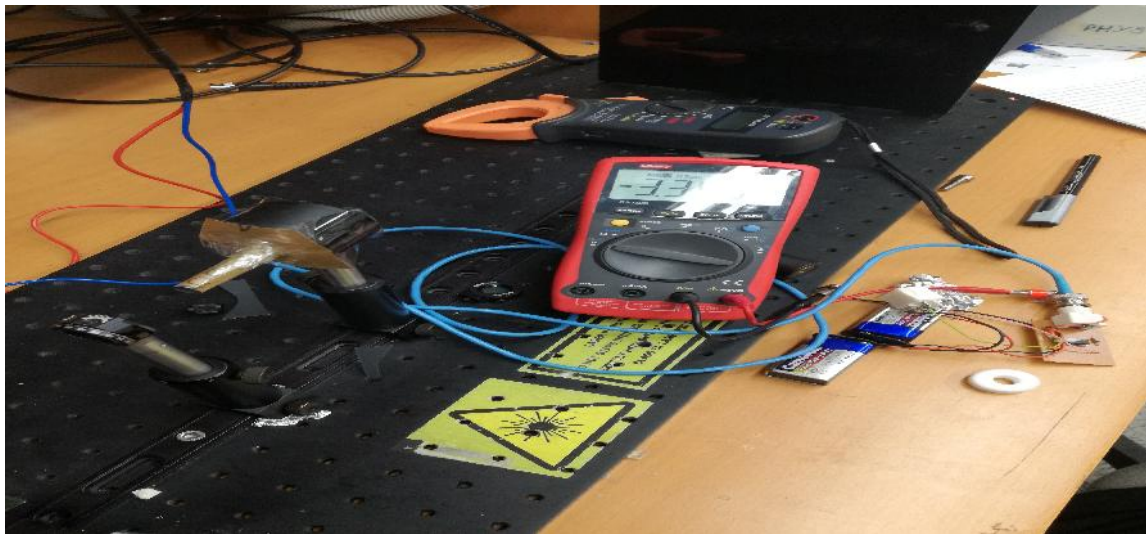


Figure 9: Covered the Photo diode to avoid stray light

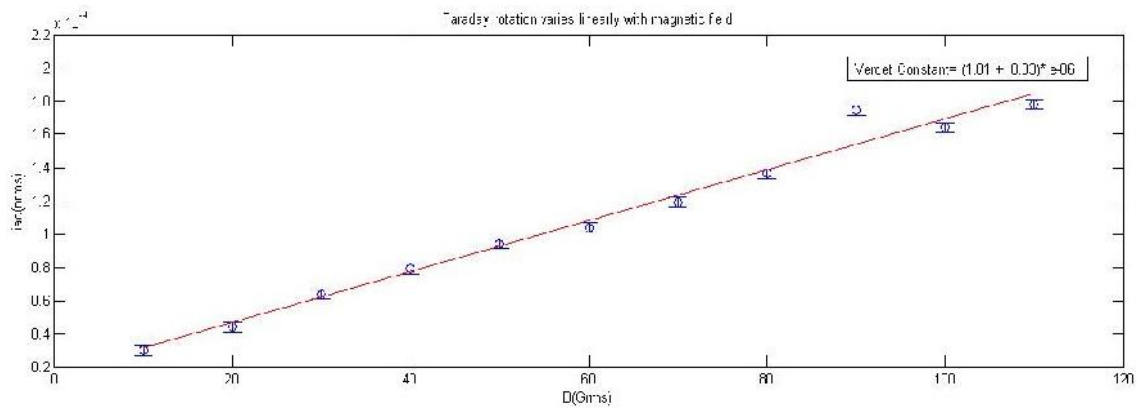


Figure 10: Verdet constant of air

```

1 x=[10:10:110];
2 y=[0.3, 0.440, .638, .790, .940 , 1.037, 1.193, 1.363, 1.743, 1.640,
   1.779].*1e-9;
3 e=0.03.*1e-9;
4 plot(x,y,'o')
5 hold on
6 errorbar(x,y,e,'o');
7 hold on

```

```

8 a=lsqcurvefit(@line123,[1 1],x,y);
9 x1=10:0.01:110;
10 y1=line123(a,x1);
11 hold on
12
13 plot(x1,y1,'r');
14 title('Faraday rotation varies linearly with magnetic field');
15 xlabel('B(Grms)');
16 ylabel('iac(nrms)');
17
18 %% Slope calculation
19 l=0;
20 m=0;
21 xmean=mean(x);
22 for c=1:1:11
23     l=l+(y(c).*(x(c)-xmean));
24     m=m+(x(c)-xmean).^2;
25 end
26 slope=l/m
27
28 %% Uncertainty in slope
29 uiny=0.03e-9
30 uinslope= uiny*(sqrt(11/(11*sum(x.^2)-(sum(x)).^2)))
31
32 %% Calculation of verdet constant
33 v=slope/(0.549e-6*(sqrt(2))^2*13.843)
34 uinv=sqrt((uinslope/(0.549e-6*sqrt(2)*13.843))^2+((v*(0.003e-9))/
    0.549e-6)^2+ ((v*(0.2)/13.843)^2))

```

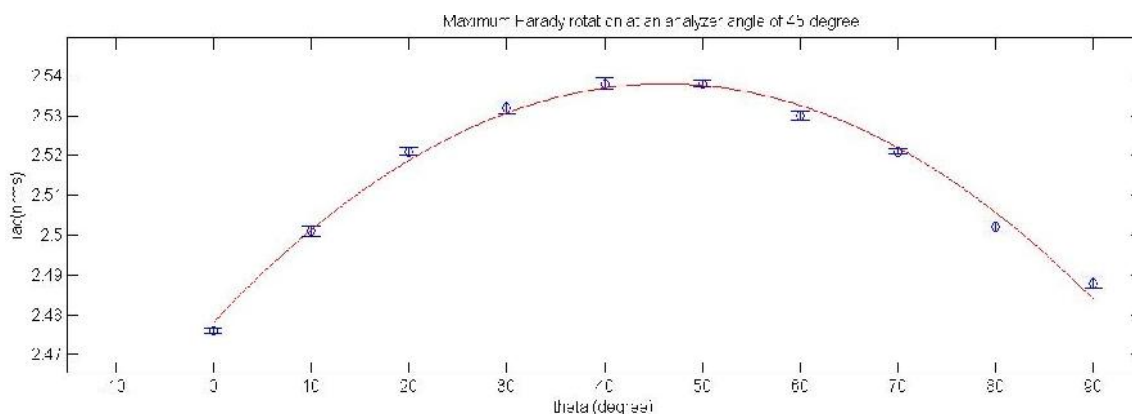


Figure 11: Faraday rotation varies with analyzer angle

```

1 x=[0:10:90];
2 y=[2.476, 2.501, 2.521, 2.532, 2.538,2.538,2.530,2.521,2.502, 2.488]
3 e=[0.013, 0.024, 0.017, 0.031, 0.027, 0.019, 0.022, 0.014, 0.025,
    0.03].*0.5e-1
4 plot(x,y,'o')
5 hold on
6 errorbar(x,y,e,'o');
7 hold on
8 a=lsqcurvefit(@quad123,[1 1 1],x,y);
9 x1=0:0.01:90;
10 y1=quad123(a,x1);
11 plot(x1,y1,'r');
12 title('Maximum Faraday rotation at an analyzer angle of 45 degree');
13 xlabel('theta');
14 ylabel('iac(nrms)');
15 axis tight

```

4.3 Verdet constant for Sugar solution

For sugar solution all the setup arrangement was same as that for water solution except that now instead of water we had sugar solution in the sample container. Again following the same procedure we found out Verdet constant of sugar solution with a concentration of 0.1g/mol from the slope of the graph using the equation $\theta_{rms} = V B_{rms} d$ (for uniform magnetic field) to be $V = (3.6 \pm 0.2) \times 10^{-5} \text{ rad } G^{-1} \text{ cm}^{-1}$. We calculated the uncertainty

in our measurement of Verdet constant using error analysis techniques learned in first few lectures of this course.

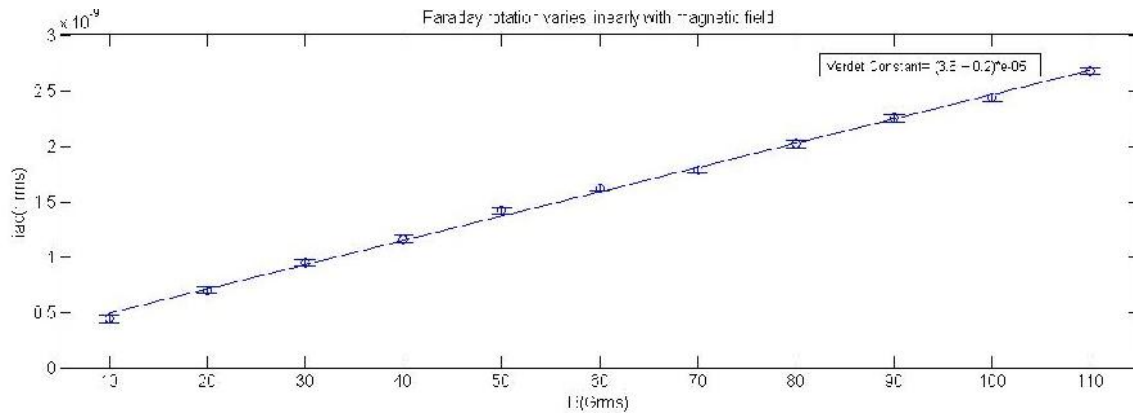


Figure 12: Verdet constant of sugar solution

```

1 x=[10:10:110];
2 y=[0.443, 0.701, .950, 1.163, 1.417, 1.622, 1.784, 2.020, 2.251,
   2.433, 2.675].*1e-9;
3 e=[0.03, 0.03, 0.03, 0.03, 0.03, 0.03, 0.03, 0.03, 0.03, 0.03,
   0.03].*1e-9
4 plot(x,y,'o')
5 hold on
6 errorbar(x,y,e,'o');
7 hold on
8 a=lsqcurvefit(@line123,[1 1],x,y);
9 x1=10:0.01:110;
10 y1=line123(a,x1);
11 plot(x1,y1);
12 title('Faraday rotation varies linearly with magnetic field');
13 xlabel('B(Grms)');
14 ylabel('iac(nrms)');
15
16 %% Slope calculation
17 l=0;
18 m=0;
19 xmean=mean(x);
20 for c=1:1:11

```

```

21     l=l+(y(c).*(x(c)-xmean));
22     m=m+(x(c)-xmean).^2;
23 end
24 slope=l/m
25
26 %% Uncertainty in slope
27 uiny=0.03e-9
28 uinslope= uiny*(sqrt(11/(11*sum(x.^2)-(sum(x)).^2)))
29
30 %% Calculation of verdet constant
31 v=slope/(72e-9*(sqrt(2))^2*4.285)
32 uinv=sqrt((uinslope/(72e-9*sqrt(2)*4.285))^2+((v*(0.003e-9))/ 72e-9)
    ^2+ ((v*(0.2)/4.285)^2))

```

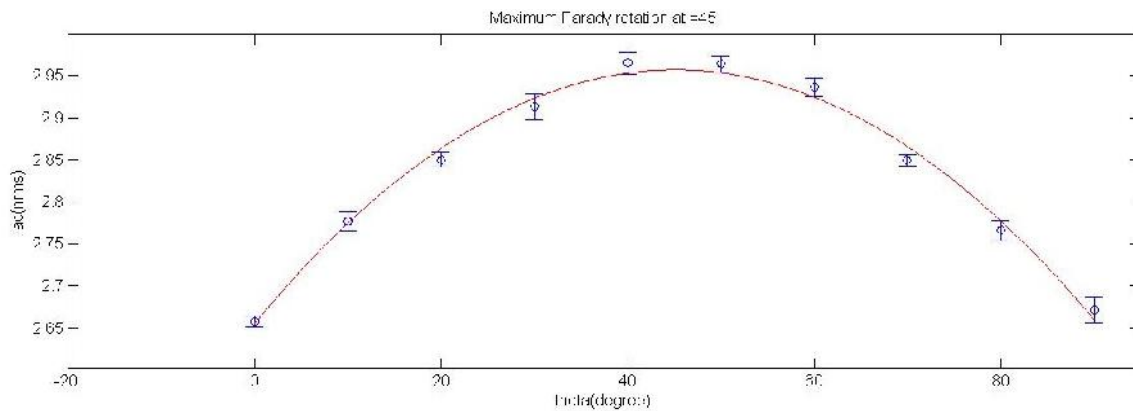


Figure 13: Faraday rotation varies with analyzer angle

```

1 x=[0:10:90];
2 y=[2.658, 2.777, 2.850, 2.913, 2.965, 2.964, 2.936, 2.850, 2.766,
    2.671]
3 e=[0.013, 0.024, 0.017, 0.031, 0.027, 0.019, 0.022, 0.014, 0.025,
    0.03].*0.5
4 plot(x,y,'o')
5 hold on
6 errorbar(x,y,e,'o');
7 hold on
8 a=lsqcurvefit(@quad123,[1 1 1],x,y);

```

```

9 x1=0:0.01:90;
10 y1=quad123(a,x1);
11 plot(x1,y1,'r');
12 title('Maximum Farady rotation at an analyzer angle of 45 degree');
13 xlabel('theta');
14 ylabel('iac(nrms)');

```

4.4 Verdet constant for Isopropanol

Again for Isopropanol we performed the experiment and found out the value of Verdet constant from the slope of the graph using the equation $\theta_{rms} = V B_{rms} d$ (for uniform magnetic field) we get $V = (2.7 \pm 0.4) \times 10^{-5} \text{ rad } G^{-1} \text{ cm}^{-1}$. Here again we calculated the uncertainty in our measurement using error analysis techniques learned in first few lectures of this course.

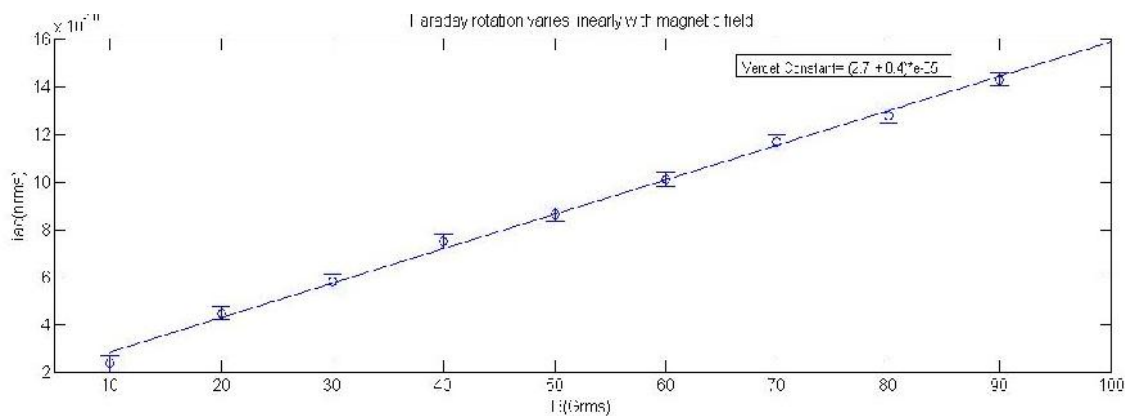


Figure 14: Verdet constant of isopropanol

```

1 x=[10:10:90];
2 y=[0.2376, 0.4479, .5802, 0.7501, 0.8627 , 1.0109, 1.1674, 1.2787,
   1.4311].*1e-9;
3 e=[0.03, 0.03, 0.03, 0.03, 0.03, 0.03, 0.03, 0.03, 0.03].*1e-9
4 plot(x,y,'o')
5 hold on
6 errorbar(x,y,e,'o');
7 hold on
8 a=lsqcurvefit(@line123,[1 1],x,y);

```

```

9  x1=10:0.01:110;
10 y1=line123(a,x1);
11 plot(x1,y1);
12 title('Faraday rotation varies linearly with magnetic field');
13 xlabel('B(Grms)');
14 ylabel('iac(nrms)');
15
16 %% Slope calculation
17 l=0;
18 m=0;
19 xmean=mean(x);
20 for c=1:1:9
21     l=l+(y(c).*(x(c)-xmean));
22     m=m+(x(c)-xmean).^2;
23 end
24 slope=l/m
25
26 %% Uncertainty in slope
27 uiny=0.03e-9
28 uinslope= uiny*(sqrt(9/m))
29
30 %% Calculation of verdet constant
31 v=slope/(65.96e-9*(sqrt(2))^2*4.285)
32 uinv=sqrt((uinslope/(56.96e-9*sqrt(2)*4.285))^2+((v*(0.003e-9))/ 56.96
    e-9)^2+ ((v*(0.2)/4.285)^2))

```

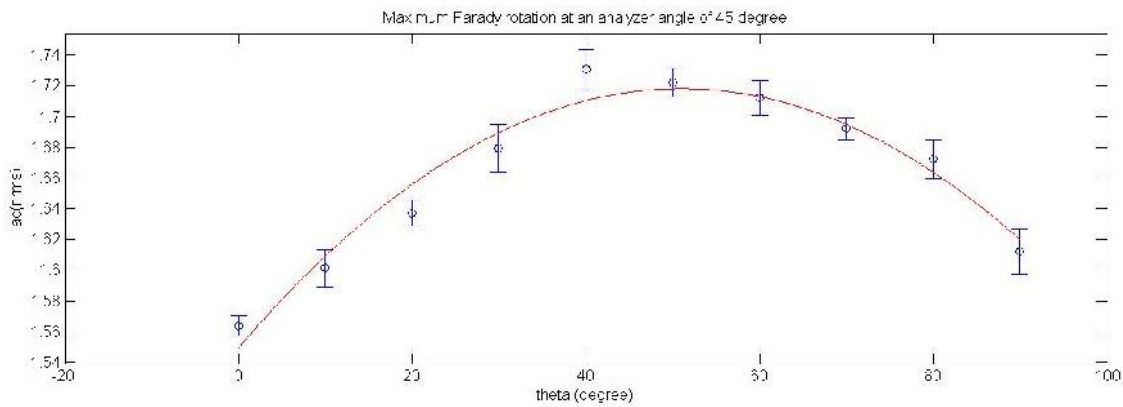


Figure 15: Faraday rotation varies with analyzer angle

```

1 x=[0:10:90];
2 y=[1.5636, 1.6012, 1.6371, 1.6793, 1.7307, 1.7221, 1.7121, 1.6921,
    1.6721,1.6123]
3 e=[0.013, 0.024, 0.017, 0.031, 0.027, 0.019, 0.022, 0.014, 0.025,
    0.03].*0.5
4 plot(x,y,'o')
5 hold on
6 errorbar(x,y,e,'o');
7 hold on
8 a=lsqcurvefit(@quad123,[1 1 1],x,y);
9 x1=0:0.01:90;
10 y1=quad123(a,x1);
11 plot(x1,y1,'r');
12 title('Maximum Faraday rotation at an analyzer angle of 45 degree');
13 xlabel('theta');
14 ylabel('iac(nrms)');

```

4.5 Table of the verdet constant of the our materials

Sample	Wavelength (nm)	Verdet Constant (rad/G cm)
Air	405	$(1.01 \pm 0.03) \times 10^{-6}$
Sugar Solutions	405	$(3.6 \pm 0.2) \times 10^{-5}$
Isopropanol	405	$(2.7 \pm 0.4) \times 10^{-5}$
Water	405	$(8.8 \pm 0.9) \times 10^{-6}$

Table 1: Verdet Constant of the materials

5 Conclusion

In the conclusion we summarize results of our project. Initially we tried to measure the Verdet constant of Air. For that we made certain changes to our already designed experimental setup as shown in pictures above but after performing the experiment our results varied quite significantly from the published value $1.39 \times 10^{-9} \text{ rad } G^{-1} \text{ cm}^{-1}$ at 634.8 nm [9]. The huge difference could be associated to the fact that we tried to measure the Verdet constant of air which is of the order of nano rad $G^{-1} \text{ cm}^{-1}$. So the experiment required quite a sensitive way to measure it, but the modification we did were not quite up to the mark or may be we were not able to fully eliminate the effect of field in the surroundings. Because whether the field is parallel to the direction of light or not makes a huge difference in the overall results. Also the electronic devices placed around our experimental setup might as well have disturbed our measurements. After that we tried to calculate the Verdet constant for different other materials which was in good agreement with the published values. For water published value was $3.35 \times 10^{-6} \text{ rad } G^{-1} \text{ cm}^{-1}$ at 20° C at a wavelength of 632.8 nm [10]. We calculated the value $8.8 \times 10^{-6} \text{ rad } G^{-1} \text{ cm}^{-1}$ at 405 nm. Similarly for Isopropanol already found out value given on Physlab website (final year thesis presentation) was close to $2.2 \times 10^{-5} \text{ rad } G^{-1} \text{ cm}^{-1}$ at 20° C at a wavelength of 405 nm and we calculated the value $2.7 \times 10^{-5} \text{ rad } G^{-1} \text{ cm}^{-1}$ at 405 nm. For the sugar solution we were not able to find the suitable reference value so it is being reported without any reference.

6 References

1. www.bbvaopenmind.com/en/faraday-electromagnetic-theory-light/
2. Student manual Physlab <http://physlab.org/experiment/faradays-effect/>

3. Optics and Laser Physics Laboratory Linear Polarization of Light, Miami University, 2014.
4. Physics Experiment, University of Michigan, 341(4), 2010, 1-18.
5. H. Becquerel, The Faraday and Zeeman Effects, *Comptes Rendus* 125, 679 (1897).
6. F.L. Pedrotti and P. Bandettini, Faraday rotation in the undergraduate advanced laboratory, *Am. J. Phys.* 58, 542 (1990),
7. C.G. Darwin and W.H. Watson, The Constants of Magnetic Dispersion of Light, *Proc. Roy. Soc. London A* 114, 27 (1927),
8. R.D. Herpst, Huge Verdet Constant (International Crystal Laboratories),
9. Chia-Yu Chang, *Review of Scientific Instruments* 82, 063112 (2011); <https://doi.org/10.1063/1.3602927>
10. A. B. Villaverde and D. A. Donatti, "Verdet Constant of Liquids," *Journal Chemical Physics*. 71 (10), 4021 - 4024 (1979).

Newton's cradle

Muhammad Shiraz Ahmad and Muhammad Sabieh Anwar*

Department of Physics, Syed Babar Ali School of Science and Engineering

May 6, 2019, Version 2019-01

Newton's cradle¹ is a device that demonstrates conservation of momentum and energy using a series of swinging spheres. When one sphere at the end is lifted and released, it strikes the stationary spheres, transmitting a force through the stationary spheres that pushes the last sphere upward. The last sphere swings back and strikes the still nearly stationary spheres, repeating the effect in the opposite direction. In this experiment, we will verify energy conservation laws using video tracking.

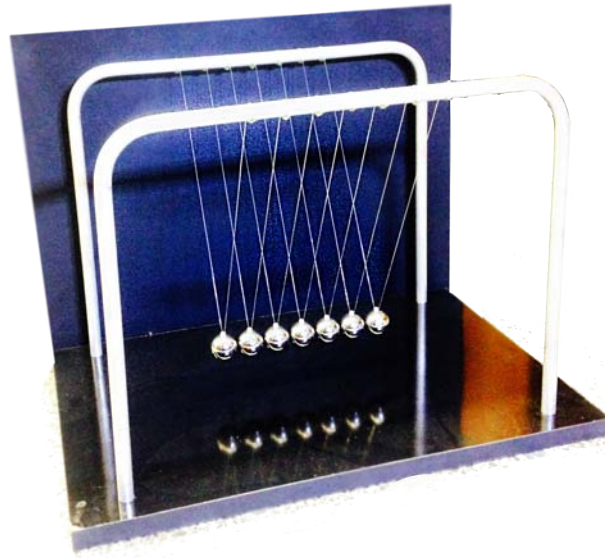


Figure 1: Newton's cradle consists of aligned spheres.

Major specifications of Newton's cradle

Number of spheres	07
Radius of each sphere	1.25 cm
Mass of each sphere	66.1 g

*This document is released under the CC-BY-SA License. Please attribute to the authors.

¹The device is named after the 17th-century English scientist Sir Isaac Newton. It is also known as Newton's Balls or Executive Ball Clicker.

1 Objectives

In this experiment, we will,

1. track the motion of Newton's cradle, by recording video a camera, in the following configurations:
 - (a) The far right ball is pulled away and let go.
 - (b) The far right and the far left balls are simultaneously pulled away and let go.
 - (c) A set of two balls from the far right are pulled away and let go.
2. Further more, using recorded videos of these experiments, we will obtain graphs of:
 - (a) K.E. of all balls,
 - (b) P.E. of all balls,
 - (c) velocities of all balls, and
 - (d) acceleration of all balls.

Your instructor will guide you on which experimental configurations will you be required to test.

2 The Experiment

The experimental configuration is shown in Figure 2. This experiment employs video based tracking using PhysTrack—our MATLAB based solution for videos tracking. The video should be recorded with high frame rate (i.e. 240 frames per second). The latest version can be downloaded from the website http://bit.ly/PhysLab_PhysTrack. Interpret your data and discuss with the instructor.

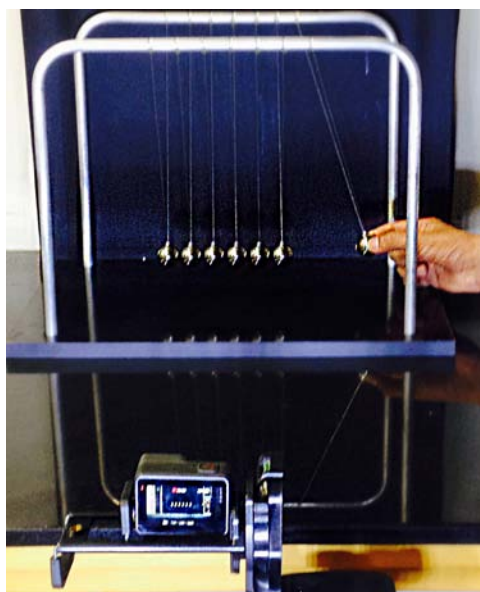


Figure 2: Releasing the right most sphere in Newton's cradle.

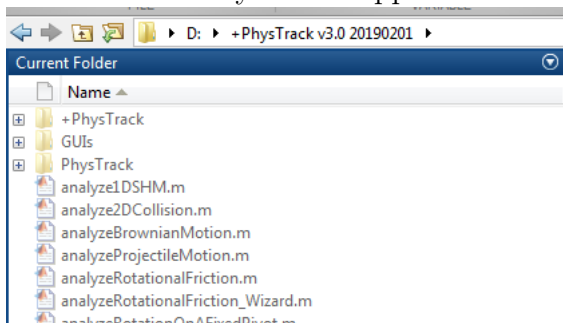
3 Tracking the Recorded Videos

The heart of this experiment is to extract the kinematics from recorded videos. At this point, we expect that you have recorded the video. By going through the following steps, you can extract the experimental data from the video using **PhysTrack**:

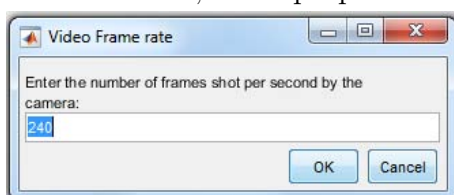
1. Download the Phystrack (the zipped file) from the url http://bit.ly/PhysLab_PhysTrack
2. Extract the downloaded zipped file into your PC's local directory.

Name	Date modified	Type	Size
+PhysTrack	5/6/2019 1:16 PM	File folder	
GUIs	5/6/2019 1:16 PM	File folder	
PhysTrack	5/6/2019 1:16 PM	File folder	
analyze1DSHM	1/1/2019 5:06 PM	Wolfram Mathem...	4 KB
analyze2DCollision	1/1/2019 5:06 PM	Wolfram Mathem...	12 KB
analyzeBrownianMotion	1/2/2019 1:30 PM	Wolfram Mathem...	4 KB
analyzeProjectileMotion	1/1/2019 4:31 PM	Wolfram Mathem...	6 KB
analyzeRotationalFriction	1/2/2019 3:33 PM	Wolfram Mathem...	11 KB
analyzeRotationalFriction_Wizard	1/1/2019 1:31 PM	Wolfram Mathem...	1 KB
analyzeRotationOnAFixedPivot	1/1/2019 5:06 PM	Wolfram Mathem...	4 KB
analyzeSlidingFriction	1/2/2019 1:33 PM	Wolfram Mathem...	5 KB
analyzeWilberforcePendulum	1/1/2019 5:05 PM	Wolfram Mathem...	4 KB
analyzeWilberforcePendulum_DCS	10/5/2018 6:08 PM	Wolfram Mathem...	1 KB
GeneralPurposeTracker	1/1/2019 5:05 PM	Wolfram Mathem...	3 KB
RunWizard	1/2/2019 3:55 PM	Wolfram Mathem...	1 KB
Start	1/2/2019 3:59 PM	Wolfram Mathem...	1 KB

3. Run MATLAB and change it's current folder to the same directory where you have extracted the PhysTrack zipped file.



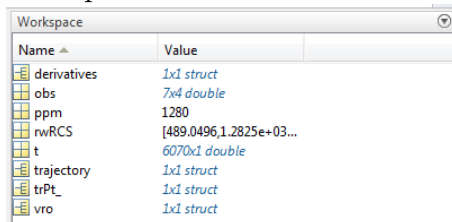
4. In the command window, type “GeneralPurposeTracker” and press **Enter**.
5. A new option will pop up to select the desired video, pick the video to be processed.
6. After selecting the video, a option will appear asking for the frame rate of the selected video, write proper frame rate and click on **OK**.



7. Video trimming option will emerge; pick the proper **mark--in** and **mark--out** frame and click on **Close** .



8. The “Object Selector Option” will pop up. Mark all the spheres as an object by clicking on “Manually mark an object” and then select the spheres one by one. After that, click on **Close** .
9. Now, KLTGUI named option will pop up, click on the button **Begin** and wait for the process to complete.
10. After completing these steps, the script will generate a lot of useful variables in the workspace of MATLAB that can be used as required.

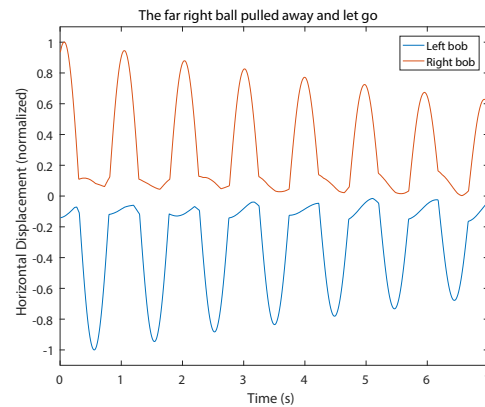
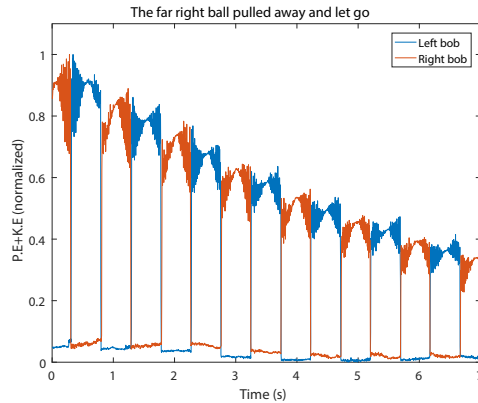
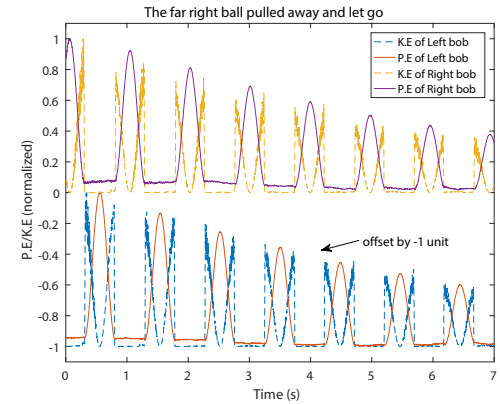
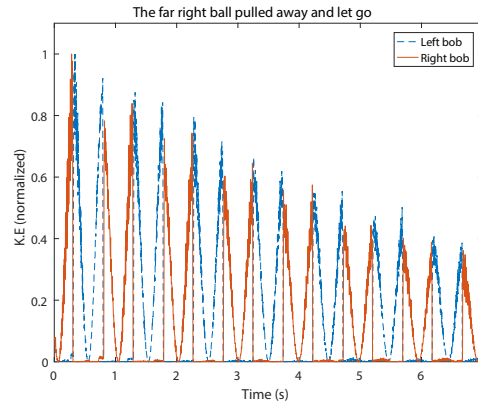
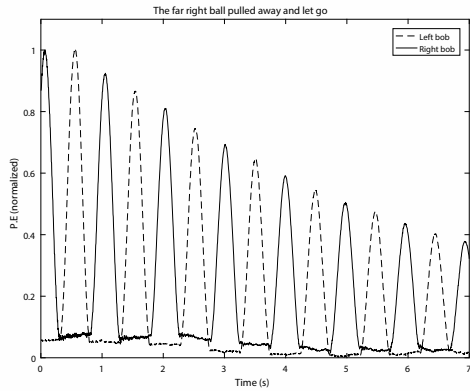


11. Following are the variables that will be used in this experiment:

List of useful variables	
t	time (s)
trajectory.tp1.x	x profile of first sphere
trajectory.tp1.y	y profile of first sphere
trajectory.tp2.x	x profile of second sphere
trajectory.tp2.y	y profile of second sphere
⋮	⋮

12. **Numerical Differentiation:** For speeds and accelerations, we need to determine numerical derivatives. For this purpose, one could use the following command.
`[xd, yd] = PhysTrack.deriv(xdata, ydata, order)`

Newton's cradle: video tracking and analysis with matlab



Experimenting with a linear air track

Muhammad Shiraz Ahmad and Muhammad Sabieh Anwar*

Syed Babar Ali School of Science and Engineering, LUMS

May 27, 2019
Version 2019-v1

An air track is a perforated rail which is connected to an air blower. Compressed air is sprayed from the holes and forms a thin layer on the surface of the track. This layer fills the space between the air track and the inner surface of a glider. As a result, the movement of the glider can be regarded as almost friction-free. This apparatus can be used to experimentally study important concepts in kinematics such as velocity, acceleration, momentum, collisions, and kinetic energy. It is an ideal teaching aid for physics. In this experiment, we provide students with an opportunity to explore some of these ideas through experiments that they can devise on their own.

KEYWORDS

Speed; acceleration; momentum; kinetic energy; friction; acceleration due to gravity; free body diagram; photogate

1 Objectives

In this experiment, we will,

1. understand concepts of instantaneous and average speeds and measure them using a photogate;
2. measure acceleration;
3. find momentum and its possible conservation during collisions;
4. learn how to use graphical data to infer physical quantities and commenting on their uncertainties;
5. learn about a free body diagram and observe Newton's force law in action;
6. measure effects of friction and energy losses.

*This document is released under the CC-BY-SA License. Please attribute to the authors.

Your instructor will guide you on which experimental configurations you will be required to investigate. We largely expect students to come up with their own experimental strategy to investigate various phenomena. Now let's get you started.

2 The Experiment

The experimental setup comprising the air track connected with an air blower and a pulley affixed on its edge is shown in Figure 1. The glider is a V-shaped metal frame that glides on the air cushion. Each glider has two flags attached on its edges. Their motion is detected with the help of photogates which are connected with the computer through Physlogger, which is our data logging device. During its motion, when glider passes through the inverted U shaped arms of the photogate, the Physlogger channel detects two rectangular pulses, one when the flag at the entering edge of the glider passes through the photogate and second when the flag at the leaving edge passes through the photogate.

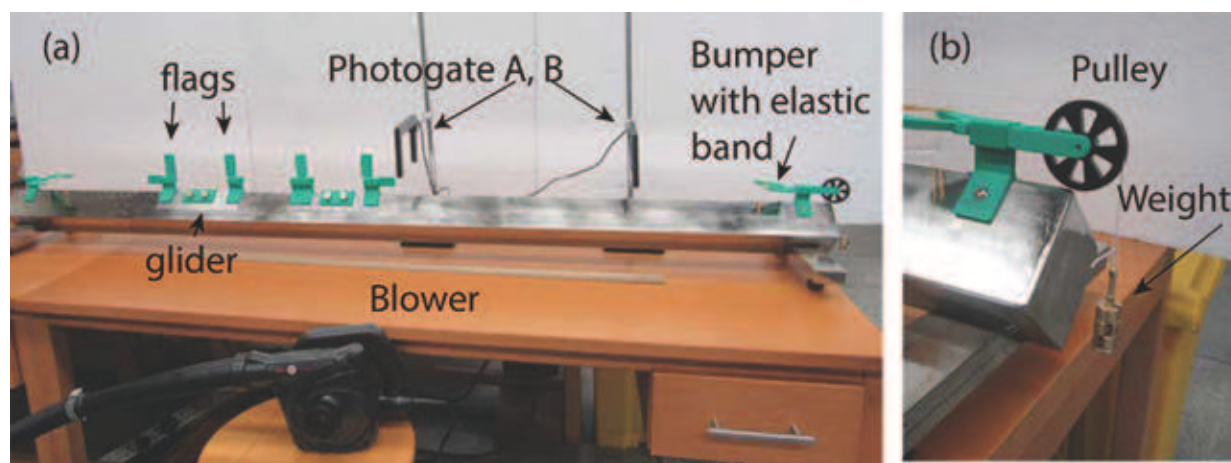


Figure 1: A photograph showing the (a) air track with all its accessories and (b) a close-up of the end pulley which allows a weight to be hung from a thread.

3 Preparing for the experiment

Before starting the experiment, make sure to verify the following aspects.

1. The air blower is turned on. **Turn on the air blower only when required. Do not keep the blower on for more than ten minutes. This will prevent over heating and damage to the blower. The experiments are brief and should be briskly conducted. The blower should be turned off during the data analysis stage.**
2. The air track level is adjusted with the help of leveling screws at the bottom of the track. When the track is balanced, a glider will not appreciably move in either direction.

3. Photogate A is connected to channel 1 and Photogate B is connected to channel 2 of Physlogger. The wires labeled **Photo** are connected to the terminals labeled **A+** and **B+** while **G** is connected to the identically named terminal on Physlogger.
4. **Notes about configuring Physlogger:**
 - (a) Ensure that Physlogger is connected to the PC using the USB cable.
 - (b) The channel types are each set to **Analog In RSE** mode, and
 - (c) the individual input ranges are set to ± 6 V.

When connected, if the Physlogger app is showing the photogate signal on its channels and responding to obstacles detected by the photogates, it means that the apparatus is ready to use. Your instructor will provide you more details about using Physlogger. Alternatively, you can download the user manual from this website [1].

4 A basic exercise

Let's do a basic exercise of detecting a signal when the glider passes through the photogates,

1. Place photogate A 45 cm away from the left edge of air track and photogate B 100 cm away from photogate A.
2. Connect photogate A to channel 1 of Physlogger and photogate B to channel 2 of Physlogger.
3. Starting from the extreme left, slightly push the glider by hand and let it cruise to the right end. First this glider will intercept photogate A and at some later time photogate B.
4. For example, Physlogger's channel 1 will show two rectangular pulse signals when the glider intercepts Photogate A (see Figure 2). Likewise, two pulses will be detected for photogate B and displayed on Channel 2. The two pulses correspond to the flags on the glider. You are provided with measuring rules to measure the lengths and mutual distances between these flags.

Now let's do some interesting exercises on this apparatus.

5 Idea Experiments

1. **Measure speeds and finding their uncertainties:** Using a single slider move across the air track, measure the speeds of the (a) flags, and the (b) glider on the locations of the two photogates placed ≈ 100 cm apart. In this experiment, you can find the speed of a flag by measuring, say, $t_2 - t_1$ and the speed of a glider by measuring $t_3 - t_1$ or $t_4 - t_2$. Other schemes are also possible. In which of these quantities do you see the

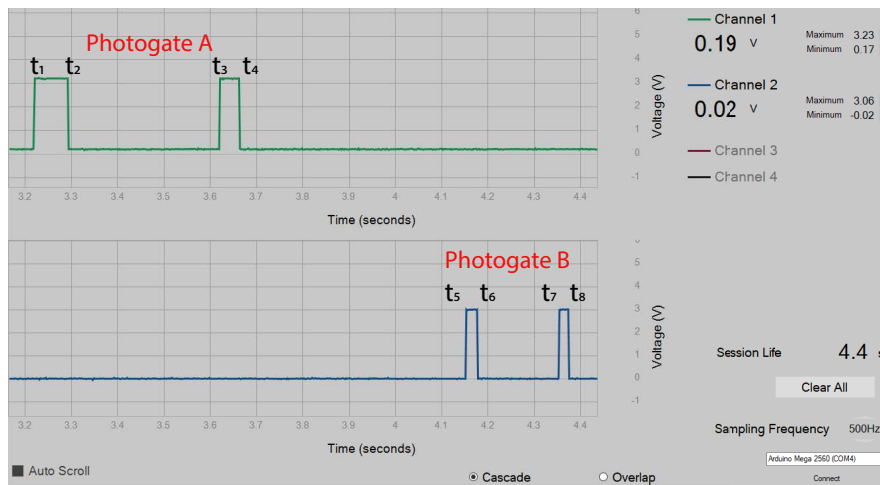


Figure 2: The waveforms acquired on Physlogger when a single glider passes through the photogates A and B spaced 100 cm apart. The markers t_1 through t_8 are also marked.

largest variation? Comment on the uncertainties of the speeds. What's a more precise estimate of the speed of the glider? Are these speeds measures of *instantaneous* or *average* speeds?

2. **Average speeds:** Find the average speed of a glider between locations A and B. There are different time intervals you could use for determining the average speed. Recognize these various methods and estimate the average speed. Discuss with your instructor.
3. **Energy and momentum losses:** How does the momentum and the energy of the slider decay as it makes multiple round trips on the air track? Connect the rubber bands on the end bumpers on both ends for this part of the experiment. Could you plot these energy and momentum losses and explain the origin of these losses? How do the speeds and momentums change when two gliders collide with one another. Is the collision elastic?
4. **Acceleration and free body diagram:** Measure the mass m of the glider with the provided weigh balance. Tie a thread to the neck of a flag that is attached to the glider on the end closest to the end-pulley. Attach a weight M to the weight hanger and hang it to the end of the thread which passes over the pulley. Adjust the length of the thread and the location of the photogates such that that when the weight M is at its highest location, the glider finds the opportunity to intersect both the photogates in the weight's downward descent. Measure the average acceleration a of the glider. Repeat the experiment a few times with the same mass M . Subsequently, repeat for different masses M .

Draw a free body diagram for the hanging weight and the glider, showing the tension in the string and the acceleration of the objects. Derive a formula showing the relationship between m , M and a . Does your experimental data verify this relationship? Draw a graph to elaborate your findings. Can you modify your formula to elicit a linear relationship? Finally, estimate the value of the acceleration due to gravity g deduced from your data.

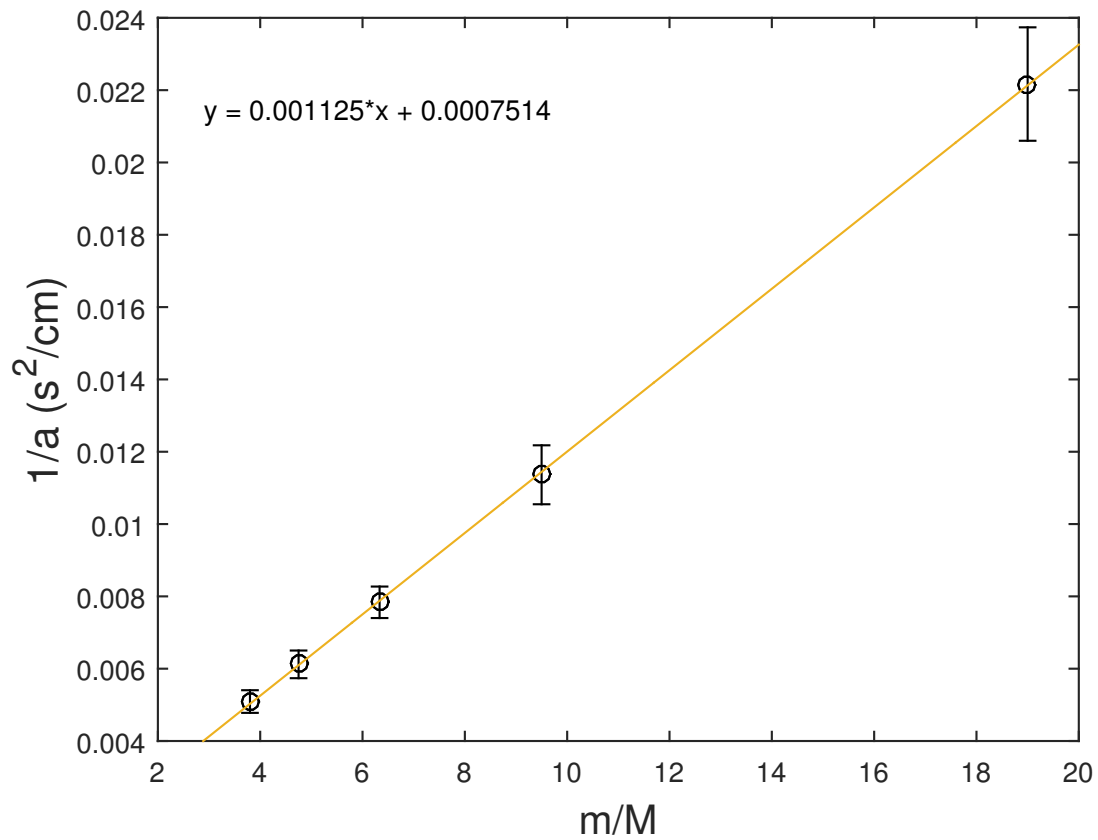
5. **Automating calculation of the acceleration** Could you write a computer program that takes the data saved from the Physlogger's session and computes the acceleration? Well, if you can try this on your own, then bravo! If you don't want to try, you could also draw from a collection of Matlab scripts from our website that automatically computes the acceleration for you. Put all of these files *and* your data files recorded from Physlogger into the same folder. Suppose your filename with the recorded data is `example.txt`. Typing the following command in Matlab's command window will compute the acceleration in cm s^{-2} for the dimensions and sizes of the provided air track accessories.

```
AirTrackAcc('example.txt')
```

References

- [1] Details on the Physlogger and the user manual can be read from here: <https://www.physlab.org/facility/physlogger/>.

Experiments with a linear air track: Sample Results



S#	m	M	Average acceleration in each trial: a_{avg}					a_{avg}^{mean}	m/M
			Trial 1	Trial 2	Trial 3	Trial 4	Trial 5		
1	190	10	45 ± 2	45 ± 2	46 ± 2	45 ± 2	45 ± 1	45 ± 3	19
2	190	20	88 ± 5	88 ± 5	88 ± 4	89 ± 4	88 ± 4	88 ± 6	9.50
3	190	30	127 ± 5	128 ± 5	128 ± 5	127 ± 5	129 ± 7	128 ± 7	6.33
4	190	40	163 ± 9	164 ± 8	160 ± 8	$160 \pm U$	167 ± 8	$160 \pm U$	4.75
5	190	50	$198 \pm U$	$197 \pm U$	$196 \pm U$	$200 \pm U$	$192 \pm U$	$196 \pm U$	3.80

$U = 1 \times 10^1$

Tuning a Laser Diode*

Muhammad Shiraz Ahmad, Alamdar Hussain,
Rabiya Salman and Muhammad Sabieh Anwar
Syed Babar Ali School of Science and Engineering, LUMS

Version 2019-1; July 23, 2019

The output of a laser diode can be modulated by varying its temperature and current. In this experiment, we will develop an understanding of how a laser diode's optical power and wavelength can be varied by controlling its temperature and operating current. Furthermore, we will use the proportional integral (PI) feedback control system to stabilize and tune the temperature of the diode laser.

Essential pre-lab reading: “*Laser Diode (L785P100) Specifications*” by Thorlabs.

“*Laser Diode Mount (TCLDM9) Manual*” by Thorlabs (Understand the internal configuration of the mount).

“*Laser Diode Driver Manual*” by Thorlabs.

Optional Reading: “*Feedback control of Dynamic Systems*” by Frankline, Powell and E-Naeini, Pearson (Section 4.3).

1 Overview of the Experiment

In this experiment, we will control the temperature and the current through the laser diode and observe the effects on the light output. The schematic of the control system is shown in Figure 1. Now follow this discussion closely.

The setup is divided into four different blocks. The laser diode is placed in a laser diode mount; the mount is shown as block *A* in the figure. The laser diode package contains a laser diode and a photodiode for monitoring its output. These two components are then connected to a *laser diode current driver* depicted overall as block *B*. Within block *A*, the laser diode package is in thermal contact with a thermistor and a Peltier heater. Using these two components, the temperature controlling system, comprising boxes *C* and *D*, is designed to control the temperature. Block *C* contains a current source to drive the temperature sensor (thermistor)

*No part of this document can be used without the explicit permission of Dr. Muhammad Sabieh Anwar. We like to thank Muhammad Hamza Waseem, Faizan e Ilahi, Zahra Tariq and Mahpara Iqbal for improving this experiment and the associated write-up in 2018.

and a transistor (50N06) which acts as a switch for operating the Peltier heater. The output of the temperature sensor, $y(t)$, is fed into block D where it is compared with the desired temperature y_s . The difference $e(t)$ is then used to create a control signal $u(t)$ which is then converted to a voltage signal $z(t)$. Block D is implemented through the data acquisition system (DAQ). Finally this voltage signal is fed to the transistor in block C which accordingly switches the current through the Peltier heater.

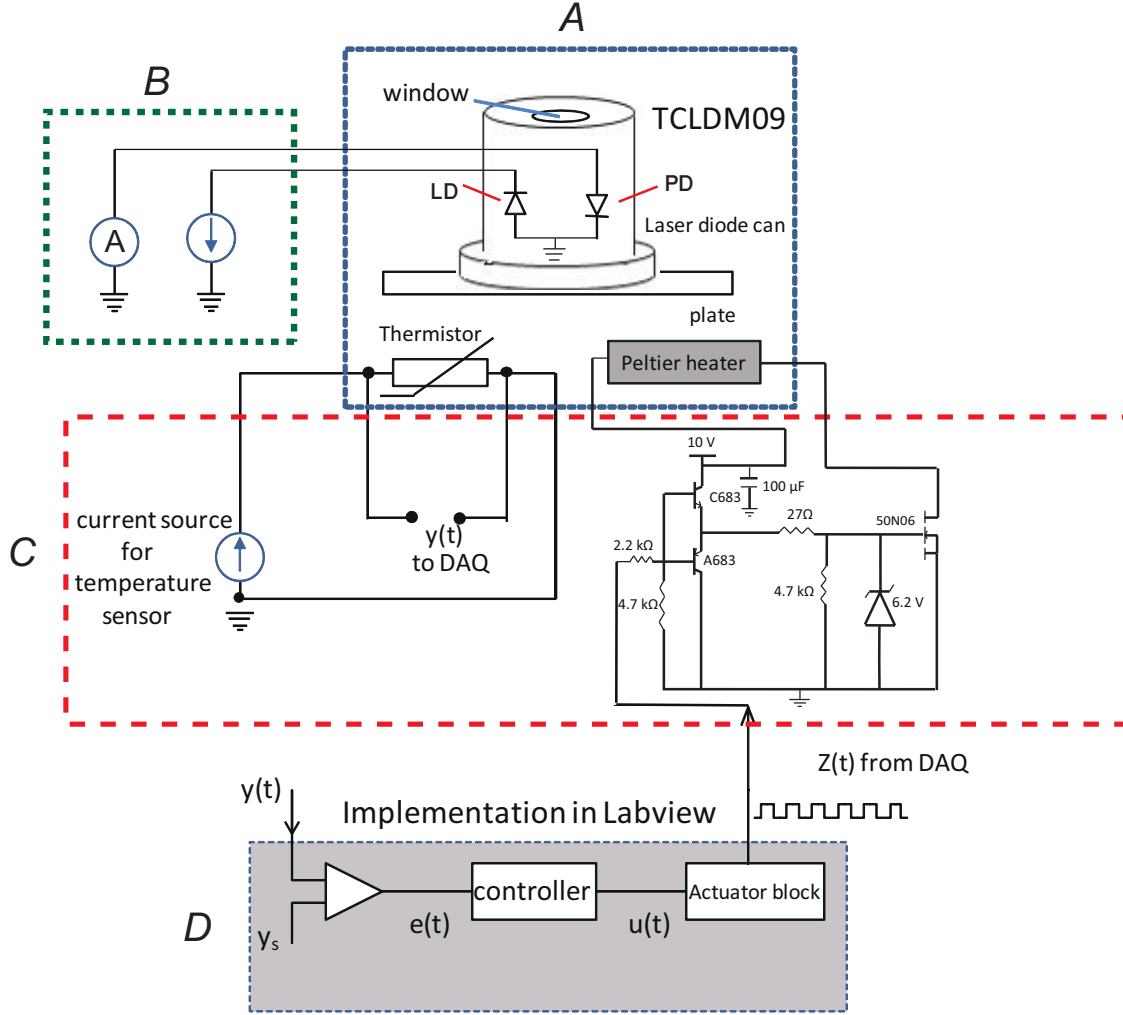


Figure 1: Schematic for the tuning experiment. A represents the laser diode mount, B is the laser diode current controller, C is the temperature controller box and D represents the control algorithm implemented in LabView. This figure is seen best in color. LD = laser diode and PD = monitor photodiode.

2 Preparing for the Experiment

Before starting the experiment, make sure to have following components available,

1. 100 μ A current source.
2. Laser mount (Thorlabs TCLDM09).
3. Temperature controller circuit (Homemade).
4. NI DAQ USB-6001.
5. Laser diode controller (Thorlabs LDC 205 C).
6. 9 V voltage source.
7. PC with LabVIEW installed.

Now, follow these steps to make your setup ready for use,

1. Connect the 100 μ m current source, 9 V voltage source and DAQ USB-6001 to the temperature controller as per the schematic of Figure 2 where wires are labelled with the same colours as of the apparatus.
2. Connect laser mount (TCLDM9) to the laser diode controller (LDC 205 C) with DB9M-to-DB9F cable. The laser diode is already mounted in the laser mount for your convenience.
3. Connect the DB9M connector of temperature controller to TEC Controller connector of laser mount.
4. Connect the green and white wire from the temperature controller to the “AI 0” and “AI 4” terminals of DAQ, these wires are directly connected to the thermister in Laser mount. these wires give the potential drop as a function of temperature. In this configuration, DAQ can read the temperature of Laser diode on its terminals “AI 0” and “AI 4”.
5. Connect the red and black wires from the temperature controller to the “AO 0” and “AO 1” terminals of DAQ, these wires act as a switch, when high voltage of 5 volts is applied on these terminals via DAQ, the temperature controller circuit switches on the Peltier heater, of the laser mount, which is in thermal contact with the laser diode and thermister.
6. Run the Labview file “tempcontroller.vi” (see index for GUI) which implements the PI based temperature controller. The front panel of PI control is shown in Figure 2b. Assign the weights $P = 10$ and $I = 0.015$ to proportional and integral controls respectively. These values are chosen such that temperature rises rapidly when the error is large and then changes slowly when the error diminishes.

This setup can further be configured in two different ways as shown in Figure 3 depending on the need.

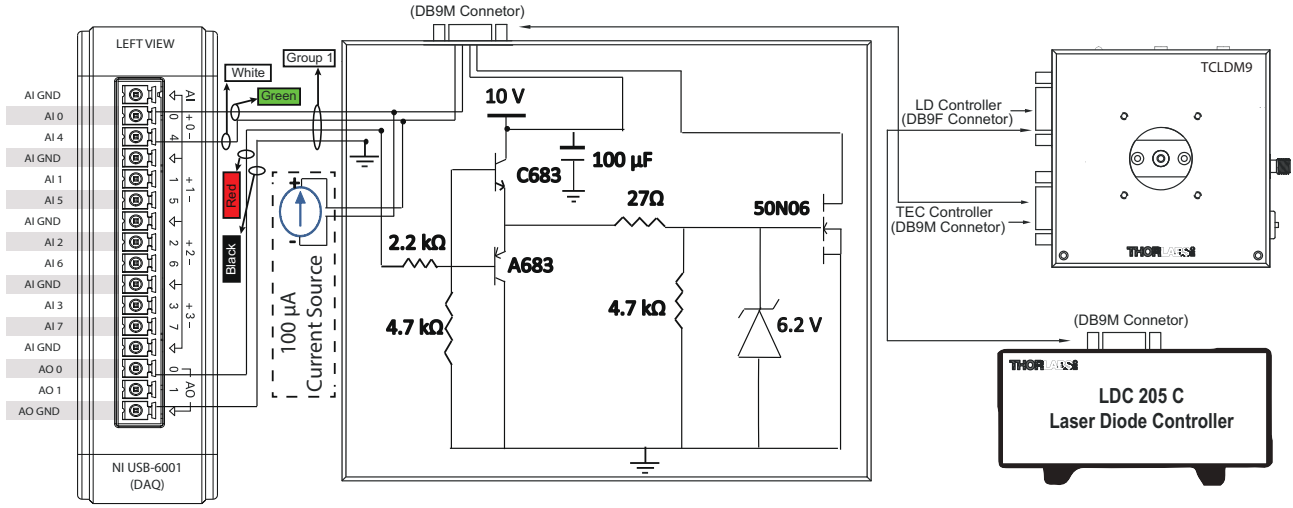


Figure 2: (a) The temperature control box and (b) the front panel of PI based temperature controller. These were represented by blocks C and D in Figure 1 respectively.

2.1 Measuring Optical power versus injection current at room temperature.

Arrange the apparatus as shown in Figure 3a. Increase the injection current of the laser diode in regular intervals from zero to 150 mA (since the maximum operation current is 160 mA). Note down the output of the external photodiode and the current produced by the internal photodiode at each step. The monitor photodiode outputs current proportional to the power incident on it.

Q 1. Using proper conversion factor plot the external photodiode current as a function of the injection current. Find the *threshold current* and explain the shape of graph.

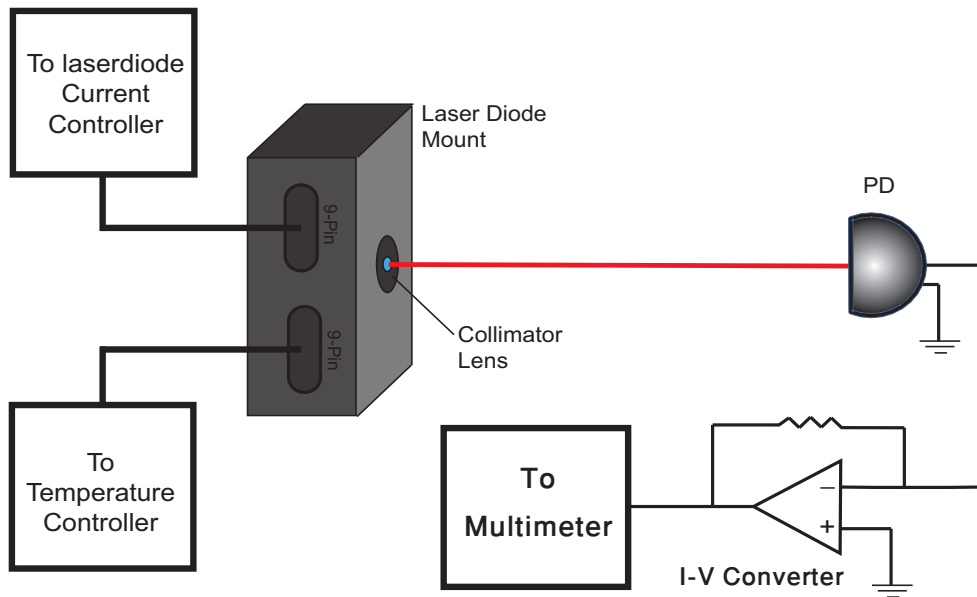
Q 2. Similarly plot the internal photodiode's photo-current and confirm the value of the *threshold current*.

Q 3. Utilize the external photodiode current to plot the power emitted by the laser diode using the proper conversion factor. The responsivity of the external photodiode is 0.48 A/W.

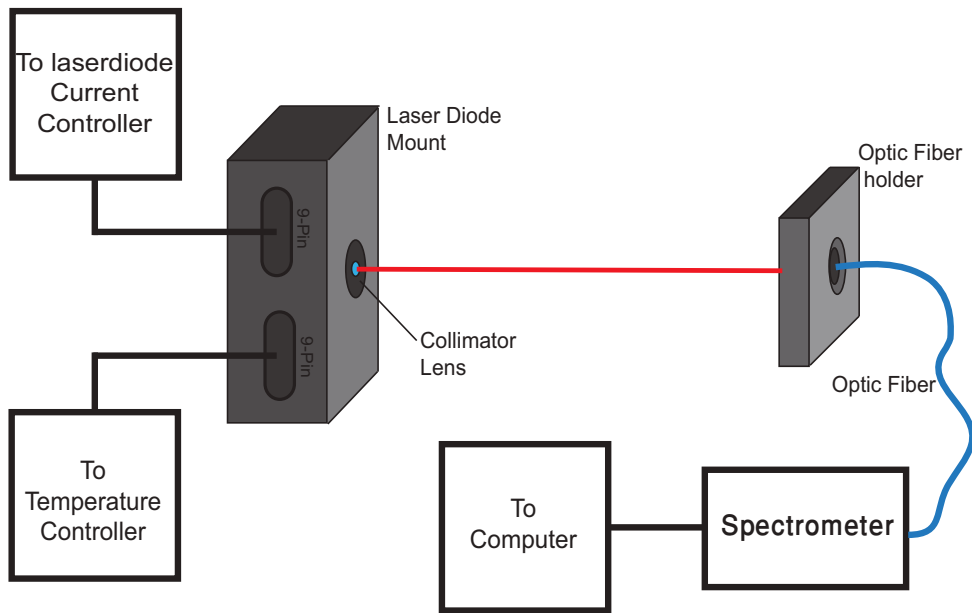
2.2 Measuring optical power versus temperature

Now set the injection current to 115 mA and set temperature to 50°C from LabVIEW based control panel. When diode temperature reaches to 50°C, set its temperature to the room temperature. Temperature will start decreasing slowly, keep measuring optical power with temperature. Measure the output power using the external photodiode at each step.

Q 4. Plot the optical power as a function of the temperature.



a

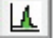


b

Figure 3: Schematic for measuring (a) the output intensity of the laser diode and (b) the wavelength of laser diode. The red line shows the perceived path of laser (the picture is seen best in color).

2.3 Measuring wavelength versus temperature

Finally let the laser diode cool down to room temperature and then set the apparatus as shown in Figure 3B . Connect the fiber optic spectrometer (StellarNet Blue Wave Spectrometer) to

the computer and open its software named *SpectraWiz*. It will immediately start acquiring the spectrum. To measure the wavelength of the laser, right click on the spectrum peak and press the *peak wavelength* button indicated by . Increase the temperature up to 50°C in regular steps and measure the wavelength of the laser. You may need to change the value of injection current at each step so that the peak is identifiable as well as the observable within the software window. You can also change the limits of the y-axis scale.

Q 5. Plot the wavelength as a function of temperature. What is the best estimate of $\frac{d\lambda}{dT}$? What's the uncertainty?

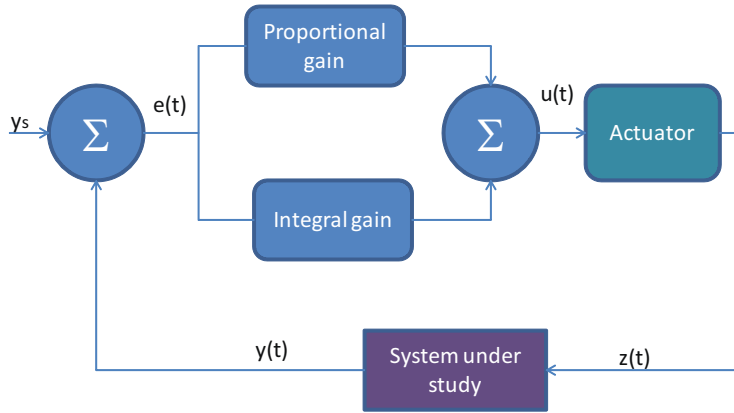


Figure 4: Block diagram of a typical PI Controller.

Appendix

Feedback Control

In a feedback control system the variable that is to be controlled is measured. This measurement is compared with a set point. The controller takes the difference between the current value of the parameter and the set point and decides what action should be taken to compensate for, and hence remove, the error. The ultimate goal is to train or steer the control variable to the desired set point.

A PI controller, implemented in the current experiment, is special kind of controller. A PI controller works by summing the current controller error and the integral of all previous errors. If we define the error as

$$\begin{aligned} e(t) &= (\text{set point}) - (\text{current measured variable}), \\ &= y_s - y(t), \end{aligned}$$

then the output of the PI controller would be,

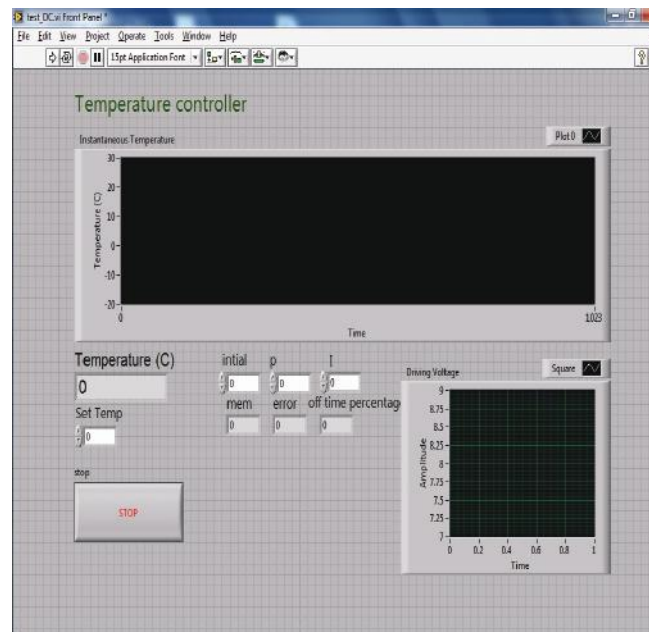
$$u(t) = K_p e(t) + K_I \int_{\tau=0}^t e(\tau) d\tau,$$

where K_P = proportional gain and K_I = integral gain are approximately chosen weighting factors.

PI controllers work in a closed-loop feedback system as shown in Figure 4. A sensor measures the parameter, the measurand being $y(t)$ is then fed back into the comparator, and compared against the set point y_s . This signal $u(t)$ is then sent to the actuator, and the output $z(t)$ is obtained. The signal $z(t)$ actuates some mechanism enabling the system to restore its parameters.

This control loop is ultimately an iterative process. In each iteration, the controller takes this new error signal and computes integral. In this experiment, the PI controller is implemented in the LabView program, while $y(t)$ is the measured temperature, y_s is the set temperature and $z(t)$ is the signal that is fed into the heater.

The front panel of PI based temperature controller

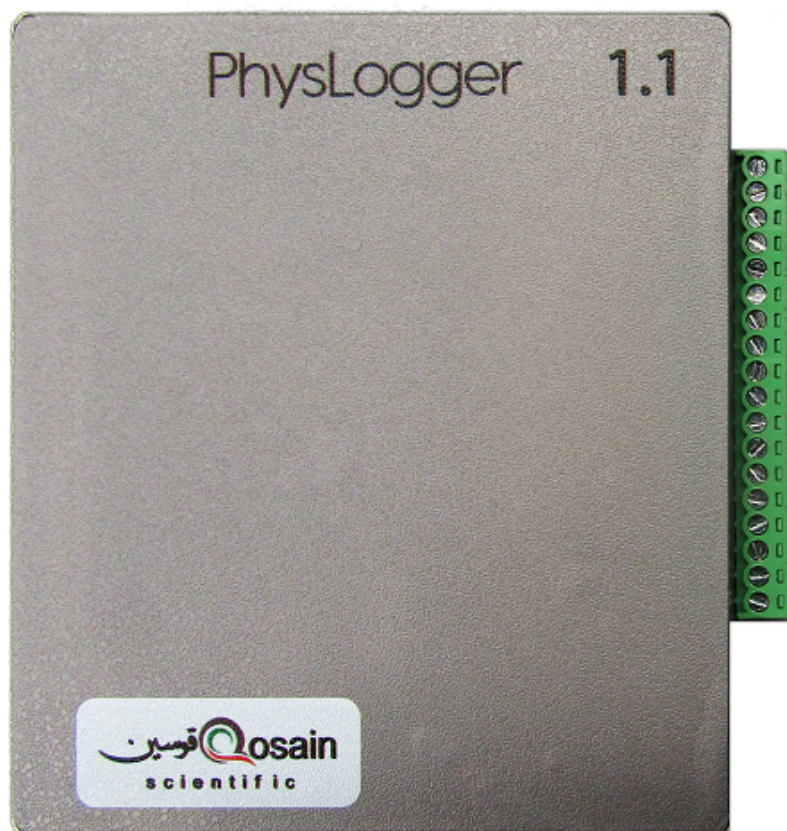


PhysLogger – Quick start Guide (App)

v. 2019-I

Muhammad Umar Hassan, Muhammad Shiraz Ahmad,
Muhammad Sabieh Anwar

April 22, 2019



Introduction

PhysLogger can adapt to any voltage measurement application that you might encounter. From pressure to torque and load to force, sensors convert mechanical properties to a voltage and PhysLogger can record that information, from single to multiple channels. This manual provides an overview of how the app, that goes with the same name, can be used to interface with the physical device. So happy logging!

Contents

1	Overview to PhysLogger Device	3
2	Using PhysLogger App	4
2.1	App Start-up	4
2.2	PhysLogger Desktop.	4
2.3	Customizing the channels	5
2.3.1	Channel options	5
2.3.2	Labelling channel names	5
2.3.3	Graph scaling	6
2.3.4	Channel display modes	6
2.4	Exporting Data	7
2.5	Saving/Opening Projects	7
3	Example: Using PhysLogger in an Optical Experiment: verifying Malus's law	7
4	Appendix	8
4.1	Prerequisites to run PhysLogger App	9
4.2	Frequently asked questions	9
4.2.1	How to install Arduino drivers in PC	9
4.2.2	How to update the Firmware into PhysLogger device.	10

I Overview to PhysLogger Device

PhysLogger is shown in Figure 1. It has a total of 18 pin connections and one USB port to connect it with the PC. The functionality of these pins will now be described.

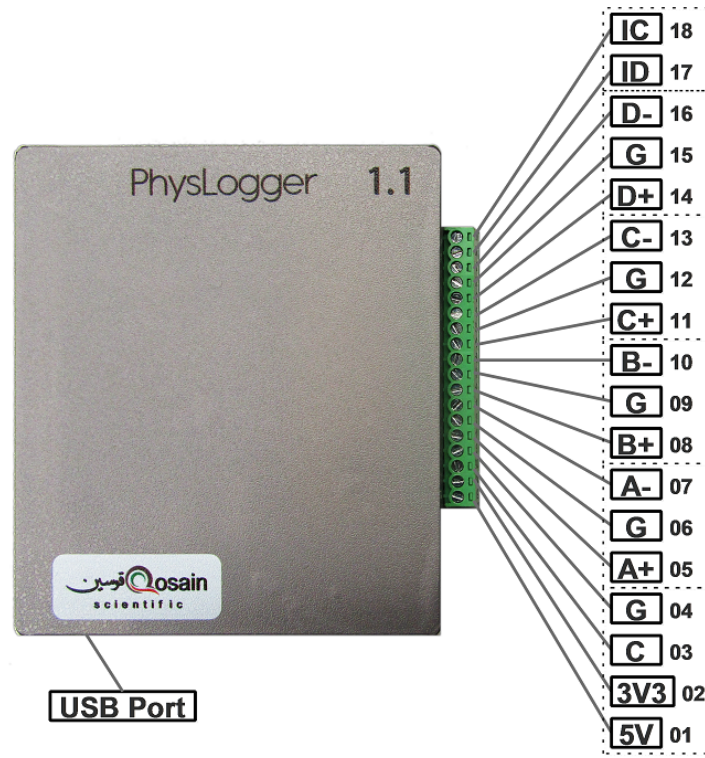


Figure 1: PhysLogger Device.

Pins 01 and 02 are built in power sources of voltages 5 V and 3.3 V. These pins are used as power source for commonly available transducers. Pins 05, 08, 11 and 14 which are labelled as A+, B+, C+ and D+ are four input channels to read voltage levels. These channels can read data in different modes such as Analog RSE or Analog Differential. The pairs:

A+(05), G(06);

B+(08), G(09);

C+(11), G(12);

D+(14), G(15);

are the combinations used in RSE Differential mode and the pairs:

A+(05), A-(07);

B+(08), B-(10);

C+(11), C-(13);

D+(14), D-(16);

are used for Analog Differential mode. All the G(04, 06, 09, 12 and 15) pins are physically connected inside the device. The pin C(3) is reserved for calibration purposed.

The pins IC(18) and ID(17) are meant for inputting digital I^2C data.

2 Using PhysLogger App

2.1 App Start-up

To run PhysLogger App:

1. Insert the product CD in your PC, open the E: drive or letter of your CD-ROM drive.
2. Under the directory **CD** > **Release**, run the file **PhysLogger.exe**.

■ To run the app, your PC must meet all basic requirements mentioned in the Appendix.

2.2 PhysLogger Desktop.

When you start PhysLogger, PhysLogger desktop appears (see Figure 2), containing all the tools, required to control the acquisition and display of all signals.

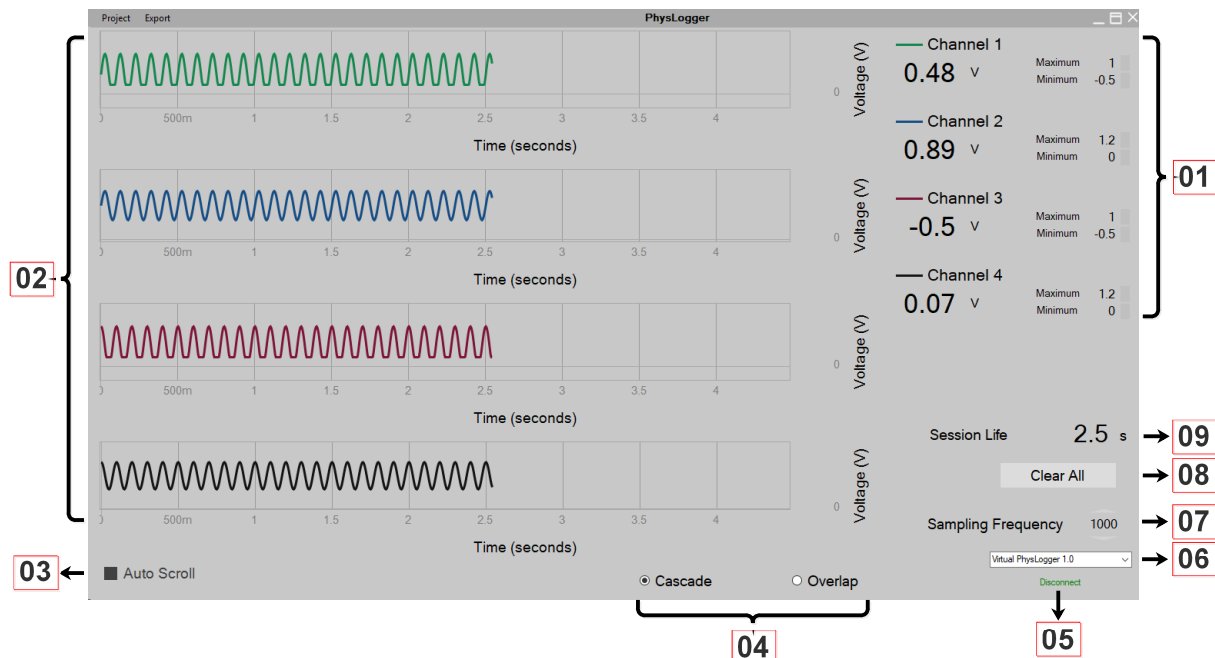


Figure 2: PhysLogger Desktop.

Here is a description of the various menu items visible on PhysLogger Desktop.

1. Controls of each channel.
2. The live plots of the acquired electronic signals.
3. Locks or unlocks auto scrolling.
4. Toggle switch between cascade and overlap modes. The latter mode puts all signals onto the same screen.
5. Connects or disconnects PhysLogger with the device through the USB port.
6. Device port selector.

7. Sampling frequency selector.
8. Resets the live session plot. It clears all data points in the buffer and continues acquiring the electronic signals afresh.
9. Time since last reset.

2.3 Customizing the channels

This section provide a quick introduction to PhysLogger 's desktop tools.

2.3.1 Channel options

PhysLogger supports up to four (4) channels. One of the channels could be on I^2C protocol. All have similar controls. They all have very similar controls. To activate any channel, hover the mouse over the **line** before the channel label. A check-box will appear (see Figure 3). Click on that check-box to activate the corresponding channel. The channels can be accessed by hovering the mouse over the live-plot of that channel and right clicking on it. The following options for each channel will be exposed upon right clicking:

1. Display Options

Color, thickness or opacity of the live-plot can be changed through this option.

2. Channel Options

- (a) **Input Range:** Through this option you can change scale values on your live-plots. This switches the onboard amplifiers giving you a higher resolved view of small sized signals, for example.

■ Input range can be set to one of the following values: 6 V, 0.6 V or 30 mV.

- (b) **Type:** As PhysLogger can measure voltage changes from the sensors connected to its channels, hence some mathematical function is required to convert these voltage changes into corresponding required units. This is called scaling. Following are some inbuilt transfer functions

- i. Analog Differential: Differential analog voltage signal, e.g. between A+ and A-, B+ and B-, C+ and C-, D+ and D-
- ii. Analog RSE: Single ended analog signal measurement
- iii. Physbar 1.0: Pressure measurement
- iv. Physlab Thermocouple Module: Temperature measurement
- v. PhysLoad 1.0: Measurement of forces using a load cell
- vi. PhysDisp: Linear displacement measurement

These functions can be accessed under menu Channel Options Type.

2.3.2 Labelling channel names

Channels are labeled as **Channel 1**, **Channel 2** ... by default. To relabel any channel name, click on it's label (see Figure 3) and type in any desired name.

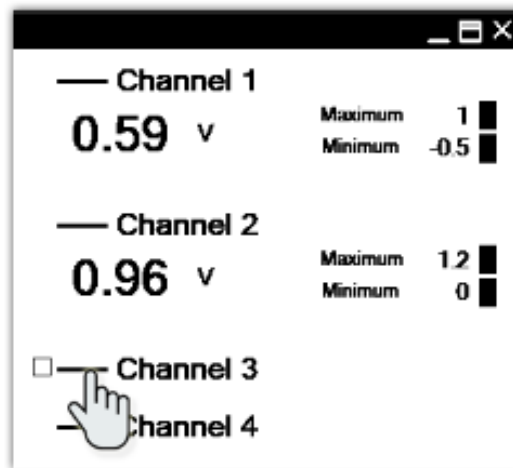


Figure 3: Check-box appeared with hovering mouse.

2.3.3 Graph scaling

To change the time scale on a graph of any channel (see Figure 4), click on a space just above the Time (seconds) caption and drag horizontally (left or right). Similarly, to change the voltage scale, click on a space left to the Voltage (V) caption and drag vertically (up or down).

To auto scale incoming data on live-plot, right click on a space left to the Voltage (V) and select/deselect auto scale option.

The time scale of all channels is synchronized, changing the time scale of any channel uniformly effects all channels whereas voltage scales can be changed independently.

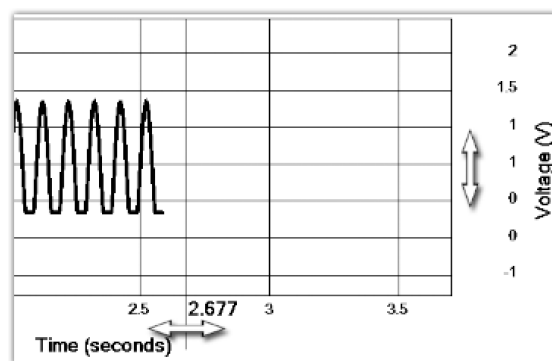


Figure 4: Graph scaling options.

2.3.4 Channel display modes

PhysLogger displays the output of all channels on separate graphs by default, but they can also be displayed on the same graph by changing the mode from Cascade to Overlap (see Figure 5).

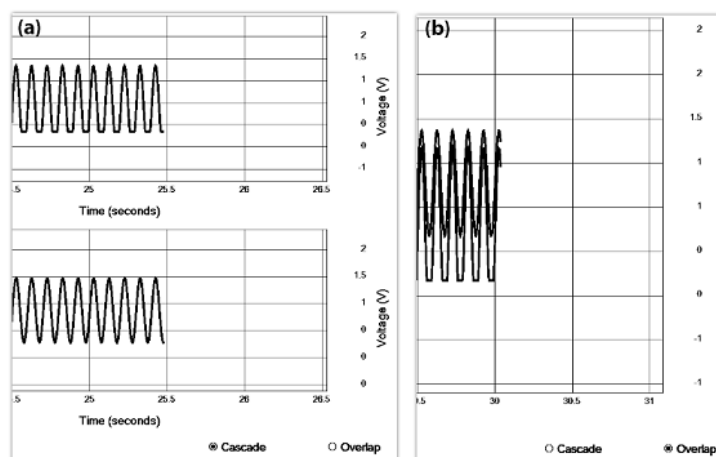


Figure 5: a) Cascade mode. b) Overlap mode.

2.4 Exporting Data

The following data sets export options are available in PhysLogger :

1. Tab-Delimited (.txt): Readable by software like Excel, Origin etc.
 - (a) To export data without headers, select **Export** **Data File** **Raw...** from the menu,
 - (b) To export data with headers, select **Export** **Data File** **With Headers...** from the menu.
 2. Copy to Clipboard: Copies all the recorded data directly to the clipboard.
 - (a) To copy data without headers, select **Export** **Copy to Clipboard** **Raw...** from the menu,
 - (b) To copy data with headers, select **Export** **Copy to Clipboard** **With Headers...** from the menu.
- PhysLogger exports data in tab-separated columns with the following sequence,
- | Sr.No. | time_s | Channel 1 | Channel 2 | Channel 3 | Channel 4 |
|--------|--------|-----------|-----------|-----------|-----------|
|--------|--------|-----------|-----------|-----------|-----------|
3. Take Screen Shot: To take screen shot of current window of PhysLogger , select **Export** **Screen Shot**.

2.5 Saving/Opening Projects

The whole work space of PhysLogger , including all the recorded data and configuration, can be saved through menu **Project** **Save** and can be opened any time again same work space through menu **Project** **Open**.

3 Example: Using PhysLogger in an Optical Experiment: verifying Malus's law

To test our PhysLogger in an optical setup, we used the configuration shown in Figure 6. An optical beam produced by a laser is passed through the polarizer and the analyzer and is finally detected on a photodiode. The photodiode converts this interrupted optical signal into

an electrical current which is converted to proportional voltage using a current-to-voltage amplifier. Finally, this signal is measured on **PhysLogger**. Here, output wires of current-to-voltage amplifier are connected with the pins A+(05) and A-(07) of **PhysLogger** with Analog Differential mode inside the app.

Figure 7 shows the experimental curve which agrees almost perfectly with the theoretical prediction of the square of cosine relationship. In our experiment, we fixed the orientation of the polarizer while rotated the angle θ of the analyzer.

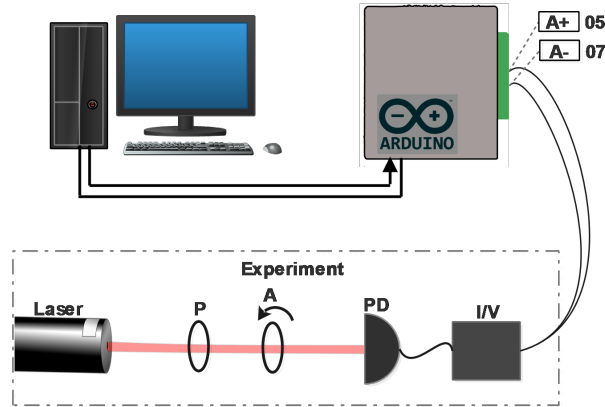


Figure 6: Schematic diagram of the experiment to verify the Malus's law where "P" represents the polarizer, "A" represents the analyzer.

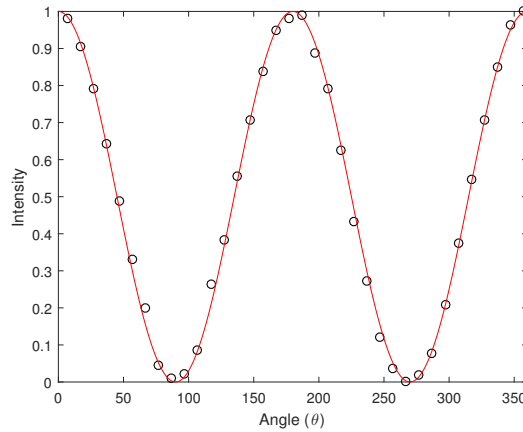


Figure 7: Intensity of an optical beam as a function of angle between two crossed polarizers, curve fitted on square of cosine, which satisfies Malus's law.

4 Appendix

If the app does not run when the **PhysLogger** executor file is run, one needs to ensure that few prerequisites are satisfied.

4.1 Prerequisites to run PhysLogger App

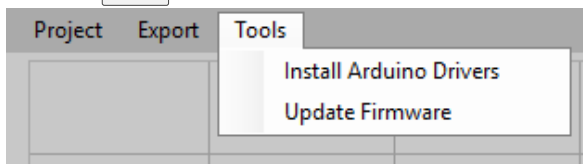
To run PhysLogger App, you must have,

1. Arduino drivers properly installed on your PC.
2. PhysLogger device is connected to PC via USB cable.
3. Firmware is installed into PhysLogger device.
4. We have already installed .NET Framework of version 4.5.2 or greater.

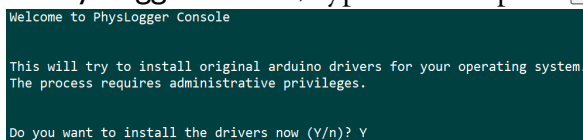
4.2 Frequently asked questions

4.2.1 How to install Arduino drivers in PC

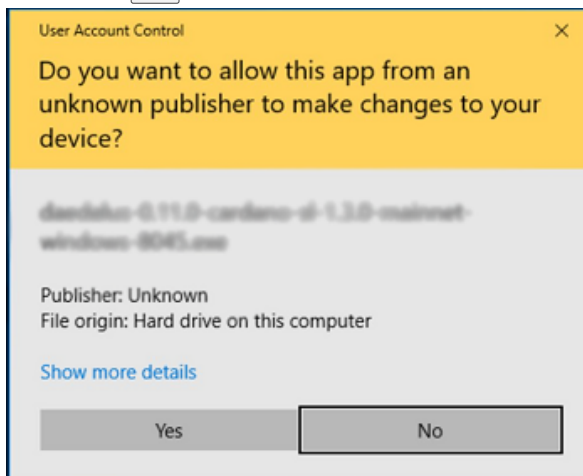
1. Insert the product CD in your PC, open the E: drive or letter of your CD-ROM drive.
2. Under the directory **CD** > **Release**, run the program PhysLogger.exe
3. Under **Tools** click on "Install Arduino Drivers".



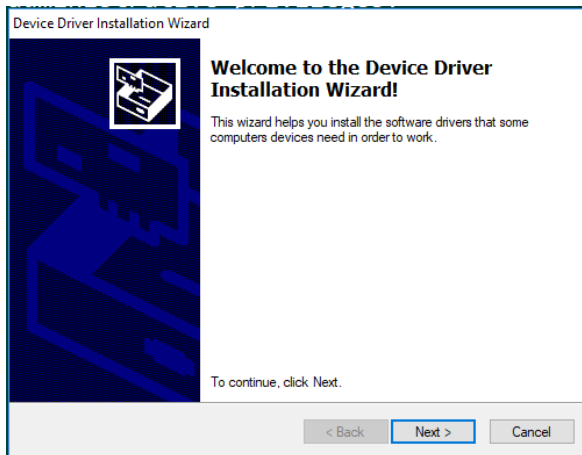
4. In PhysLogger console, type "Y" and press **Enter**.



5. Click on **Yes** button on User Account Control pop-up.

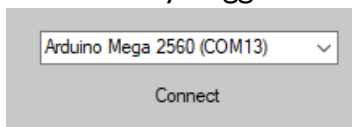


6. In Device Driver Installation Wizard, click on the button **Next** and then click on the button **Finish**.

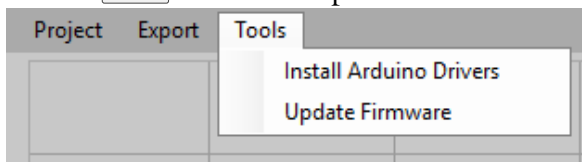


4.2.2 How to update the Firmware into PhysLogger device.

1. Insert the product CD in your PC, open the E: drive or letter of your CD-ROM drive.
2. Under the directory `CD \Release`, run the program `PhysLogger.exe`
3. Connect PhysLogger device with the App.



4. Under `Tools` click on "Update Firmware".



5. In PhysLogger console, type "Y" and press `Enter`.

```
PhysLogger Update Console
You are about to update the PhysLogger firmware to v1.1. This will update the firmware on the PhysLogger
hardware which might raise conflicts if not done properly.
If you are not sure what you are doing, you might want to quit it now.

Do you still want to continue with the update (Y/n)? Y
```

6. Wait for the message "Press any key to exit...", when it appears, press any key.

```
All done, shutting down!
The process completed

Press any key to exit...
```